

ENGINEERING RESEARCH INSTITUTE  
UNIVERSITY OF MICHIGAN  
ANN ARBOR

*John G. Lewis*

PROMOTION OF SOME CHEMICAL REACTIONS  
WITH GAMMA RADIATION

Reported by: JOHN G. LEWIS

Supervisor: J. J. MARTIN

Project M943-4

U. S. ATOMIC ENERGY COMMISSION  
CONTRACT NO. AT (11-1)-162

January, 1954

## PREFACE

The author wishes to acknowledge the assistance, direction, and support of all who have made this report possible:

Dr. L. C. Anderson	Mr. R. L. Kinney
Mr. F. Bashore	Dr. J. J. Martin
Dr. L. E. Brownell	Mr. R. D. Pierce
Mr. F. H. Chadsey	Mr. E. M. Rosen
Dr. H. J. Gomberg	Mr. S. A. Stolton
Mr. J. R. Hallman	Dr. L. Thomassen
Mr. D. E. Harmer	Mr. L. E. Wagner
Dr. L. M. Hobbs	

## TABLE OF CONTENTS

	Page
PREFACE	ii
LIST OF TABLES	v
LIST OF FIGURES	vi
ABSTRACT	ix
INTRODUCTION	1
APPARATUS	3
General Description	3
Design and Construction of a Pressure Reactor	3
Hydrostatic Test of the Reactor	8
Operation of the Reactor	9
ANALYSIS OF DOSE RATES NEAR HOLLOW CYLINDRICAL SOURCES OF GAMMA RADIATION	28
Experimental Procedure	29
Calculation Procedure	32
DOSE RATES WITHIN A CYLINDRICAL PRESSURE REACTOR	60
PRELIMINARY INVESTIGATIONS	72
Synthesis of Ammonia	72
Beta Radiation from Palladium-109	74
Partial Polymerization of Natural Oils	76
Polymerization of Acetylene	78
Chlorination of Kerosene and Benzene	79
Oxidation of Sulphur Dioxide	81
Reaction of Carbon Dioxide with Hydrogen	84
Polymerization of Isobutylene	85
Polymerization of Propylene	85
Polymerization of Ethylene	85
DISCUSSION OF PRELIMINARY INVESTIGATION	86
POLYMERIZATION OF ETHYLENE	90
Prior Work	90
Polymerization of Ethylene by Means of Gamma Radiation	91
DISCUSSION OF POLYMERIZATION OF ETHYLENE	97
EVALUATION OF POLYETHYLENE PRODUCT	99

	Page
SUGGESTIONS FOR FUTURE WORK IN THE PROMOTION OF CHEMICAL REACTIONS BY GAMMA IRRADIATION	121
Polymerization of Ethylene	121
Other Reactions	122
CONCLUSIONS	123
APPENDIX	125
Design Data for Bomb	125
Assembly Instructions for Bomb	125
Operating Instructions for Bomb	126
Definition of Radiation Yield	126
BIBLIOGRAPHY	129



## LIST OF TABLES

Table No.		Page
I	Irradiation of Ferrous Sulfate Solutions in Cobalt-60 Source - Dosimetry by Method of Weiss	31
II	Dose Rates on Axis of 10-KC Source	36
III	Dose Rates on Mid-Plane of 10-KC Source	37
IV	Estimates of Activities from Measurements of Dose Rates	38
V	Dose Rates on Axis of 1-KC Source	40
VI	Irradiation of Mixture of Nitrogen and Hydrogen with Palladium-109 Beta Rays	73
VII	Results of Irradiation of Natural Oils with Palladium-109 Beta Rays	75
VIII	Changes in Viscosity of Soya Oil after Irradiation and Subsequent Heating	77
IX	Irradiation of Mixtures of Kerosene and Chlorine in 1-KC Cobalt-60 Gamma Source	80
X	Irradiation of Mixtures of Benzene and Chlorine in 1-KC Cobalt-60 Gamma Source	82
XI	Irradiation of Mixtures of Sulfur Dioxide and Oxygen in 1-KC Cobalt-60 Gamma Source	83
XII	Irradiation of Propylene	83
XIII	Irradiation of Ethylene	92
XIV	Analyses of Ethylene from Storage Cylinders and from Reactor	95
XV	Properties of Polyethylene Produced	103

## LIST OF FIGURES

Figure		Page
1	Working Drawing for the Construction of the Reactor	11
2	Pressure Reactor and Auxiliary Fittings	12
3	Pressure Reactor Disassembled	13
4	Electrical Connections of Pressure Reactor	14
5	Drawing of Plug Gauge	15
6	Pressure Reactor with 150 psi Rupture Disc	16
7	Plug Gauge and Body of Reactor	16
8	Adapter Fitting: Cone Joint to Iron Pipe Thread	17
9	Adapter Fitting: Cone Joint to Iron Pipe Thread	18
10	Pressure Reactor: X-rays of First Welds Showing Locations at Head	19
11	Pressure Reactor: X-rays of First Welds Showing Locations at Body	20
12	Pressure Reactor: X-rays of Second Welds Showing Locations	21
13	X-ray B2: Weld in Upper Body - First Attempt	22
14	X-ray of Weld in Upper Body - Second Attempt	22
15	X-ray C3: Weld at Head - First Attempt	23
16	X-ray of Weld at Head - Second Attempt	23
17	Pressure Reactor: Drawing of Rack	24
18	Pressure Reactor: Drawing of Sling	25
19	Extension Legs for Rack	26
20	Pressure Reactor Behind Lucite Shield for Palladium-109 Experiments	27
21	Insertion of Pressure Reactor into 1-Kilocurie Gamma Source	43

## LIST OF FIGURES (Cont)

Figure		Page
22	Pressure Reactor in 1-Kilocurie Gamma Source	43
23	Rack and Sling for Pressure Reactor	44
24	Pressure Reactor: Tubing Assembly and Gas Cylinder	44
25	Pressure Reactor in 10-Kilocurie Gamma Source Room	45
26	Sectional View of Cobalt-60 Vault	46
27	1-Kilocurie Cobalt-60 Source with Shielding	47
28	10-Kilocurie Source: Elevator and Well	48
29	10-Kilocurie Source: Rack for Rods	49
30	Cobalt Rod for 10-Kilocurie Source	50
31	Source with Negligible Wall Thickness	51
32	Source with Finite Wall Thickness	52
33	Dose Rate Equations for Source with Finite Wall Thickness	53
34	Dose Rate on Mid-Plane of 10-Kilocurie Source	54
35	Dose Rate on Axis of 10-Kilocurie Source	55
36	Dose Rate on Axis of 1-Kilocurie Source	56
37	Location of Dosimetry Samples for Run 132307 with 10-Kilocurie Source	57
38	Location of Dosimetry Samples for Run 132308 with 10-Kilocurie Source	58
39	Dose Rates Parallel to Mid-Plane, Interpolated from Measurements with 10-Kilocurie Source	59
40	Dose Rates Parallel to Axis, Interpolated from Measurements with 10-Kilocurie Source	65
41	Isodose Surfaces Interpolated from Measurements with 10-Kilocurie Source	66
42	Calculated Dose Rates Parallel to Mid-Plane with 1-Kilocurie Source	67
43	Calculated Dose Rates Parallel to Axis with 1-Kilocurie Source	68

## LIST OF FIGURES (Cont)

Figure		Page
44	Calculated Isodose Surfaces with 1-Kilocurie Source	69
45	Diagram for Attenuation by Distance and Absorption	70
46	Diagram for Dose Rate Inside Pressure Vessel	71
47	Location of Pressure Reactor for Dose Rate Studies with 10-Kilocurie Source	87
48	Dose Rates Inside Pressure Reactor with 1-Kilocurie Source	88
49	Dose Rates Inside Pressure Reactor with 10-Kilocurie Source	89
50	Average Dose Rate Inside Pressure Reactor as Function of Time with 1-Kilocurie Source	106
51	Average Dose Rates Inside Pressure Reactor as Function of Time with 10-Kilocurie Source	107
52	Apparatus for Drying of Natural Oils by Palladium-109 Beta Rays	108
53	Flow Sheet for the Additive Chlorination of Benzene	109
54	Melting-Point Bar	110
55	Influence of Oxygen on Polymerization of Ethylene	111
56	Yield as Function of Order of Run in Polymerization of Ethylene	112
57	Rate as Function of Order of Run in Polymerization of Ethylene	113
58	Radiation Yield as Function of Dose of Radiation in Polymerization of Ethylene	114
59	Solution Viscosity Determinations on Polyethylene	115
60	Molecular Weight as Function of Radiation Yield of Polyethylene	116
61	Molecular Weight and Crystallinity as Functions of Radiation Dose for Polyethylene	117
62	Stress-Strain Plots for Test Specimens of Polyethylene	118
63	Crystallinity and Tensile Strength as Functions of Radiation Yield for Polyethylene	119
64	Melting Points as Functions of Radiation Yield of Polyethylene	120

## ABSTRACT

The purpose of the program of investigation described below was to study some radiation-promoted chemical reactions of potential industrial importance.

In gaseous systems the high densities which result from the application of high pressures increase the absorption of gamma radiation. Therefore pressure was thought to increase any chemical effects caused by radiation. Since many systems of interest are gaseous, it was decided to construct a pressure reactor to study such systems in the presence of radiation. A description is given of the design, construction, and successful operation of this pressure reactor used in proximity to the sources of radiation.

An analysis is presented of the dose rates caused by the sources of gamma radiation, both in air and within the reaction vessel. The resulting measure of the intensity of irradiation made possible the relating of irradiations and the chemical effects observed.

Preliminary investigations were made of the influence of gamma radiation on the following reactions: synthesis of ammonia; oxidation of drying oils and of sulfur dioxide; chlorination of kerosene and of benzene; the reaction of carbon dioxide and hydrogen; and the polymerization of soya oil, acetylene, isobutylene, propylene, and ethylene. The polymerization of ethylene to a white, solid polyethylene is described in detail. Also reported is the influence of radiation yield and of some trace impurities on molecular weight, crystallinity, tensile strength, and melting point of the solid polymers of ethylene.

## INTRODUCTION

The production of fission products as an unavoidable feature of the operation of nuclear reactors has necessitated the development of extensive storage programs for the isolation of these highly radioactive materials. It has appeared to be advisable to develop some potential applications of fission products, both in order to use the energy emitted by these materials and in order to provide an alternative to the expensive dead-storage facilities which must otherwise be provided (see Gibson<sup>25</sup>).

The fission products are chemical elements resulting from the splitting or fissioning of uranium-235 as a consequence of nuclear reaction. The most abundant fission products are those resulting from the approximate halving of the uranium-235. Most of the fission products emit gamma or beta radiation. If attention is restricted to fission products occurring in yields of more than 0.5%, of half-lives longer than 40 days, and of energy levels of more than 0.1 million electron-volts, then the energy of the emissions does not exceed about 1.5 million electron-volts for either beta or gamma radiation (see Hayner<sup>28</sup>). The beta radiation would be absorbed by the walls of most containers. Consequently the gamma radiation would be the only form of radiation usable in an installation in which the fission products are not in direct contact with the materials to be irradiated.

One possible useful function of gamma radiation is in the promotion or catalysis of chemical reactions. It seems logical to expect gamma radiation to promote chemical reactions. Gamma radiation, in common with alpha and beta radiation and x-rays, causes ionization to occur in matter in its path. Such kinds of radiation are consequently known collectively as

ionizing radiation. If ions are produced in a mixture of materials which could react chemically, then a reaction might be expected to occur in order to satisfy the electrical forces thus set up.

A program of investigation was undertaken with the objective of finding some chemical reactions so promoted by gamma radiation that they would provide industrial applications for the waste fission products.

Since it was desired to simplify the techniques of preliminary investigations and the interpretations of the results, fission products were not used as sources of gamma radiation for the work described below. One reason for not using fission products in preliminary studies is that the handling of these materials appears to be troublesome. In addition, the separation of the fission products into individual isotopes of well defined radiation spectra appears to be a formidable problem. In any event, fission products are not yet available in packaged form for use in the laboratory. In order to minimize difficulties of the kind just mentioned, cobalt-60 was used as the source of gamma radiation. Cobalt may be fabricated into convenient form for handling before being made radioactive by irradiation in a nuclear reactor. Moreover, the chief components of the spectrum of cobalt-60 are two gamma rays, of 1.17 and 1.31 million electron-volts. Consequently, by the use of cobalt-60, problems of handling the source of radiation are minimized, and a radiation of nearly uniform energy is obtained. Experimental data can then be correlated more surely with the effects of radiation.

In the following work there is presented first a brief description of some exploratory work done in an effort to discover some reactions of potential industrial usefulness which would be accelerated significantly by gamma radiation. There are then presented the results of the principal program of research followed, the polymerization of ethylene by means of gamma radiation.

## APPARATUS

### General Description

In the section on Preliminary Investigations references are made to the various pieces of apparatus used in those investigations. Most of the equipment was of standard design and presented no unusual features. However, for the conduct of the experiments under pressure, it was necessary to design and build a vessel which would permit the use of elevated pressures and temperatures for the reacting system while in close proximity to a source of gamma radiation. The description of apparatus will be limited chiefly to an explanation of the design of this pressure equipment.

### Design and Construction of a Pressure Reactor

Design Conditions. A special reactor was designed and constructed for the purpose of holding chemical systems simultaneously under pressure and in the presence of gamma radiation. Design conditions chosen were 2000 psi at 650°F. Details are shown in Fig. 1. The rate of absorption of gamma radiation of a given intensity may be considered proportional to the density of the gases within the vessel, and the density may be considered approximately proportional to the pressure. Therefore it is evident that pressures of 2000 psi will permit absorption in a perfect gas at about 130 times the rate at 1 atmosphere, neglecting absorption of radiation by the walls of the container. The use of a maximum pressure of 2000 psi permitted the use of gas cylinder pressure and minimized the need for a compressor.

It was decided that the use of pressure in proximity to the source of radiation need cause no unusual concern. It was not clear just how to define a maximum permissible temperature of operation, however. One



criterion was that sufficient clearance be allowed between the bomb and the source in order that thermal expansion would not cause the bomb to stick inside the source. The other criterion was that the temperature should not be so high that the aluminum jacketing around the cobalt would be weakened or that the air between the cobalt and the aluminum would reach a pressure high enough to cause a break in the aluminum jacket. A tentative upper limit in temperature of 575°F was set for the jacket surrounding the source.

It was necessary for the reactor to be inserted into an access hole 1-1/2 inches in diameter in a shielding block of lead (see Figs. 26 and 27) in order for the vessel to be exposed to the gamma radiation. The thickness of the walls of the vessel was kept to a minimum in order to make a maximum amount of working space available within the bomb and also to allow a maximum amount of gamma radiation to pass through to the contents.

For the use of the pressure vessel in the 1-kilocurie source, which has no auxiliary shielding, the effect of the pressure vessel on personnel shielding requirements had to be investigated. Measurements of dose rate surrounding the source indicated that no perceptible horizontal scatter was caused by a model of the bomb. Measurements made after the subsequent completion of the bomb showed the same result.

Materials of Construction. AISI 304 stainless steel was chosen as the material of construction for the body, head, and flanges of the bomb. This material would resist corrosion by many chemicals and would permit higher stresses and therefore thinner walls in the body than would carbon steel. An 18-8 austenitic steel was also desired so that chilling in dry ice would be permissible without going below the transition temperature of the steel.

The bolt studs and nuts for assembling the bomb are shown in Fig. 3. The bolt studs are of ASTM A-193. The nuts were cut from AISI 304

plate, with the transverse plane of each nut parallel to the flat direction of the plate. The plates were faced down sufficiently to remove all surface blemishes.

The flanges for the bomb were cut according to the same specifications as the nuts.

Usually the reactant materials were charged to the bomb and the product materials were removed from the bomb through the tubing assembly shown in Fig. 3. AISI 304 seamless steel tubing was used. Ermeto fittings, manufactured by the Weatherhead Corporation, were used for all connections except to the bomb and to the gauge. It was desired to avoid pipe threads at these latter two points, and consequently Fixed Nitrogen Research<sup>23</sup> metal-to metal joints were employed. In Fig. 8 are shown the details of a special fitting employed to connect a pressure gauge having an iron-pipe-size thread to a cone joint fitting. The pressure gauge fitting was machined out to provide a cone seat to match the standard cone on the end of the tubing. This kind of joint was used to provide a better seal than was thought to be possible by the use of tapered pipe threads. The assembly of tubing and fittings was originally constructed using aluminum tubing except for the cone joints. The aluminum was found to be too easily bent, and was replaced with the stainless-steel tubing. The bends shown were made cold.

Design of Component Parts. Seamless tubing was selected for the body, and it was decided to weld the bottom-end-closure to the body. This procedure was adopted in order to avoid machining a long thin-walled vessel from solid stock. A section with screw threads was to be machined from solid stock and welded to the top of the seamless tubing for the body section. The body flange was to be secured by screw threads in order to avoid welding the flange section to the much thinner body section.

A tongue-and-groove joint was used between the body and the head. The tongue was machined on the body, the walls of which were too thin to receive the groove.

The design of the head presented special problems, since the flanges were to fit within the existing opening in the vault. This opening was only 4-1/2 inches in diameter. Therefore the bolt circle was made as small as possible, both in order to fit within the vault and to prevent undue stress and deflection of the flanges. The flanges were particularly subject to deflection, having been made thin in order to keep the joint between body and head as far within the access hole as possible and thereby to reduce scatter of the primary beam of radiation into a horizontal plane. Although the bolt circle had to be as small as possible because of radiation shielding requirements, the head of the bomb had to accommodate numerous connections, namely, two electrical power leads, four thermocouple leads, an entrance line, an exit line, a pressure gauge, and a rupture disc. There was barely room to accommodate two 1/4-inch holes inside the gasket circle of the head. Space for all these required connections was obtained by using a piece of round bar for the head and running the electrical leads in through the exit opening and the thermocouple leads in through the entrance opening. These electrical fittings were sealed by means of Fixed Nitrogen Research<sup>23</sup> cone joint fittings using "Teflon" cones in holes drilled into the side of the head and intercepting the respective process holes, which were drilled longitudinally through the head. The pressure gauge and rupture disc were placed on the external tubing lines. A single-jacketed copper-clad asbestos gasket of standard size was selected for use in the head-to-body joint. These gaskets are manufactured by Goetze Gasket Division of the Johns-Manville Corporation.

Welding and Inspection of Welds. The three welded joints were welded initially using AISI 309 rod of 1/8-inch diameter at 80 amperes. The surface finish of these welds was exceptionally smooth. Some positive-print x-ray photographs of these welds appear in Figs. 13 and 15. All three joints were rejected because of regions of low density such as those shown. The joints were all cut open. Each joint contained a black material resembling slag in the regions shown by the photographs to be of low density. The joints were refaced and rewelded, using AISI 347 rod of 1/8-inch diameter at 110 amperes. Some undercutting resulted, and the exteriors of the welds appeared somewhat rough. Some positive-print x-rays of the second welds appear in Figs. 14 and 16. These welds were all accepted. Some light spots appear in the head-to-flange weld, but these could be accounted for almost entirely by the surface roughness due to undercutting.

Installation of Electrical Circuits. In Fig. 4. appears a supplementary section through the head of the bomb, showing the method of assembling the electrical connections. The installation of the power leads was accomplished by first threading a bare copper wire into the top hole and out of the bottom of the vertical hole. The wire was pulled tight to give a nearly square corner at the turn in order to assist in keeping the wire centered in the hole. The two-hole ceramic spaghetti insulation was inserted over the wire in the space between the horizontal outlets. Then a bare wire was inserted in the same manner through the lower horizontal hole. The lower ceramic spaghetti insulation was added; then the one-hole ceramic spaghetti was inserted into the horizontal holes. The circuits were checked for continuity and grounds, and then the pressure seals were assembled.

The installation of the thermocouple leads was accomplished in a similar manner. These leads were more easily threaded through the holes than were the copper wires and also carried their own insulation. The

insulation of the thermocouple leads consisted of a silicone varnish applied directly to each lead and a braided glass fabric which covered both leads. This type of thermocouple lead was a Leeds and Northrup product.

It was discovered that if the glass braid was removed from the assembly for several inches and the two wires threaded together, through the 0.040-inch hole in the "Teflon" cone, a seal could be made which would retain 2000 psig. This result was unexpected, since it was thought originally that a separate sealing cone would be required for each wire, and that the wire would have to be scraped to bare metal. After the "Teflon" cones had once been seated by the retaining nut, they were difficult to extract from their seats. It was found that if the wires were pulled out, wood screws could be driven into the wire hole, and the plug extracted by pulling on the screw. The hole would be much enlarged, but re-application of pressure by the retaining nut would re-form the "Teflon" about a wire and permit a usable seal. Often, however, the cone would be ruined in extracting it in this manner.

The thermocouples used were formed by welding matched chromel P-alumel wires in an oxygen-gas flame. Brazing flux was applied molten before the twisted couples were heated.

#### Hydrostatic Test of the Reactor

After the reactor was completed and before it was placed in regular service, it was given a hydrostatic test at 2800 psig. The electrical outlets were plugged with short stubs of wire during the hydrostatic tests. The test pressure was maintained for about one hour. All joints were then hammered with a soft-faced hammer while a pressure of 2000 psig was maintained.

After the initial welding was completed a hydrostatic test conducted as described above revealed the presence of a pin-hole leak at the location shown in the x-ray of Figs. 12 and 13.

After the second welding was completed, a hydrostatic test was conducted as indicated above. No diminution of pressure and no visible leaks occurred. An x-ray of the location after rewelding was completed appears in Fig. 14.

### Operation of the Reactor

The flanges of the reactor were tightened to the same clearance all around, with a tolerance of  $\pm 0.001$  inch measured directly opposite the bolt studs. A clearance of 0.120 inch to 0.150 inch was found to be satisfactory. The nuts were tightened to about 250 inch-pounds of torque.

Some difficulty was experienced in inserting the body of the bomb into the vault. An external diameter of 1.480 inches was specified for the bomb, and this should have been sufficiently small to clear the inside of the vault opening which was supposed to be 1-1/2 inches in diameter (see Figs. 26 and 27). The bomb would enter the hole freely for about 10 inches and then stop. In order to investigate this situation a special gauge was fabricated (see Figs. 5 and 7). The gauge was a piece of 1-1/2-inch-outside-diameter cold-rolled steel bar with a handle permitting remote manipulation over the open source. The bar was originally 1.499 to 1.500 inches O.D. This diameter permitted the bar to be inserted 12-1/4 inches. The bar was turned to 1.490 inches and could then be inserted 14-1/4 inches. The diameter was reduced by 0.010-inch increments to 1.470 inches, at which dimension it would go in 22-1/4 inches. Then it was finally turned to 1.465 inches, which dimension permitted the gauge to go in the full

24-1/8 inches with a minimum clearance of 0.005 inch on the diameter. The body of the bomb was then turned to 1.465 inches O.D., and fitted into the vault satisfactorily.

A steel rack was designed and built for the purpose of positioning the stainless-steel reactor approximately symmetrically with respect to the 10-kilocurie source (see Figs. 17 and 23 for details). Extension legs (Fig. 19) permit use of the rack to hold the reactor on the axis of the source. The steel rack was designed to accommodate the sling (Figs. 18 and 23) previously constructed for the purpose of supporting the reactor with its attached tubing in the 1-kilocurie source.





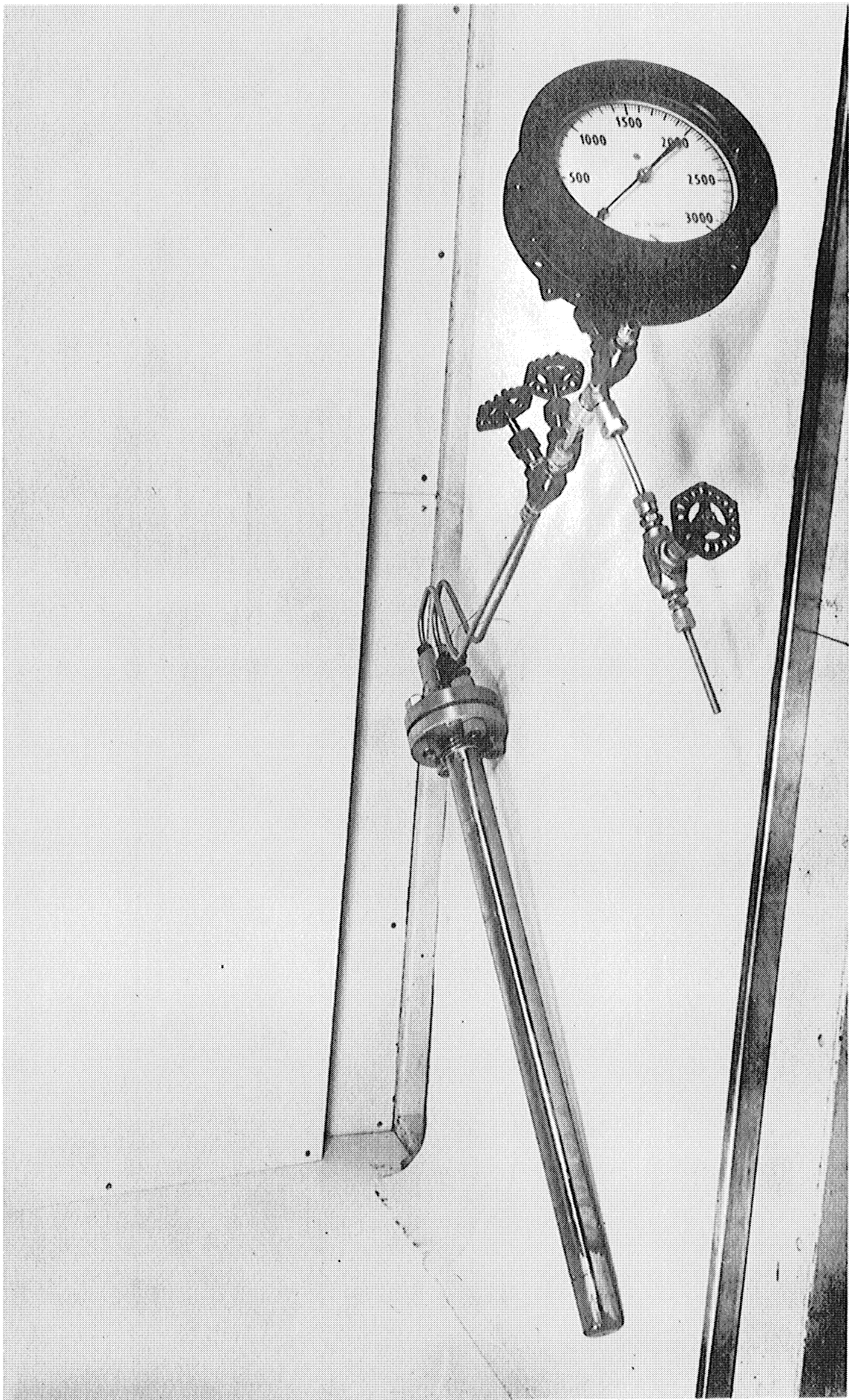


Fig. 2. Pressure Reactor and Auxiliary Fittings.

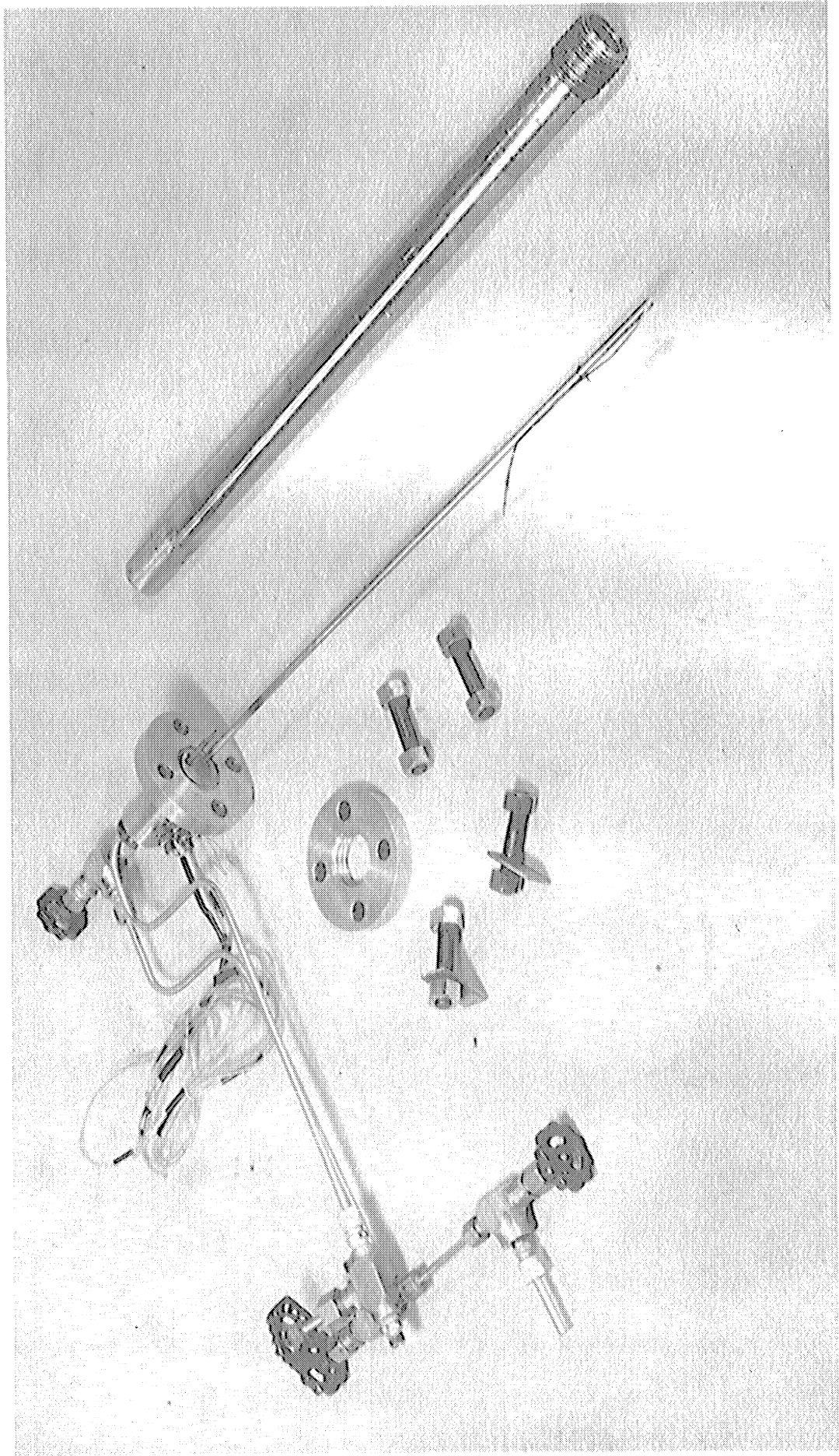
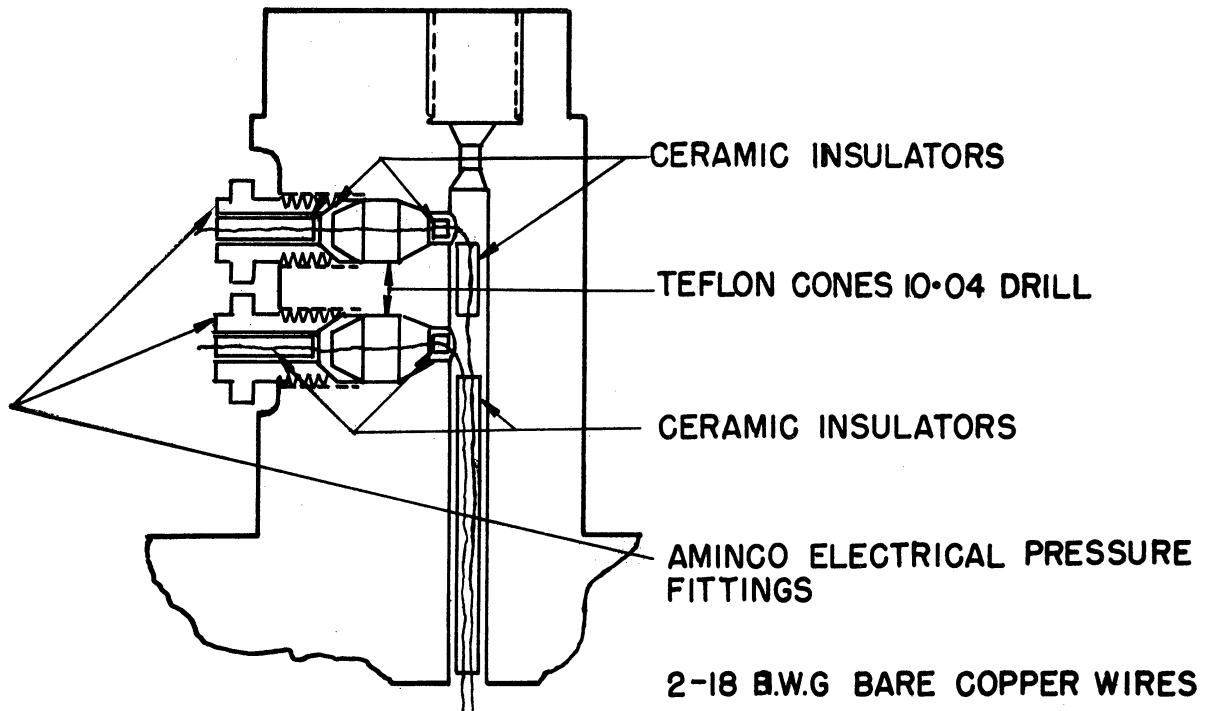
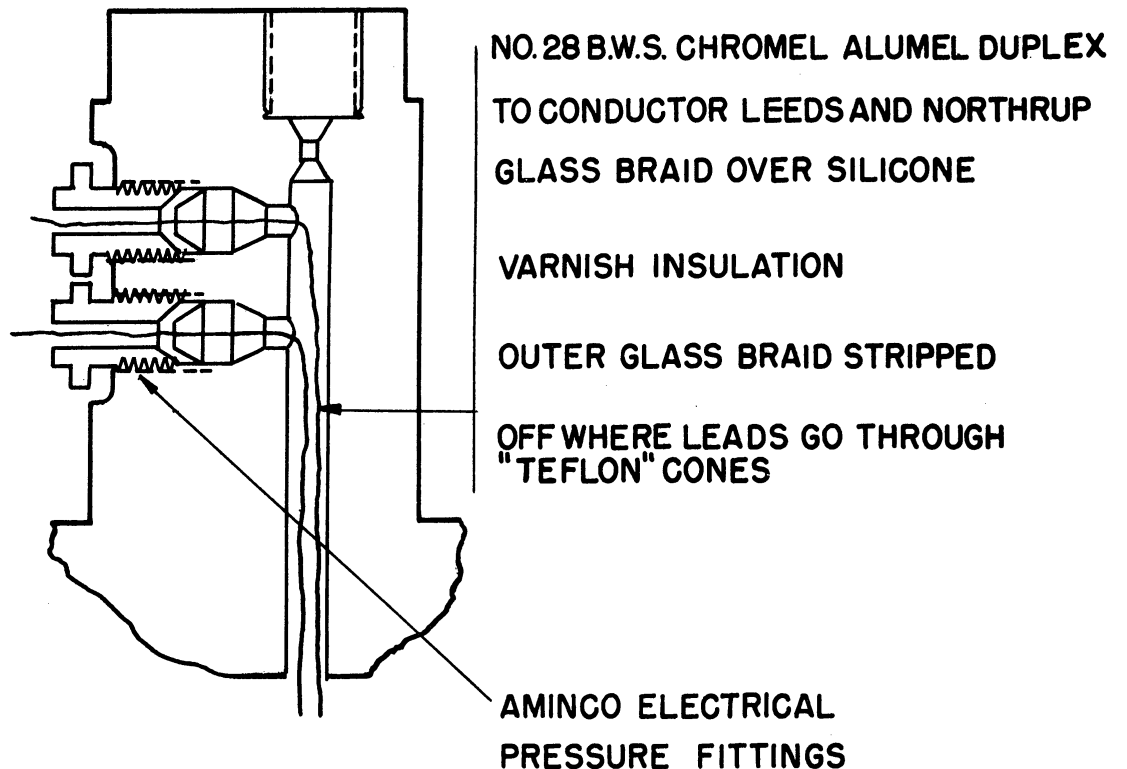


Fig. 3. Pressure Reactor Disassembled.



INSTALLATION AT  
POWER LEADS



INSTALLATION AT  
THERMOCOUPLES

Fig. 4. Electrical Connections of Pressure Reactor.

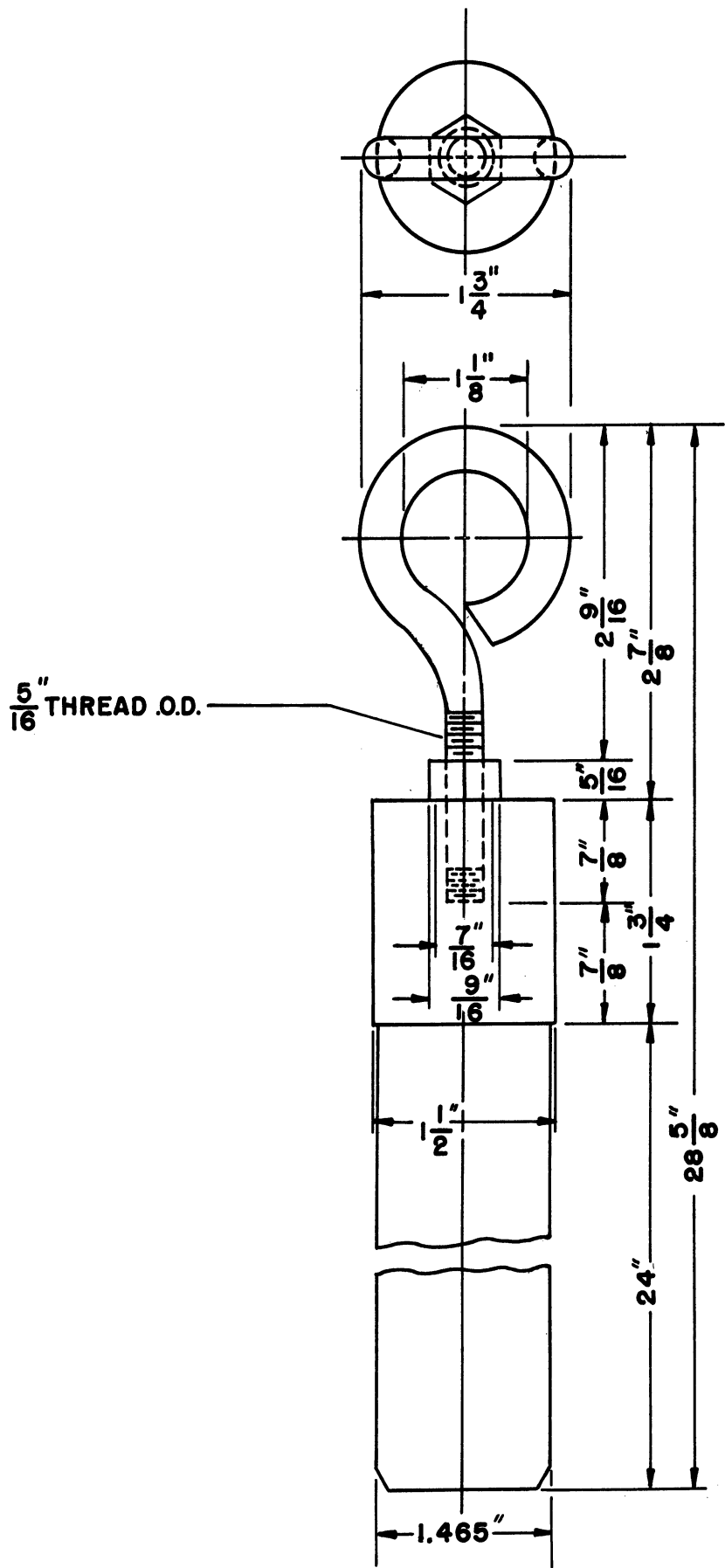


Fig. 5. Drawing of Plug Gauge.

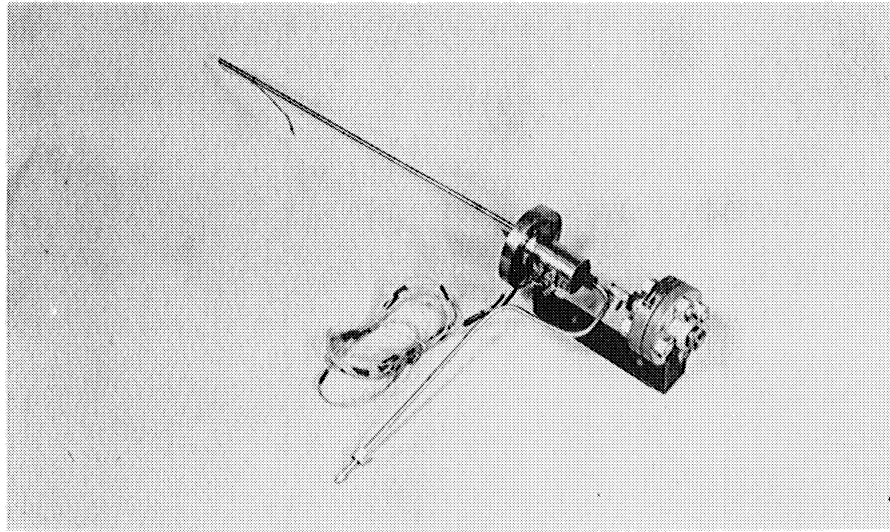


Fig. 6. Pressure Reactor with 150-psi Rupture Disc.

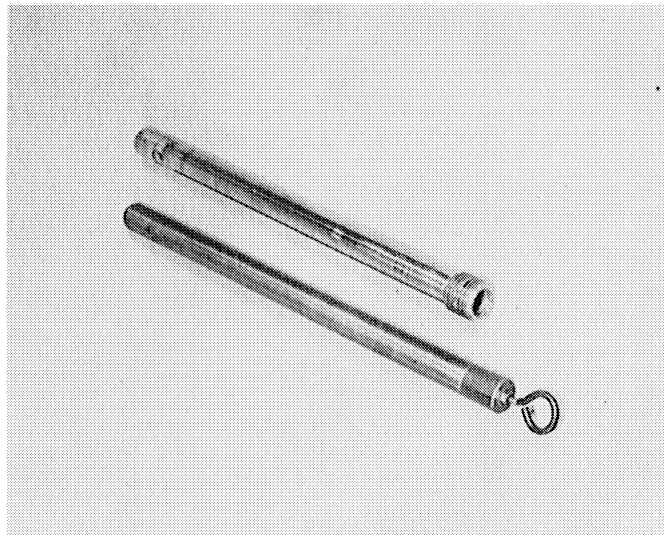


Fig. 7. Plug Gauge and Body of Reactor.

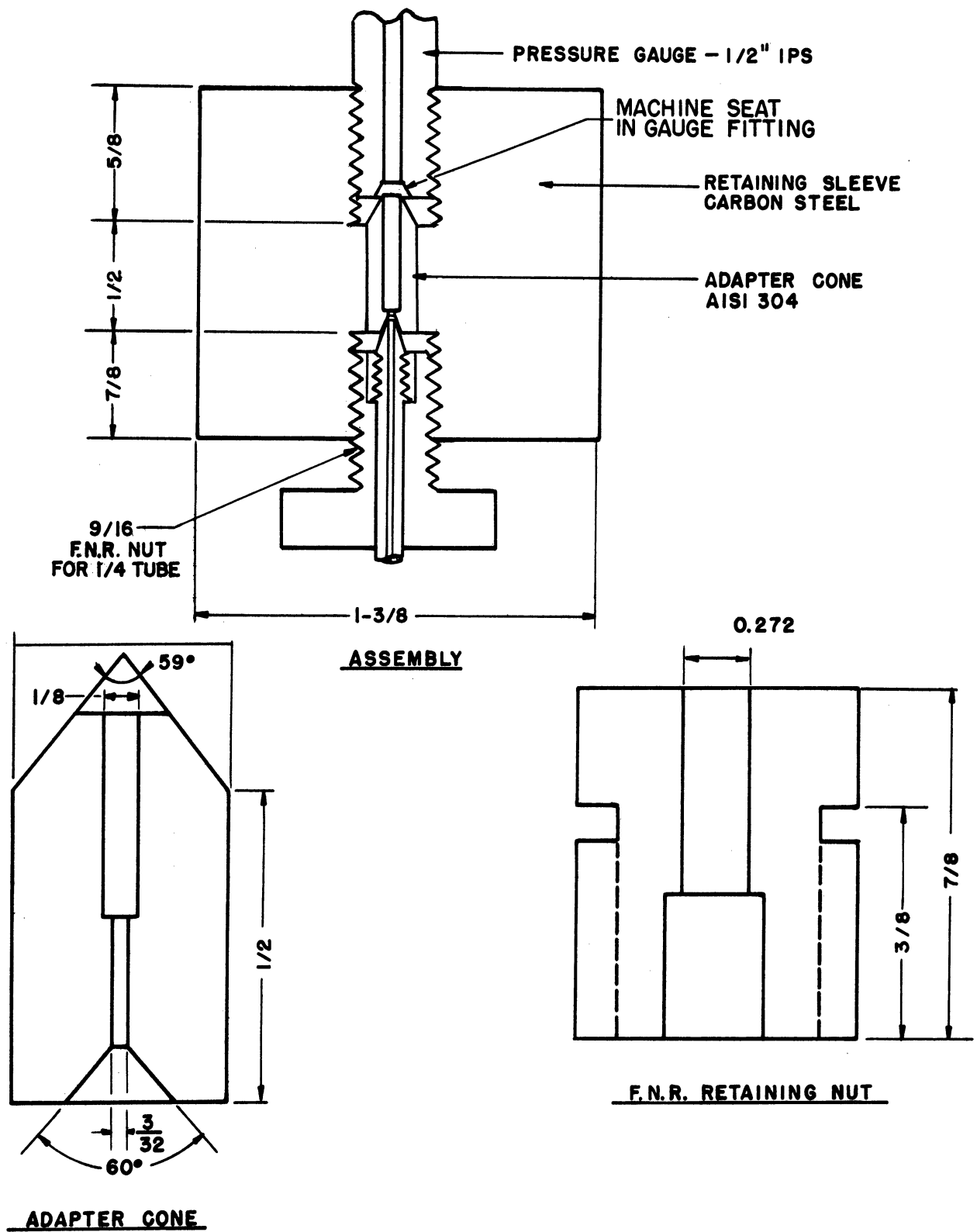
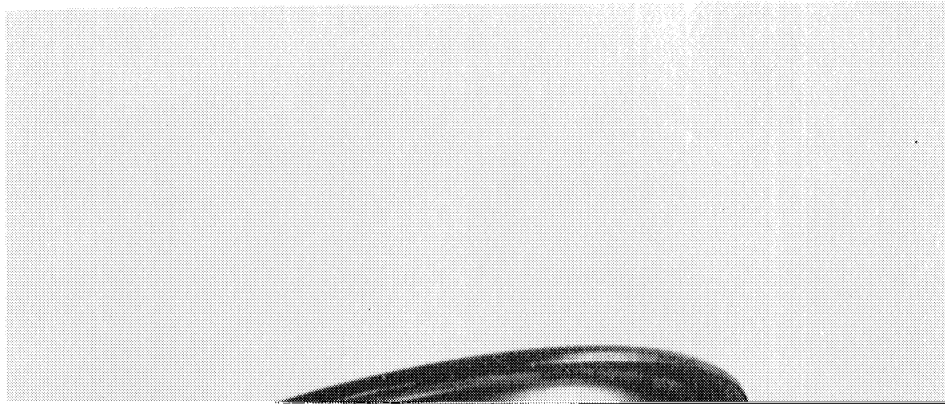
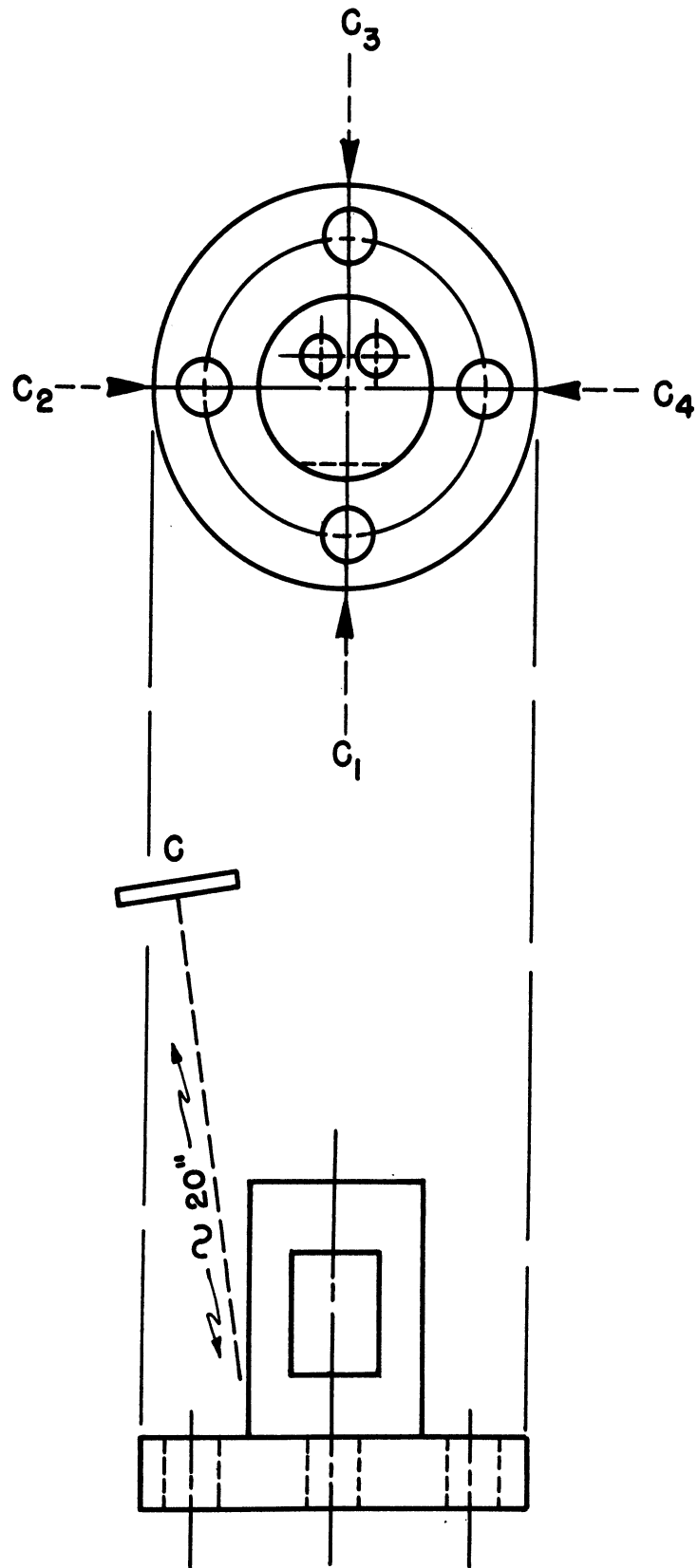


Fig. 8. Adapter Fitting: Cone Joint to Iron Pipe Thread.



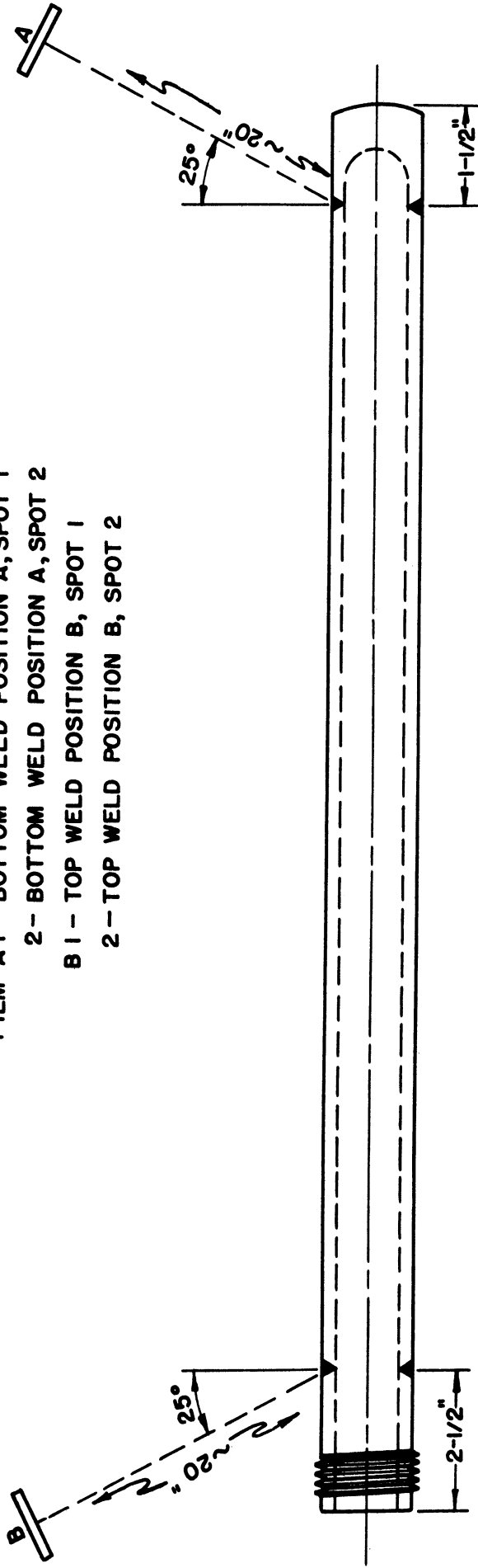


150 KVP, 5MA., 10MIN., DUPONT 506 FILM

Fig. 10. Pressure Reactor: X-rays of First Welds Showing Locations at Head.



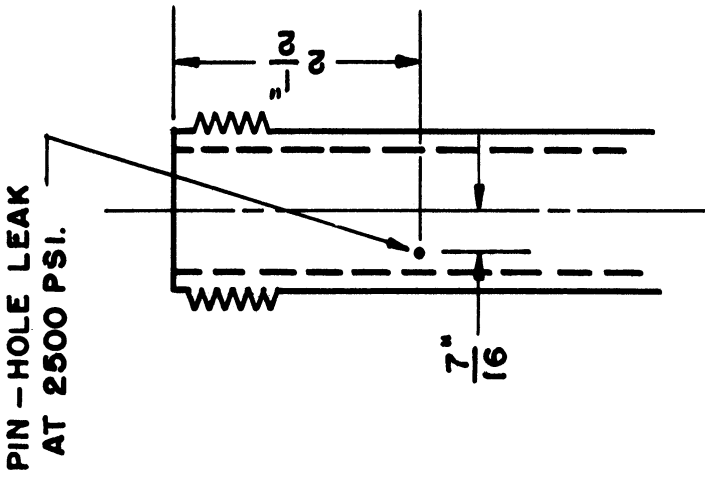
FILM A 1 - BOTTOM WELD POSITION A, SPOT 1  
 2 - BOTTOM WELD POSITION A, SPOT 2  
 B 1 - TOP WELD POSITION B, SPOT 1  
 2 - TOP WELD POSITION B, SPOT 2



SPOT 2 90° AROUND VESSEL FROM 1, MARKED ON MASKING TAPE  
 150 KVP, 5MA., 4 MIN., DUPONT 506 FILM

Fig. 11. Pressure Reactor: X-rays of First Welds Showing Locations at Body.

150 KVP, 5MA., DUPONT 506 FILM



B-2 POSITION

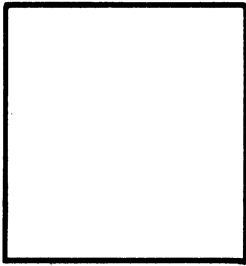


PHOTO # 1

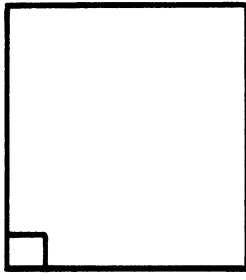
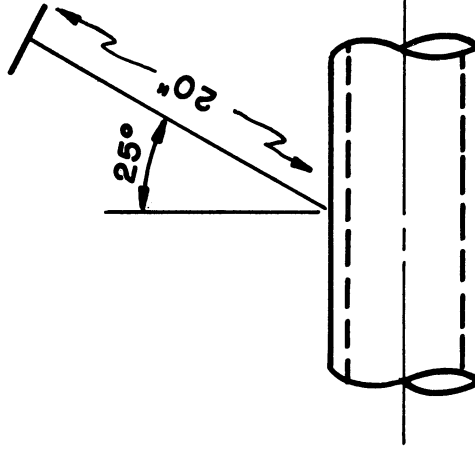
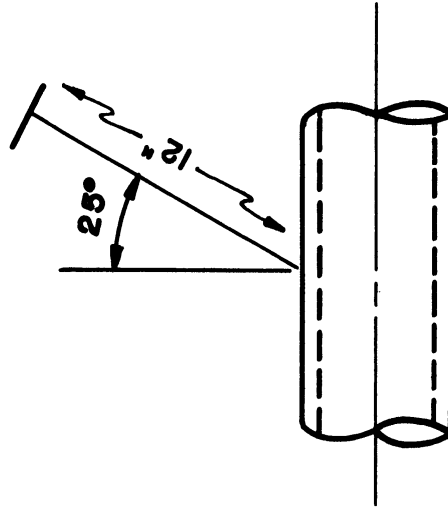


PHOTO # 2  
(CUT CORNER)



EXPOSURE O.K.  
FOR VIEW # 2



BOTH VIEWS ON SAME FILM - VIEW  
# 2 ON CUT CORNER  
FILMS OVEREXPOSED

Fig. 12. Pressure Reactor: X-rays of Second Welds Showing Locations.

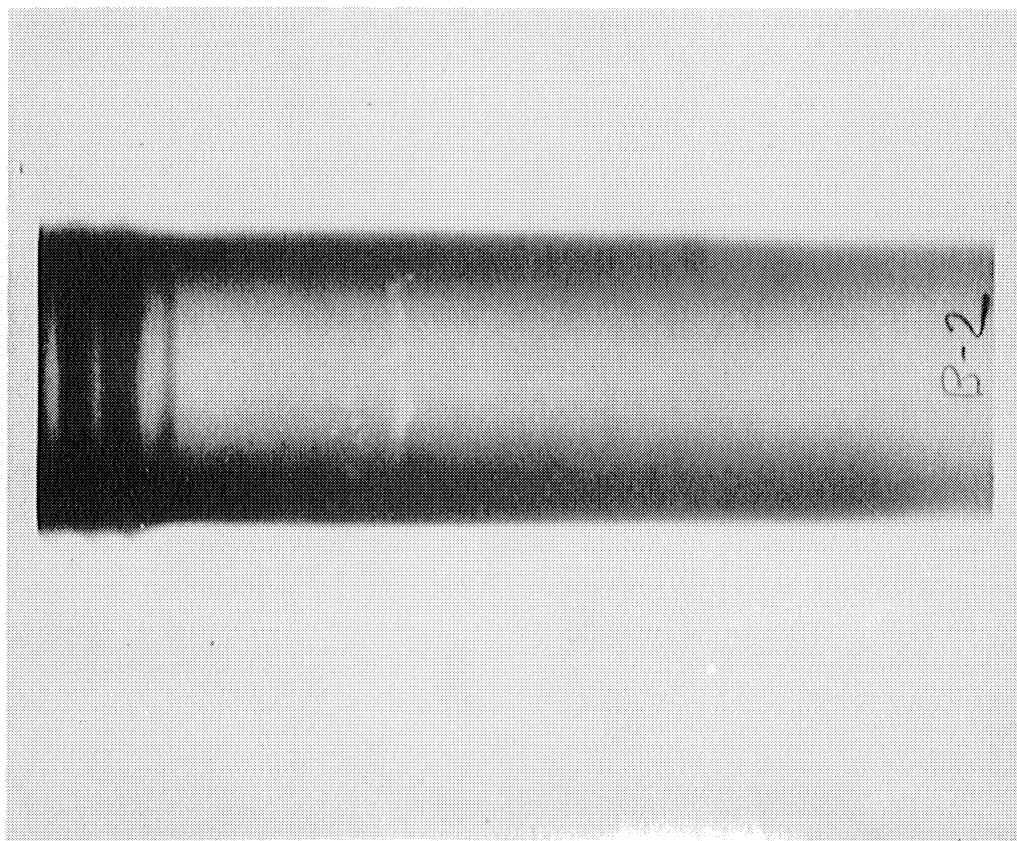


Fig. 13. X-ray B-2: Weld in Upper Body -  
First Attempt.

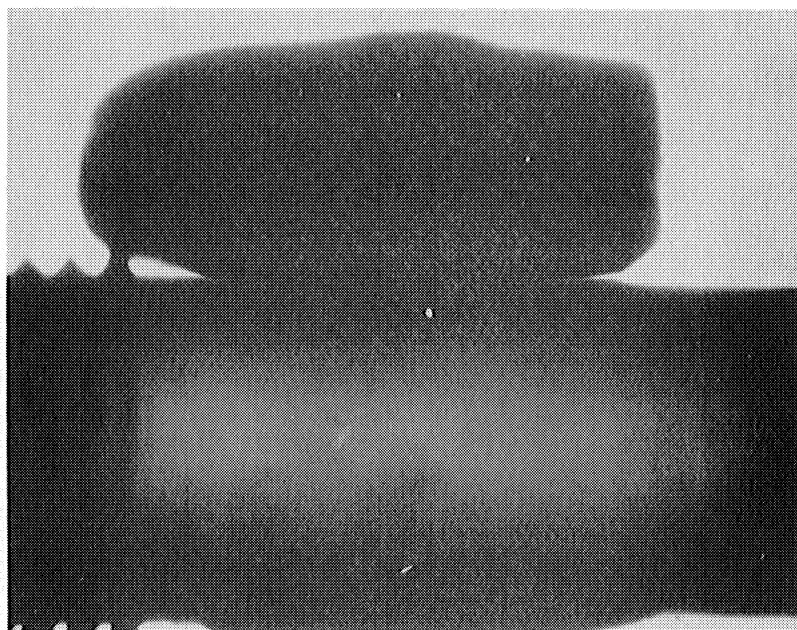


Fig. 14. X-ray of Weld in Upper Body -  
Second Attempt.

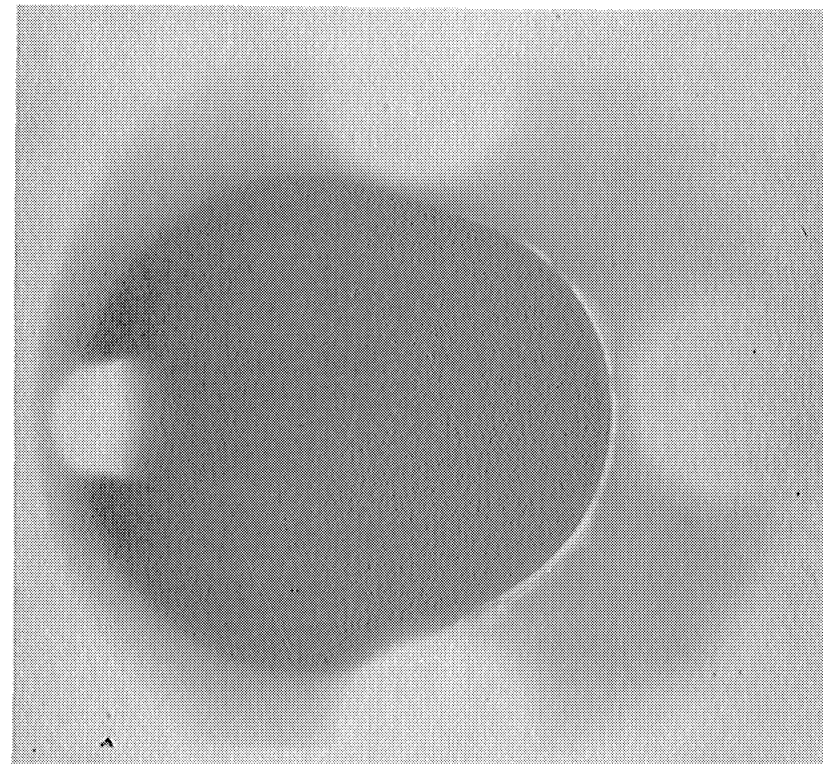


Fig. 15. X-ray C-3: Weld at Head -  
First Attempt.

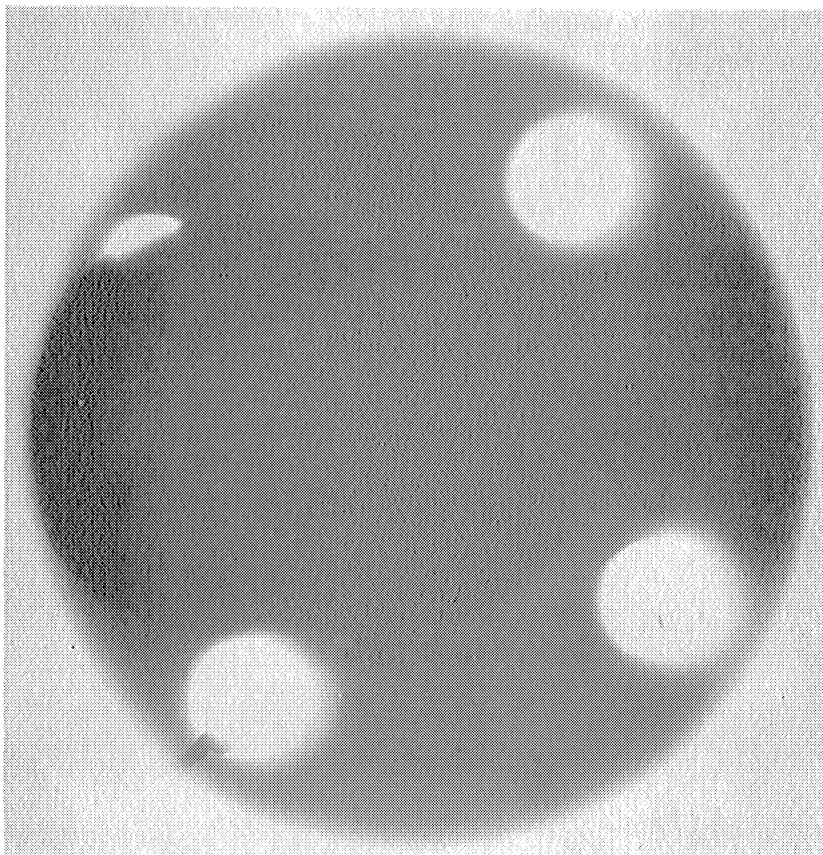
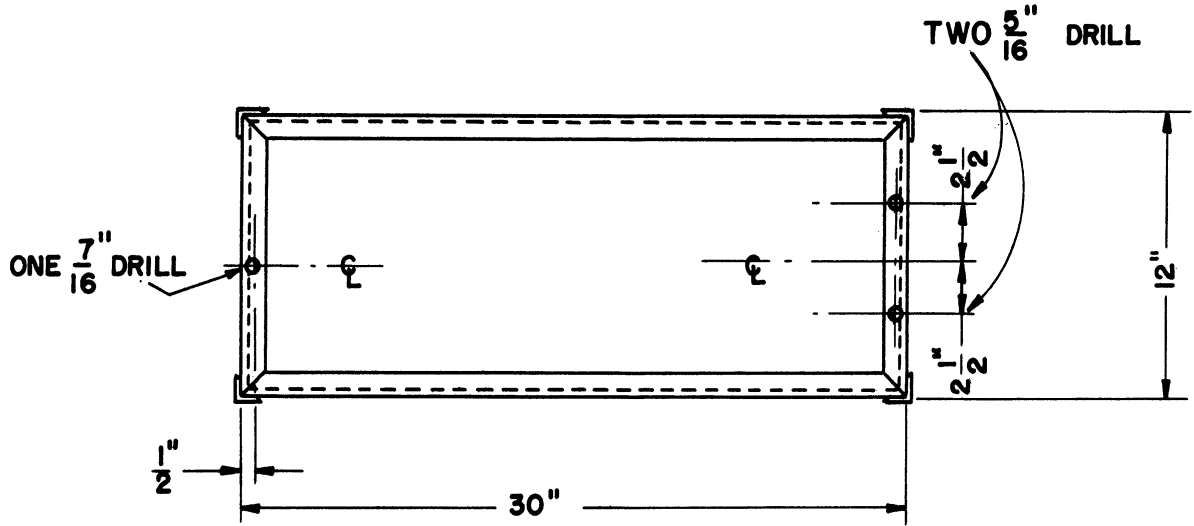
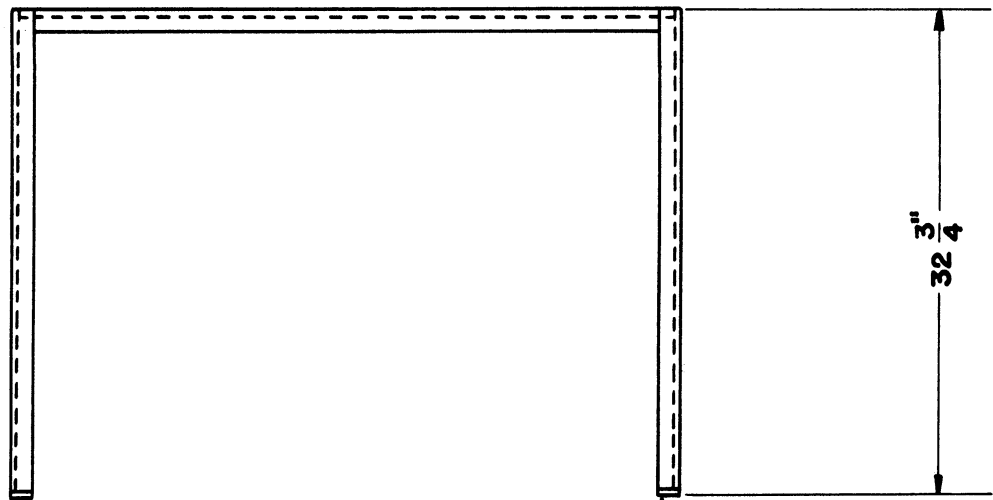


Fig. 16. X-ray of Weld at Head -  
Second Attempt.

SCALE  $1\frac{1}{2}'' = 1'-0''$



PLAN



WELD ON BASE PLATES  $\frac{1}{4}''$  THICK  
DRILL - HOLES FOR  $\frac{1}{4}''$  BOLTS

ELEVATION

Fig. 17. Pressure Reactor: Drawing of Rack.

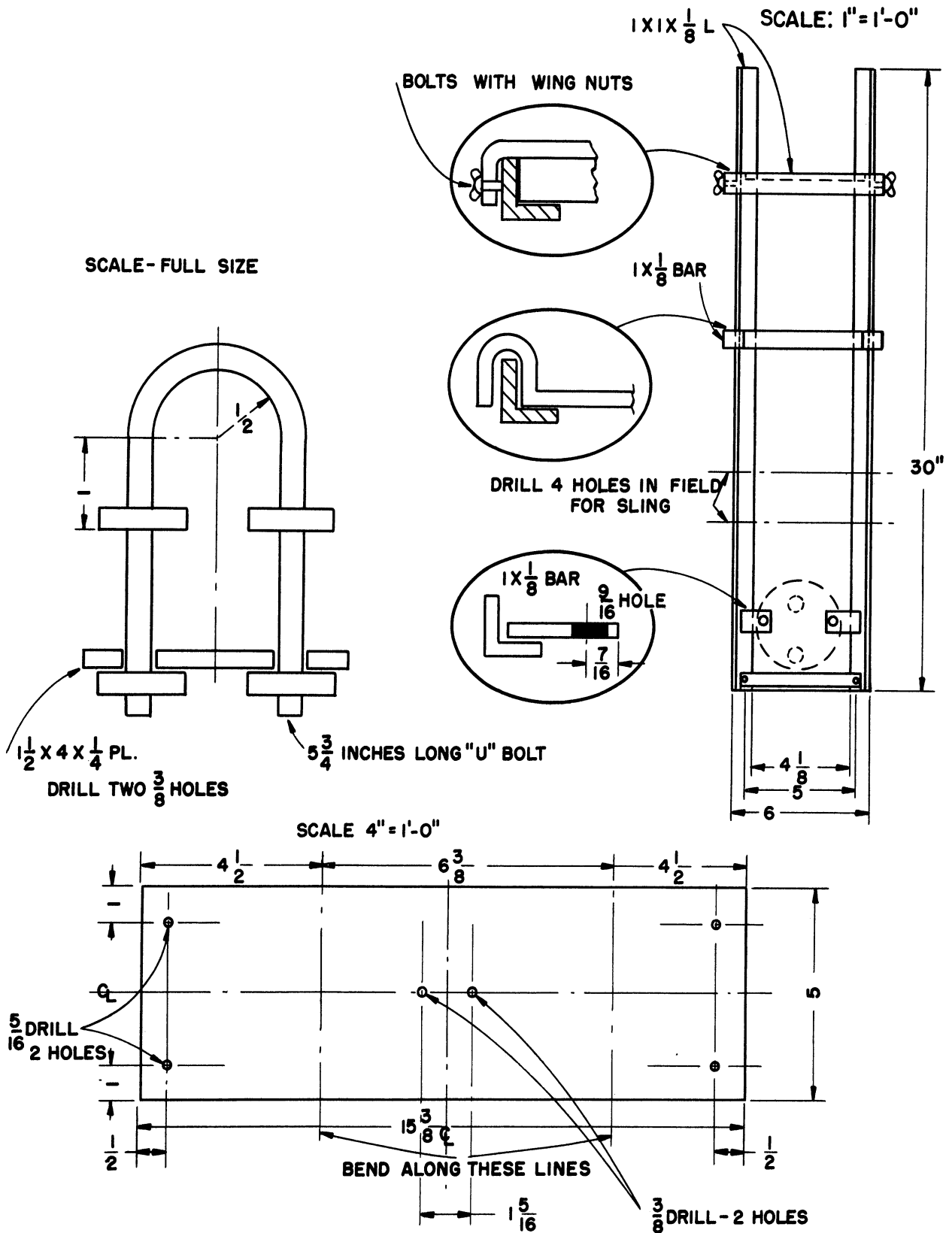


Fig. 18. Pressure Reactor: Drawing of Sling.

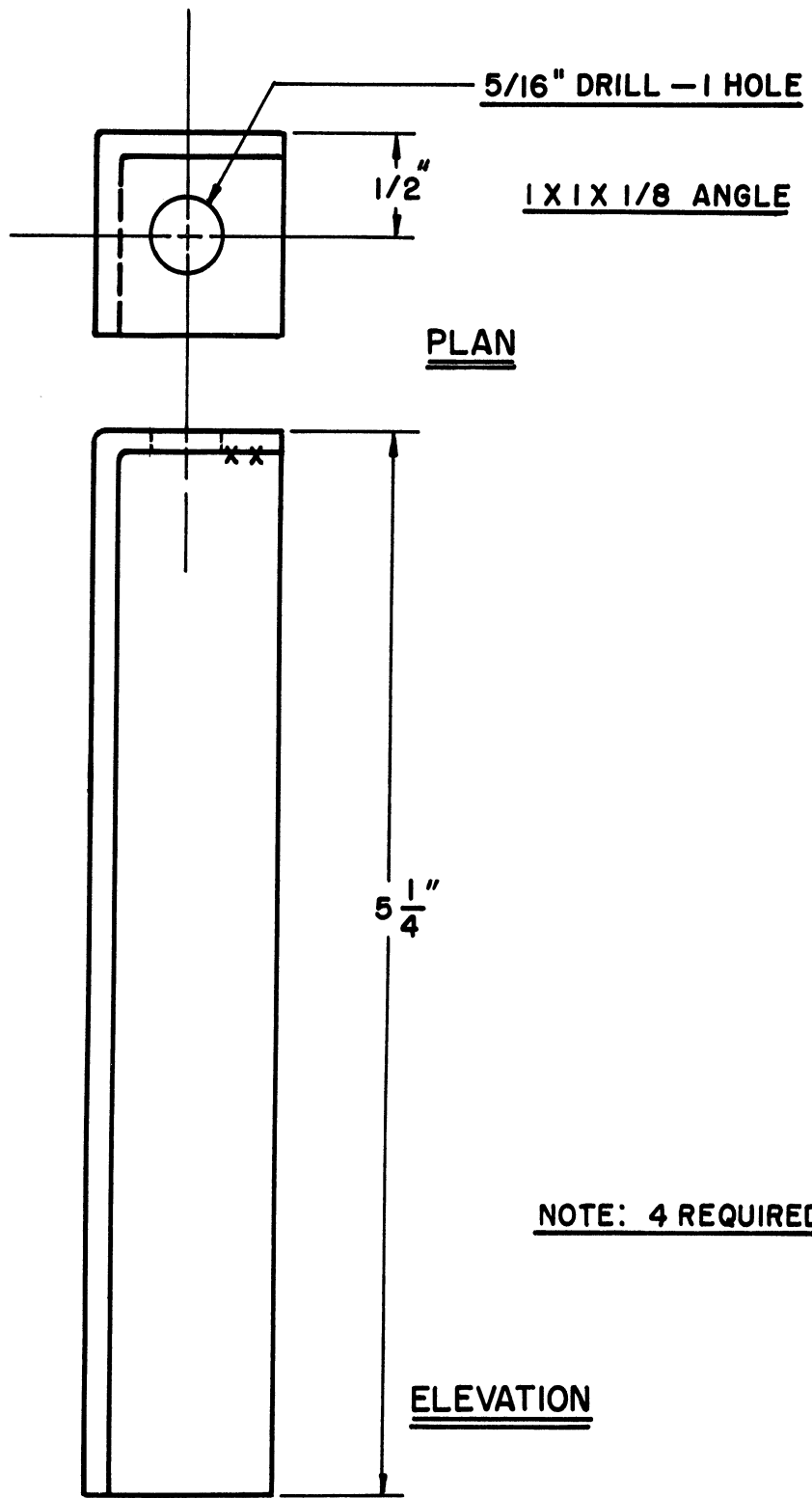


Fig. 19. Extension Legs for Rack.



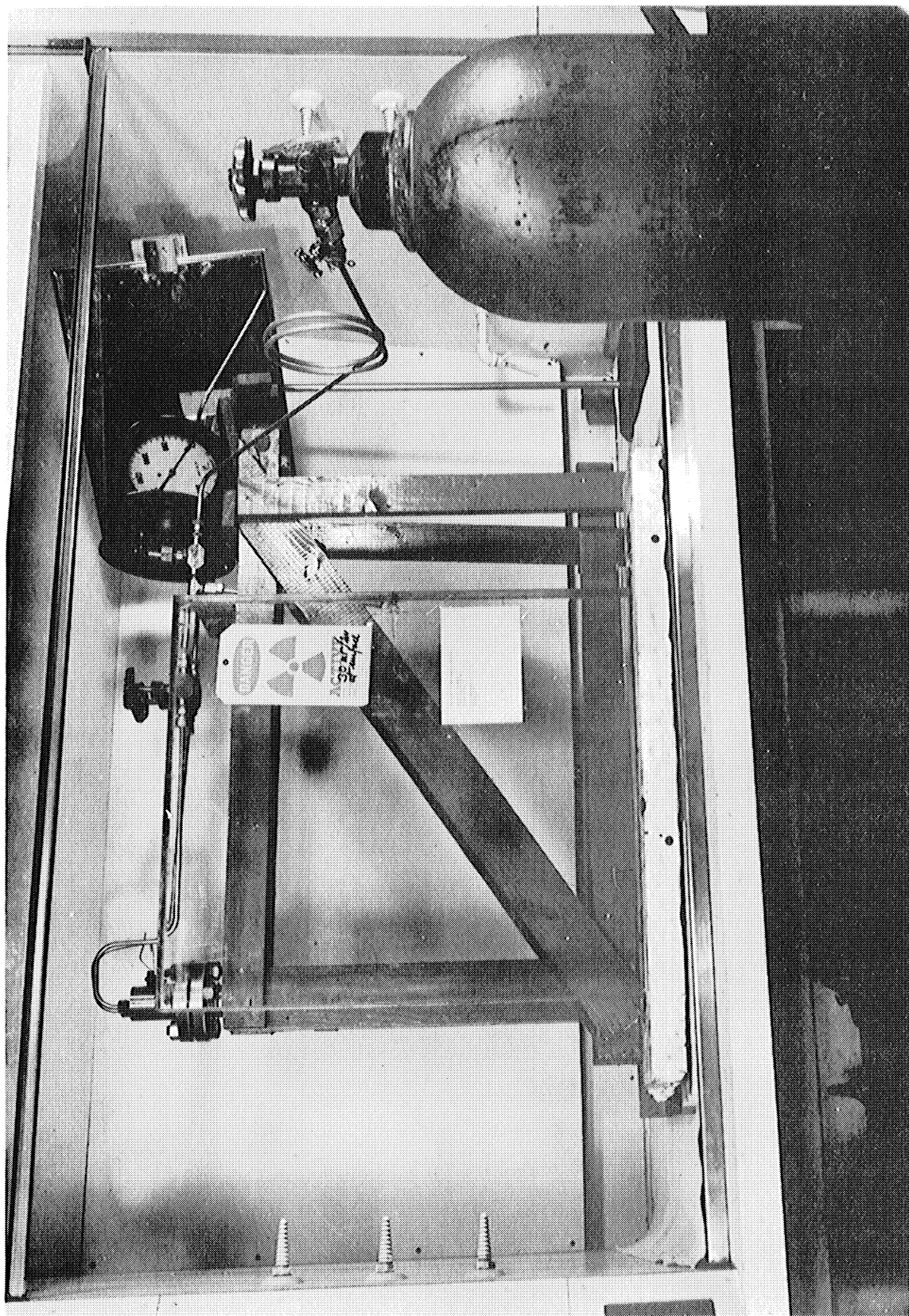


Fig. 20. Pressure Reactor Behind Lucite Shield for Palladium-109 Experiments.



ANALYSIS OF DOSE RATES NEAR HOLLOW  
CYLINDRICAL SOURCES OF GAMMA RADIATION

It was proposed to examine some effects of gamma radiation on the rate of polymerization of ethylene. For this purpose it was necessary to adopt some criterion of the effect of gamma radiation on matter. In the following treatment the rate of ionization produced in air has been used as a measure of the effect of gamma radiation. The units used are the roentgen for air subjected to electromagnetic radiation and the roentgen equivalent physical (rep) for tissue subjected to electromagnetic or to charged-particle radiation. Siri<sup>49</sup> has discussed these units. The roentgen corresponds to the absorption of about 83 ergs per gram of air, while the rep corresponds to the absorption of 93 ergs per gram of water<sup>58</sup>, and is often used to report doses for other aggregations of matter as well.

There is some evidence that the rate of reaction in a given chemical system subjected to ionizing radiation is proportional to the rate of ionization produced in that system. Lind<sup>36</sup> used an equation developed by Mund<sup>44</sup> to calculate the rate of ionization produced in a given chemical system subjected to alpha radiation. Lind found that in many systems the yield of a given reaction produced by alpha radiation alone was proportional to the ionization as calculated by Mund's equation. Lind developed the concept of the "ion yield", i.e., the ratio of molecules of product secured to ion pairs produced in the system, which he denoted as "M/N". He found that values of M/N were nearly constant for a given system and were nearly equal for many systems. Values of M/N appeared usually to range from 1 to 2, but there were a few cases in which the value was much in excess of

unity. Allen<sup>1</sup> pointed out that the observed M/N should be constant for most systems at small degrees of reaction, but should decrease to 0 at equilibrium.

The rate of ionization caused by the passage of gamma radiation through matter is a common measure of the intensity of this radiation. As seen above, the rate of ionization has been found by other workers to govern the rate of chemical reactions under some conditions. Consequently, we now wish to develop a means of predicting the rate of ionization caused by gamma rays as a function of the position of the receiving point and the geometrical configuration and composition of the source. Such a measure of the rate of ionization is known as the "dose rate" in the matter, caused by the radiation.

#### Experimental Procedure

Dose rates were measured chemically by Harmer<sup>9</sup> by the method employing the oxidation of ferrous sulfate solutions. Dilute solutions of ferrous sulfate ( $5 \times 10^{-4}$  M) in aerated 0.8 N sulfuric acid solution were exposed to gamma radiation for doses of between 5 and 20 kilorep. The ferric ion produced by the gamma radiation depends on the presence of a small amount of oxygen which is furnished by first passing air through the solution. For quantitative determinations of the ferric ion produced by irradiation, the spectrophotometric method described by J. Weiss of Brookhaven National Laboratory was employed<sup>58</sup>. This method makes use of a spectral absorption peak of ferric ion at about 304 millimicrons in the ultraviolet region. Optical densities of the irradiated solutions are measured at 305 millimicrons and compared with those of known ferric solutions made up by dilution of standardized ferric stock solution.

In converting the chemical yield to radiation dosage, a value of 15.4 micromoles per liter per kilorep was used. This value is based on the absorption of 93 ergs/gm of water for each equivalent roentgen of radiation. The solutions were irradiated in glass bottles about 3 cm in inside diameter and filled to a depth of about 4 cm.

The bottles of solution were placed inside and outside the 10-kilocurie source, as shown in Figs. 37 and 38, and were placed inside the 1-kilocurie source. (See Table I and Fig. 26.) Proper exposure times were calculated to fall within the range of the method of ferric-ion determination. Measurement of dose rate in the 1-kilocurie source was carried out at times separated by an interval of 1 year, and values were found to be consistent after corrections for radioactive decay were applied. Measurements using a ceric sulfate system were also made and found to agree within experimental error with the ferrous sulfate results.

Physical determinations of dose rate have also been carried out by Nehemias<sup>9</sup> on both sources. Two instruments have been employed in these determinations: The first was a Victoreen roentgen ratemeter, which measures the current flow between electrodes in an ionization chamber placed in the radiation field. The second was a Victoreen r-meter, which measures the drop in potential of a charged condenser due to ionization current caused by the radiation. The ratemeter was calibrated against radium standards by the manufacturer, while the r-meter was calibrated against a cobalt standard at the University of Michigan.

Within 50 cm of the center of the 10-kilocurie source the ratemeter readings were 15 to 20 percent lower than the ferrous sulfate determinations. The r-meter readings were 15 to 20 percent higher than the ferrous sulfate measurements in the 10-kilocurie source, and were 25 to

TABLE I

IRRADIATION OF FERROUS SULFATE SOLUTIONS  
IN COBALT-60 SOURCE - DOSIMETRY BY METHOD OF WEISS<sup>58</sup>

Data From 10-Kilocurie Source Unless Noted

Sample Number	Dose Rate kilorep/hr	Sample Number	Dose Rate kilorep/hr
1	280	1	144
2	250	2	194
3	242	3	249
4	244	4	261
5	292	5	266
6	342	6	281
7	38	7	243
8	102	8	234
9	80	9	248
10	8	10	274
11	57	11	168
12	60	12	86
		13	115
		14	52
		15	24
		16	13
		17	22
		18	17
		19	74
		20	42
		21	4.4
		22	2.6
		23	2.0
		1 kilocurie	55

30 percent higher in the 1-kilocurie source. The detailed significance of these differences is not clear.

### Calculation Procedure

Since gamma radiation from a point source may be assumed to follow the usual inverse-square relation, it is possible to calculate the dose rate at any position in the neighborhood of a source of known shape and total activity by an integration technique similar to that employed in radiant heat transfer. If the configuration of the source is complicated, the resulting integration may be difficult. A hollow cylinder of negligible wall thickness is a simple shape similar to that of the two cobalt-60 sources. The activity of the actual source may be assigned to such a cylinder. The dimensions of such a cylinder were taken to correspond as nearly as possible to those of the actual source, and the assigned curies were assumed to be distributed uniformly over the surface of the cylinder. Absorption and attendant effects were neglected. Then the contribution to the radiation intensity at any given point due to an element of source area,  $dA$ , at a distance  $\rho$  away was given by Equation (1). See Fig. 31.

$$dI = \alpha \frac{dA}{\rho^2} \quad (1)$$

The total intensity at the given point was obtained by summing the contributions from all elemental areas as

$$I = \int_{Z=0}^{Z=L} 2 \int_{\theta=0}^{\theta=\pi} \frac{\alpha r d\theta dZ}{R^2 + r^2 - 2Rr \cos \theta + (Z_1 - Z)^2} \quad (2)$$

Integrating Equation (2) gives

$$I = \frac{2\alpha\pi r}{R+r} \left[ F\left(\tan^{-1} \frac{R+r}{Z_1-L}, k\right) - F\left(\tan^{-1} \frac{R+r}{Z_1}, k\right) \right]$$

$$\text{for } Z_1 > L > 0, \quad R \geq 0, \quad r > 0, \quad (3)$$

$$0 \leq \tan^{-1} \frac{R+r}{Z_1-L}, \quad \tan^{-1} \frac{R+r}{Z_1} < \frac{\pi}{2}$$

and

$$I = \frac{2\alpha\pi r}{R+r} \left\{ 2K(k) - \left[ F\left(\tan^{-1} \frac{R+r}{L-Z_1}, k\right) + F\left(\tan^{-1} \frac{R+r}{Z_1}, k\right) \right] \right\}$$

$$\text{for } L \geq Z_1 > 0, \quad R \geq 0, \quad r > 0, \quad R \neq r, \quad (4)$$

$$0 \leq \tan^{-1} \frac{R+r}{L-Z_1}, \quad \tan^{-1} \frac{R+r}{Z_1} < \frac{\pi}{2} .$$

An alternative form may be obtained as shown by Equation (5).

Dewes and Goodale<sup>19</sup> have indicated the preliminary steps in this development.

$$I = \frac{2\alpha\pi r}{R+r} \left[ F\left(\tan^{-1} \frac{Z_1}{|r-R|}, k\right) - F\left(\tan^{-1} \frac{Z_1-L}{|r-R|}, k\right) \right]$$

$$\text{for } Z_1 \geq 0, \quad R \geq 0, \quad r > 0, \quad R \neq r, \quad (5)$$

$$-\frac{\pi}{2} < \tan^{-1} \frac{Z_1-L}{|r-R|} < \frac{\pi}{2}, \quad 0 \leq \tan^{-1} \frac{Z_1}{|r-R|} < \frac{\pi}{2} .$$

A relation given by Hancock<sup>27</sup> permits the transformation of Equations (3) and (4) into Equation (5), and vice versa. Equation (5) is considered more convenient in most computations, except for  $R=r$ ,  $Z_1 > L$ , where Equation (3) may be used.

The symbols used above are defined as follows:

$I$  = dose rate, equivalent roentgens per hour.

A = area of source.

$\rho$  = distance from elemental area  $dA$  to the point at which I is taken.

$$\alpha = \left( \frac{\text{total activity, curies}}{\text{area of source, cm}^2} \right) \left( \frac{1000 \text{ millicuries}}{\text{curie}} \right) \left( \frac{\text{equiv. roentgens at 1 cm}}{(\text{hour}) (\text{millicurie point source})} \right).$$

r = radius of source, and also constant radius vector of cylinder.

R = radial distance of point at which I is taken from axis of source.

$\theta$  = central angle from R to r.

Z = distance parallel to axis of source from base of source to element  $dA$ .

$Z_1$  = A coordinate of point at which I is taken.

$$k = 2\sqrt{Rr}/R+r.$$

$F(\phi, k)$  = elliptic integral of first kind of modulus k and amplitude  $\phi$ .

$K(k)$  = complete elliptic integral of first kind of modulus k.

Self absorption of a hollow cylindrical source of finite thickness may be approximated along the axis of the source by the following procedure (see Fig. 32). It will be assumed (1) that the source is of uniform unit-volume-activity and density, (2) that absorption occurs only within the source, (3) that scattered radiation due to the absorber will not affect the dose rate, (4) that radiation intensity and dose rate vary inversely with the square of the distance from a point source and inversely with an exponential function of absorber thickness, and (5) that the part of the source lying outside the cone  $\phi = \tan^{-1} r_1/(Z_1-L)$  also fulfills the foregoing assumptions. The resulting differential equation and its approximate integration are as shown in Fig. 33, where

P = distance between point and element of volume,

$\rho$  = density, grams per  $\text{cm}^3$ ,

$\mu$  = mass absorption coefficient,  $\text{cm}^2/\text{gram}$ ,

$$V = \left( \frac{\text{total activity, curies}}{\text{volume of source, cm}^3} \right) \left( 1000 \frac{\text{millicuries}}{\text{curie}} \right) \left( \frac{\text{equiv. roentgens at 1 cm}}{\text{(hour) (millicurie point source)}} \right),$$

$dv$  = element of volume of source,

and all other terms are defined as above or in Fig. 33.

Equations (5) and (8) were applied to both the 1000- and 10,000-curie sources. In the case of the 1000-curie source, it was straightforward to assume a cylinder with dimensions corresponding to the actual cobalt cylinder. In the case of the 10,000-curie source, the nest or bundle of 100 rods was assumed equivalent to a cylinder whose inside and outside diameters were the shortest and longest diametrical distances across the rod bundle. The 10,000 curies was assumed to be uniformly distributed throughout this volume and the density of the assumed cylinder was taken so that its mass equalled that of the rods themselves.

Calculated and observed values of dose rate for the 10-kilocurie source of cobalt-60 are compared in Tables II and III and are plotted in Figs. 34 and 35. The calculated values were based on an assumed activity of 10,000 curies. The observed values are considerably less than the calculated values. For any given method of measurement the observed values are a nearly constant fraction of the calculated values. In Figs. 39, 40, and 41 appear cross-plots of Equation (5) when the latter is made to agree with data from the oxidation of ferrous ion. The data were taken on the mid-plane on the axis in March, 1953. The source was irradiated at the Chalk River NRX reactor and was rated at 9250 curies on shipment from the Chalk River site in January, 1953. The activity computed from each means of measurement appears in Table IV. In the extreme right column of Table IV there appears the ratio of the curies estimated from observed values of dose rate to the 9250-curie nominal value after correction of the



TABLE II

## DOSE RATES ON AXIS OF 10-KC SOURCE

$$Z_1 - \frac{L}{2} = \text{Distance Above Mid-Plane, cm, } R = 0$$

$Z_1 - \frac{L}{2}$	Calculated Rep/hr for 10,000 curies			$Z_1 - \frac{L}{2}$	Measured Rep/hr	
	Annular Source		Sheet Source		Ferrous Oxidation	Victoreen Ratemeter
	No Absorption	With Absorption	No Absorption		13 March 1953 unless noted	
0	1,020,000	830,000	1,010,000	0	242,000 (16 March 1953)	
6.35	910,000	747,000	928,000	2.5	249,000	
12.7	665,000	527,000	662,000	2.5	234,000	
25.4	222,000	154,000	218,000	8.9	194,000	
38.1	97,000	61,000	96,000	15.2	144,000	
63.5			32,000	20.3	- - -	61,000
				21.6	74,000	- - -
				22.8	- - -	48,000
				25.4	- - -	38,000
				26.7	42,000	- - -
				38.1		16,000
				50.8		8,100
				60.8		5,000
				76.2		3,300

TABLE III

## DOSE RATES ON MID-PLANE OF 10-KC SOURCE

$$Z_1 = \frac{L}{2} = 12.7 \text{ cm}; R = \text{Distance from Axis, cm}$$

R	Rep/hr for Sheet Source, No Absorption. Calculation for 10,000 curies	R	Rep/hr for Ferrous Oxidation		R	Rep/hr for Victoreen Meters	
			13 March 1953	16 March 1953		Ratemeter	R-Meter
0	1,000,000.	0	249,000.	242,000	21.3	61,000	
		0	234,000.				
4.85	1,120,000	3.30	243,000	250,000	23.1	52,000	
8.70	1,800,000	3.30	248,000	244,000	26.2	43,000	
9.70	∞	6.30	281,000	280,000	30.8	32,000	
10.7	1,800,000	6.30	274,000	292,000	31.8	---	40,000
12.0	1,150,000	14.7	168,000		38.4	18,500	---
19.4	379,000	18.1	86,000	102,000	51.0	---	15,500
29.1	160,000	20.6	115,000	79,500	64.0	7,500	---
38.8	92,000	25.7	52,000		73.9	---	7,500
100	14,000	38.4	24,000		140	1,800	
		51.0	13,000		165	1,200	
		89.1	4,400				
		114.8	2,600				
		140.0	2,000				

20.6

82,000.  
9 June 1953

TABLE IV  
ESTIMATES OF ACTIVITIES FROM  
MEASUREMENTS OF DOSE RATES

Source	Measurements Where Method Taken		Date	Estimate of Activity, Curies			Mean Value Divided By Decayed Nominal Value
				'A' After Value Indicates Self-Absorption was Considered			
				Maximum	Minimum	Arithmetic Mean	
10 KC	Axis	Ferrous Oxidation	Mar. 53	2500	2100	2300	0.26
				3100A	2800A	2950A	0.33A
	Mid- Plane	Ferrous Oxidation	Mar. 53	1700	1400	1550	0.17
				2600A	2500A	2550A	0.28A
				2600	2200	2400	0.27
Mid- Plane	Ferrous Oxidation	Mar. 53	2500	2000	2250	0.25	
			2500	2000	2250	0.25	
Mid- Plane	Ferrous Oxidation	Mar. 53	3000	2900	2950	0.33	
			3000	2900	2950	0.33	
1 KC	Axis	Ferrous Oxidation	May 52	140			0.16
				180A			0.20A
			May 53	130			0.16
				170A			0.21A
	Mid- Plane	Ferrous Oxidation	Feb. 53	150	110	130	0.16
				190A	150A	170A	0.20A
			May 52	170			0.19
				230A			0.26A
Mid- Plane	Ferrous Oxidation	May 53	160			0.20	
			210A			0.26A	

latter value for decay. If self-absorption is not considered, the activity is estimated to be from 17 to 33 percent of the nominal value. If self-absorption is considered, the activity is estimated to be from 28 to 33 percent of the nominal value. These figures are computed from data taken both on the mid-plane and on the axis. No estimate of self-absorption was made on the mid-plane, however.

Calculated and observed values of dose rate for the 1-kilocurie source are compared in Table V and in Fig. 36. The 1-kilocurie source was irradiated at Brookhaven National Laboratory and was assumed to have a nominal activity of 1000 curies in July, 1951. The activity computed from each means of measurement is given in Table IV. The ratios of observed to decayed nominal curies appear in the right column. If self-absorption is not considered, the activity is estimated to be from 16 to 20 percent of the nominal value. If self-absorption is considered, the activity is estimated to be from 20 to 26 percent of the nominal value. These figures are computed from data taken on the axis only, since it was not possible to make measurements external to the source. However, it was desired to compare the dose rates predicted by Equation (5) for the 1-kilocurie source with those predicted for the 10-kilocurie source in order to observe differences caused by the different geometrical proportions of the two sources. Consequently Figs. 42, 43, and 44 are presented to portray the dependence of dose rate on position in the neighborhood of the 1-kilocurie source. The data for these figures were computed on the assumption that the source actually contained 1000 curies.

Judging from the above results there appears to be about a three-fold discrepancy between the curies in the 10-kilocurie source as estimated from ionization measurements and as calculated from neutron absorption. The comparisons for the 1-kilocurie source are not so meaningful, since no firm

TABLE V

## DOSE RATES ON AXIS OF 1-KC SOURCE

$$Z_1 - \frac{L}{2} = \text{Distance Above Mid-Plane, cm}$$

$$R = 0$$

$$r = 2.493 \text{ cm}$$

Calculated Rep/hr for 1,000 curies				Measured Rep/hr			
$Z_1 - \frac{L}{2}$	Annular Source		Sheet Source	$Z_1 - \frac{L}{2}$	Ferrous	Victoreen	Victoreen
	No	With	No		Oxidation	Rate-meter	R-Meter
	Absorption	Absorption	Absorption		Feb. 53		
0	442,000	341,000	460,000.	0	62,300 } May, 52 }		79,000 } May, 52 }
8.75	429,000	336,000	450,000	0	57,200 } May, 53 }		72,000 } May, 53 }
17.5	232,000	184,000	240,000	1.3		51,600	
35.0	---	---	15,200	3.8		52,800	
87.5	---	---	1,900	6.3		54,000	
				8.9		55,800	
				11.4		57,500	
				14.0		46,800	
				16.5		19,200	
				19.0		9,300	
				21.6		5,150	
				24.2		3,240	
				26.7		1,860	
				29.2		1,320	
				34.2		490	

estimate of the activity of the source was made by Brookhaven National Laboratory, which supplied the source.

The errors in the methods of calculation summarized in Equations (3), (5), and (8) probably arise chiefly from the simplifying assumptions made. The assumption that the source has no thickness is evidently justified by the agreement of values calculated on this assumption with those in which thickness of the source is considered (see Figs. 35 and 36). The results of Tables II and V show that absorption is not negligible. However, in Figs. 35 and 36 it can be seen that the plots from data and from Equations (3), (5), and (8) differ by an approximately constant factor between any pair of curves. This result is interpreted to mean that Equations (3) and (5) may be used within limits to predict the distribution of dose rates without consideration of self-absorption, but that accurate prediction of dose rates requires consideration of self-absorption.

The 1-kilocurie source is evidently not of uniform activity throughout its whole volume. This conclusion was reached from a study of Fig. 36. Note that the measured dose rates in the 1-kilocurie source do not vary with distance along the axis in the manner predicted by the calculated curves. The depression near the mid-plane is probably caused by lower unit activity inside the source in this region. The lower unit activity here is probably caused by failure of neutrons in the pile to penetrate to the interior of the cobalt cylinder near the mid-plane as abundantly as near the ends. The other assumptions introduced are thought to be reasonably acceptable, although Equation (8) converges much more slowly as  $Z_1$  is increased. The value of 13.5 equivalent roentgens per hour at one centimeter per millicurie point source of cobalt-60 was taken from the work of Marinelli, Quimby, and Hine<sup>42</sup>, and was assumed to be correct within our experimental error.

Although there were some differences between the chemical and physical dosimetry measurements, they were not sufficiently large to account for the factor of three or four between the nominal activities of the sources and those which result from the dose measurements themselves. It was concluded that the methods of analysis of dose rates and the measurements of dose rates were both correct, and that the activities of the sources should be re-computed from this information. The activities so computed are summarized in Table IV. The activities estimated from measurements of dose were about 20 to 30 percent of the values previously estimated from absorption of neutrons. Levin and Hughes<sup>34</sup> have recently noted that a factor of about 0.30 should be applied to computed activities in neutron-irradiation of cobalt in order to account for nonuniform distribution of neutrons in the sample being irradiated.

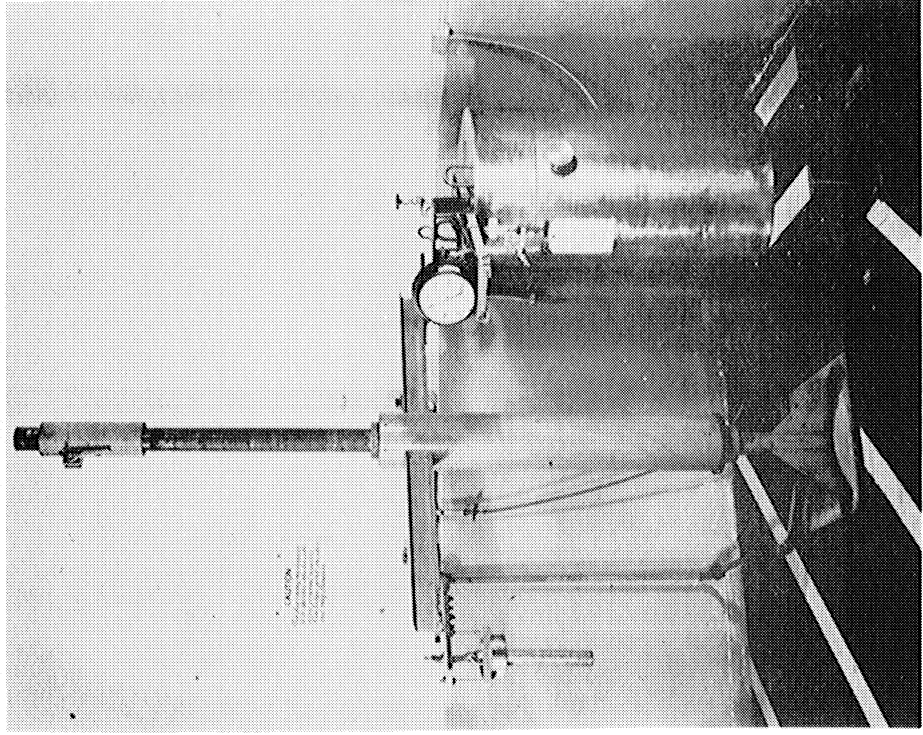


Fig. 22. Pressure Reactor in 1-K-C Gamma Source.

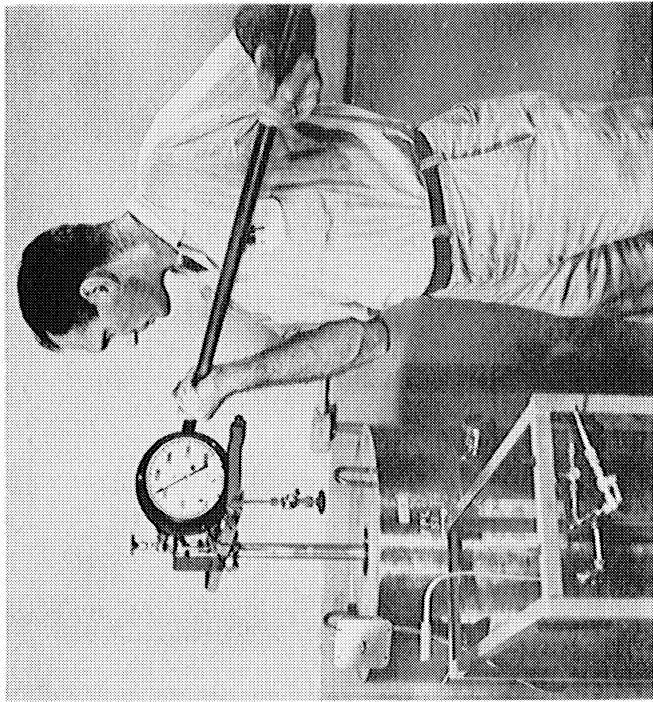


Fig. 21. Insertion of Pressure Reactor into 1-K-C Gamma Source.



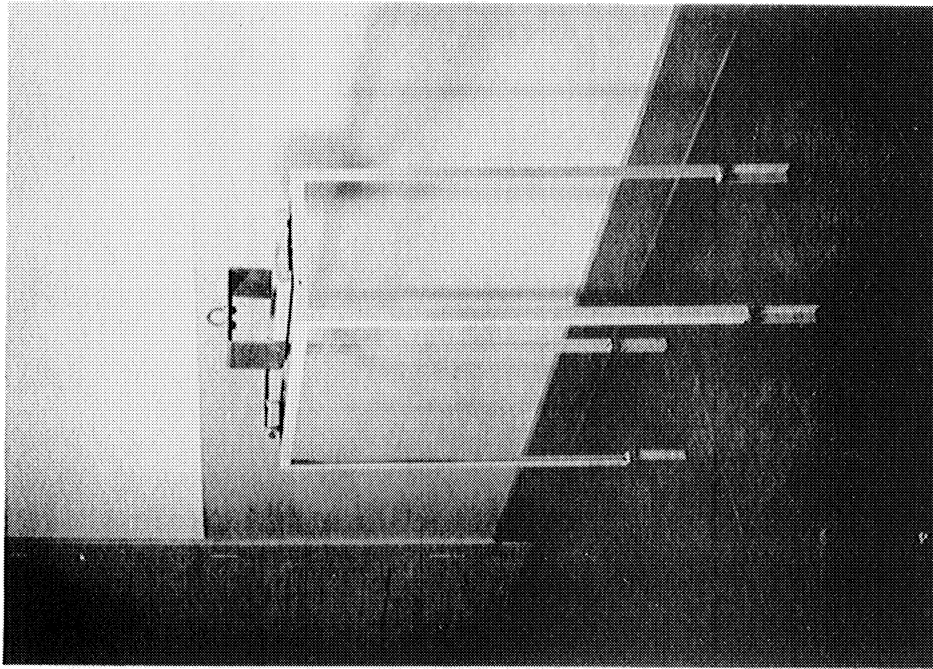


Fig. 23. Rack and Sling for Pressure Reactor.

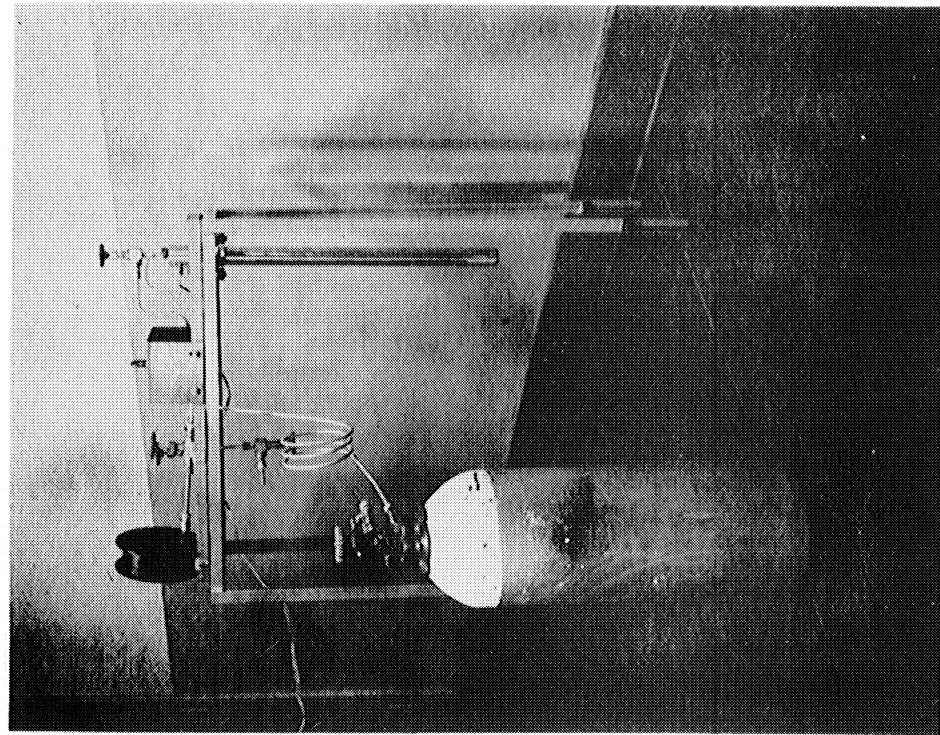


Fig. 24. Pressure Reactor: Tubing Assembly and Gas Cylinder.

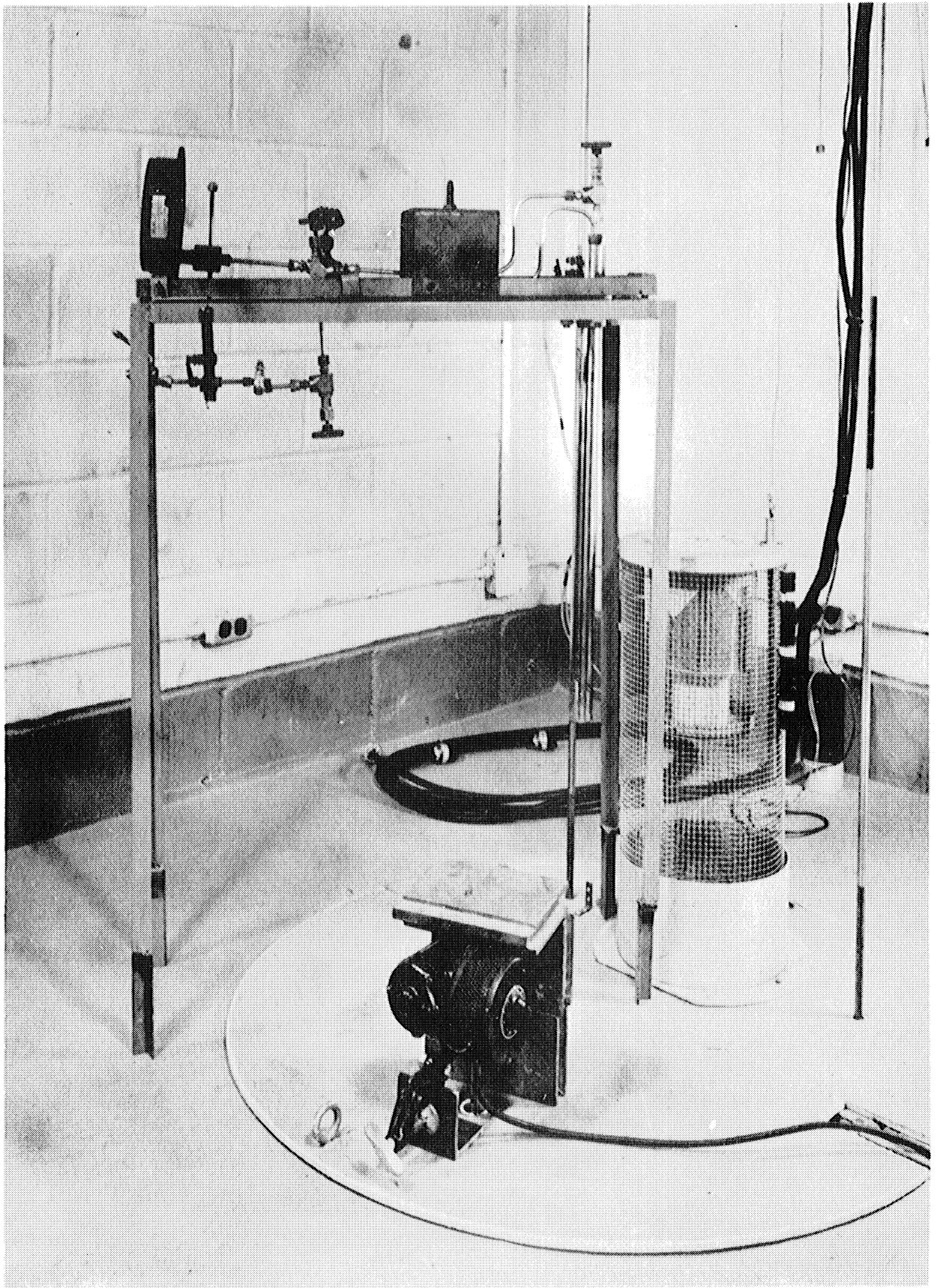


Fig. 25. Pressure Reactor in 10-K-C Gamma Source Room.



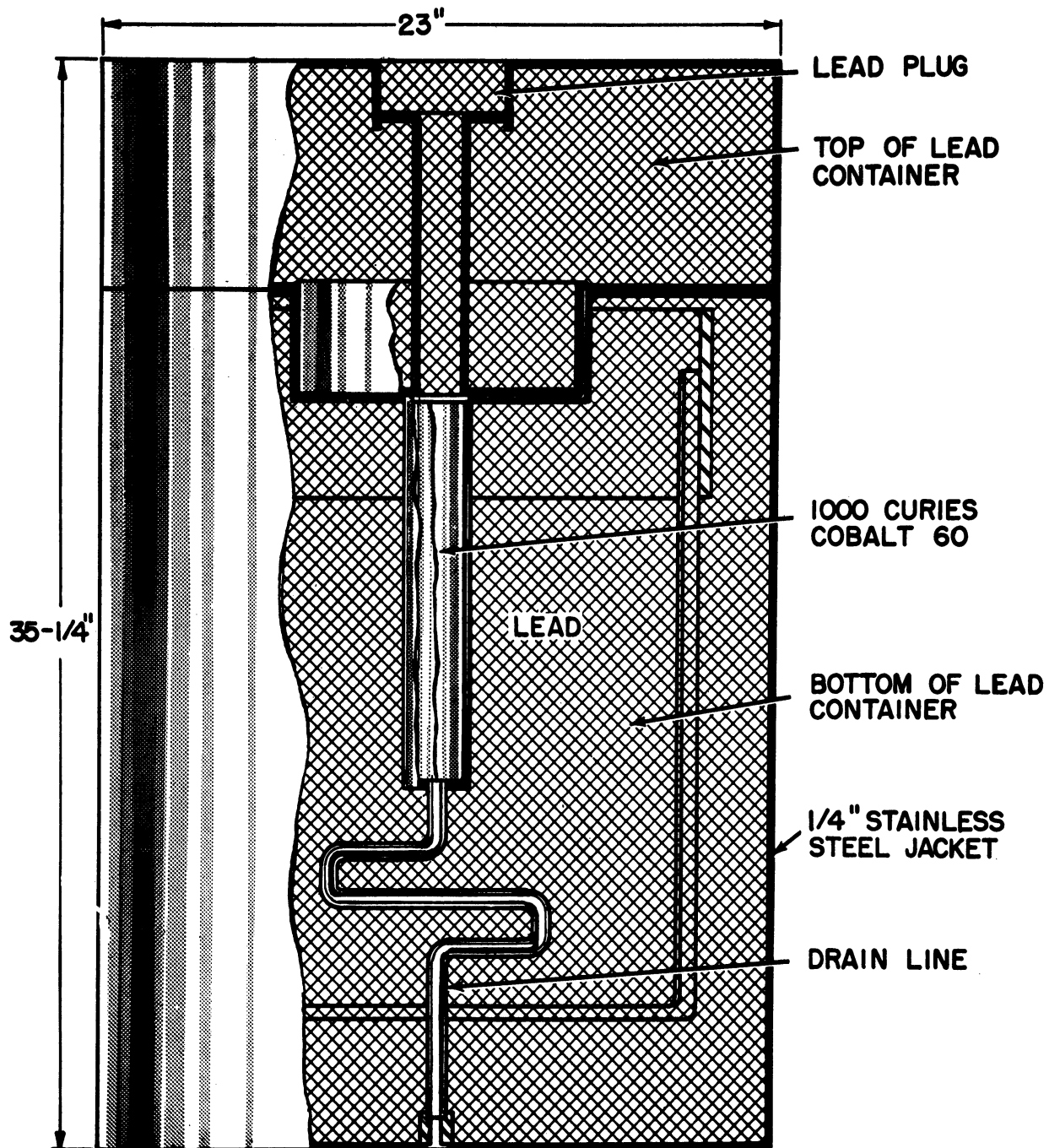


Fig. 27. 1-Kilocurie Cobalt-60 Source with Shielding.

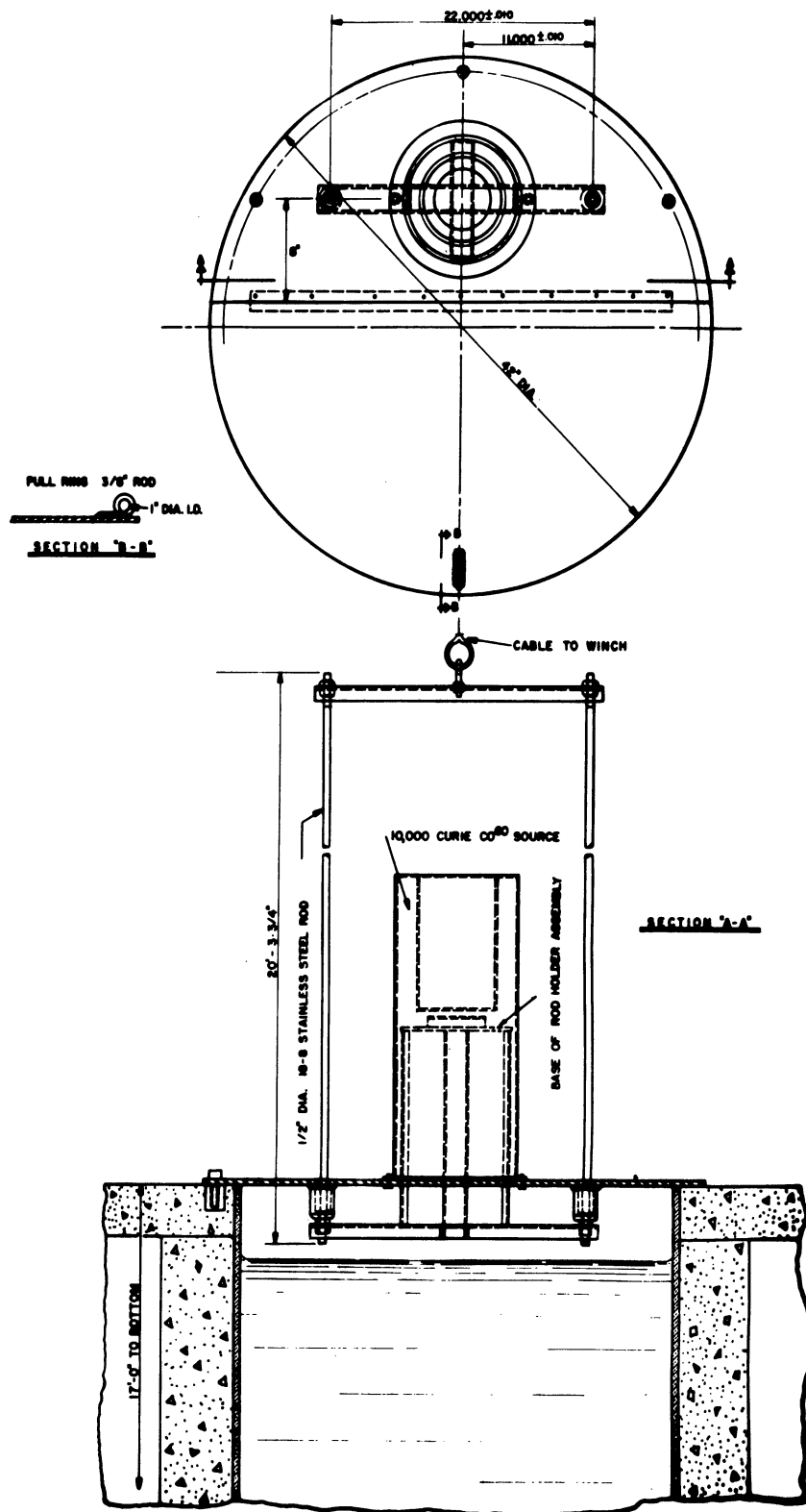


Fig. 28. 10-Kilocurie Source Elevator and Well.

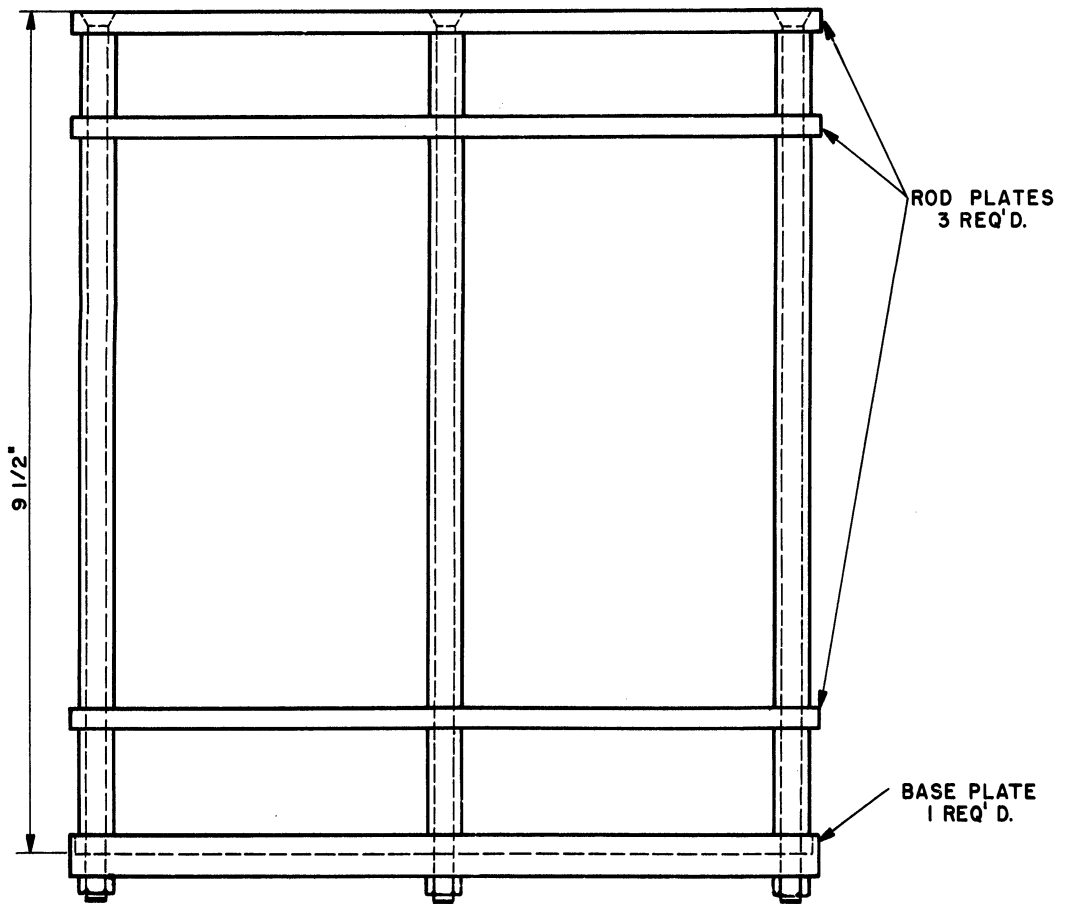
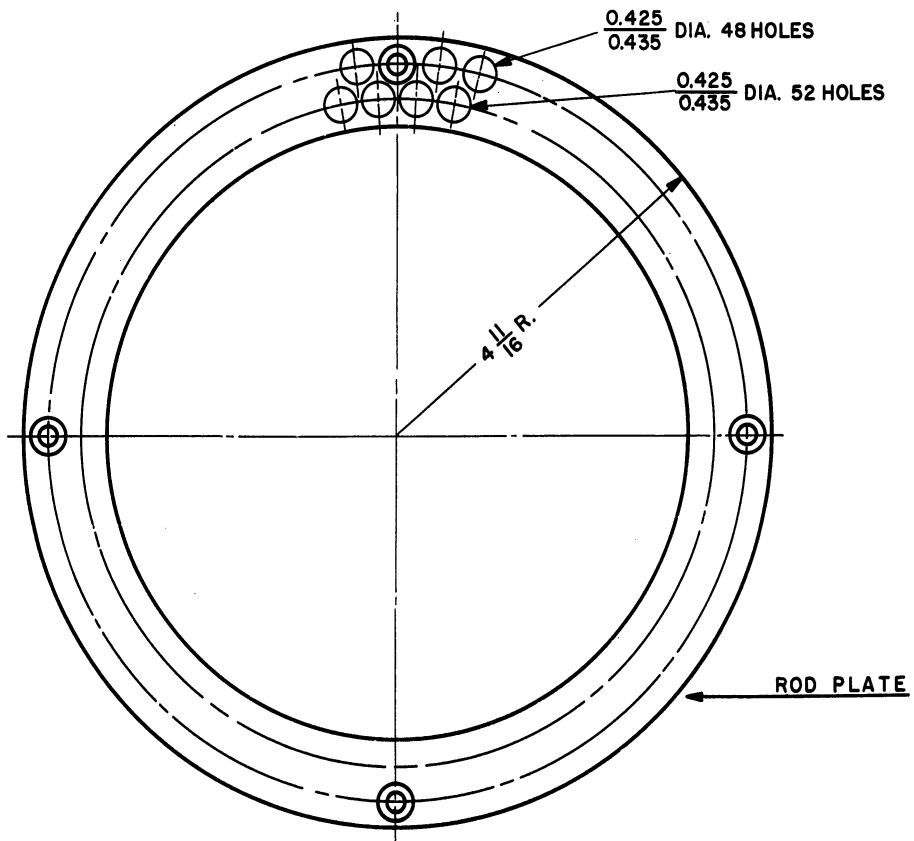
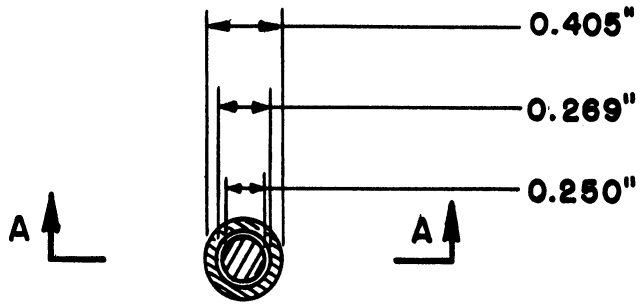
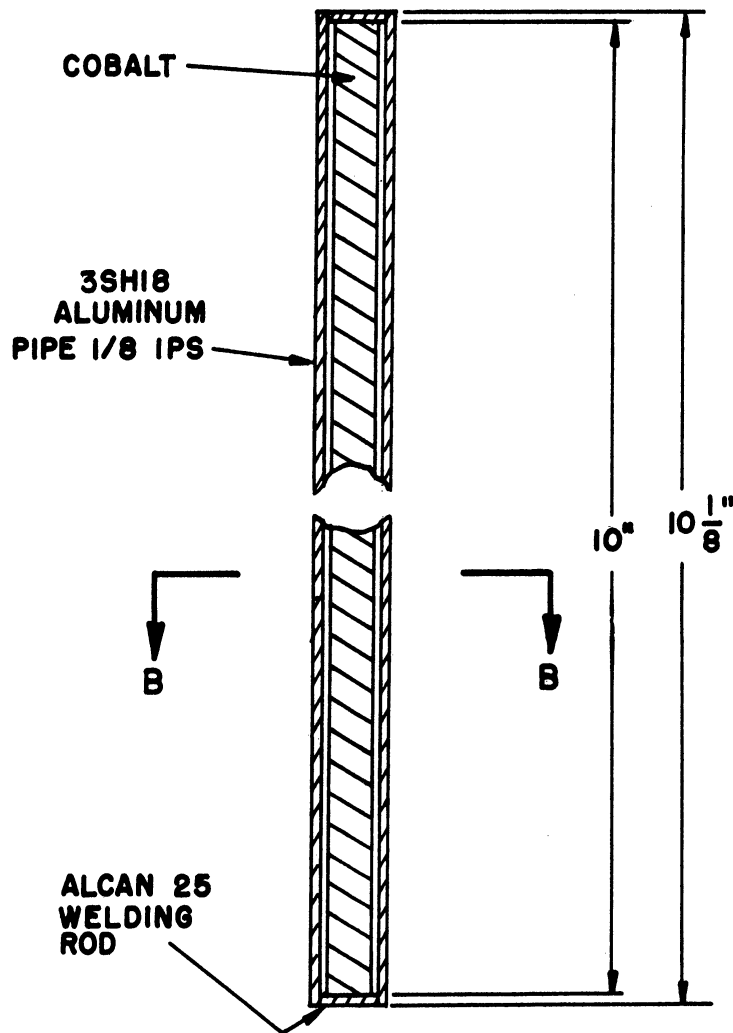


Fig. 29. 10-Kilocurie Source: Rack for Rods.



**SECTION BB**



**SECTION AA**

Fig. 30. Cobalt Rod for 10-Kilocurie Source.

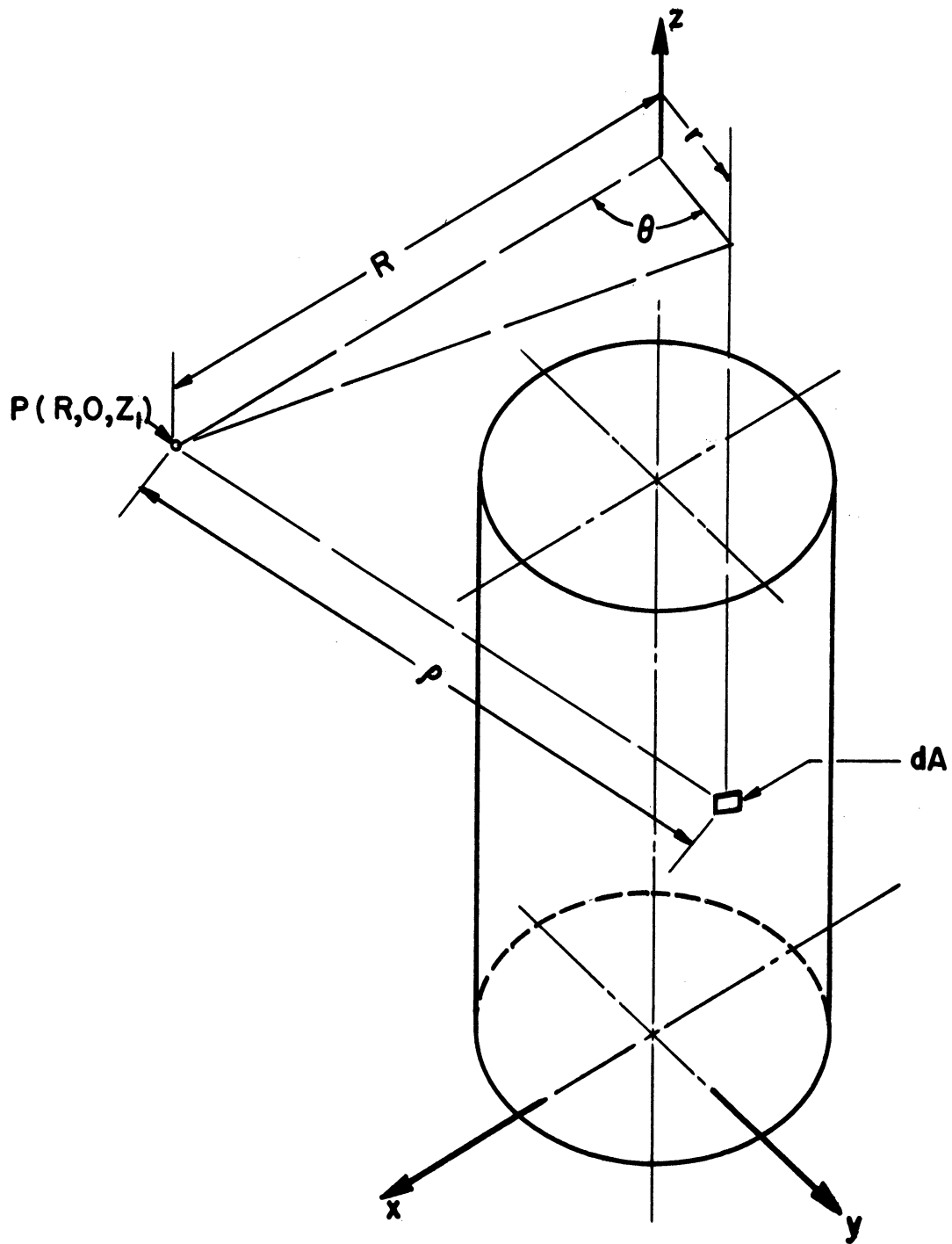


Fig. 31. Source with Negligible Wall Thickness.



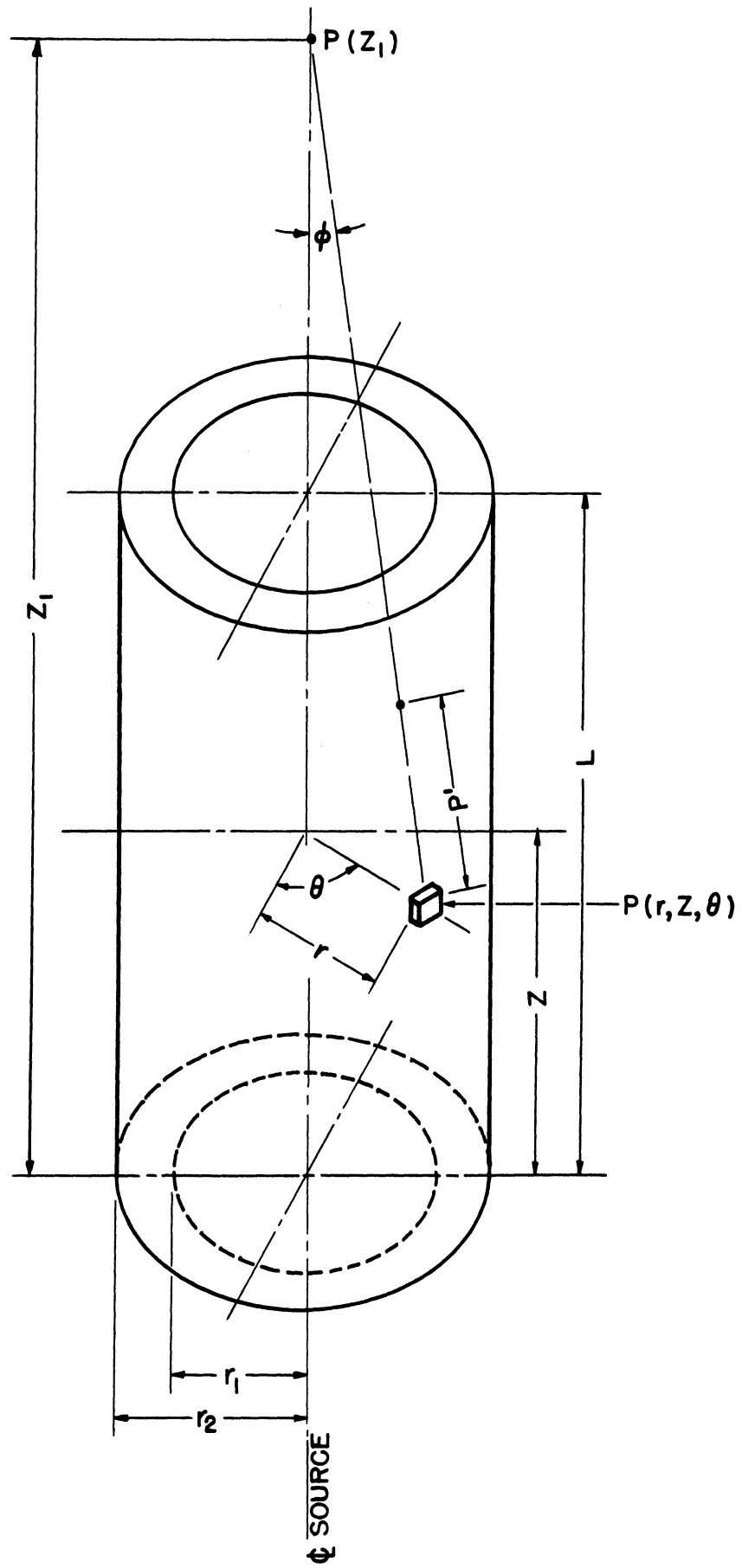


Fig. 32. Source with Finite Wall Thickness.

$$dI = V \frac{dv}{\rho^2} e^{-\mu P'} \rho \quad \text{EQ. (6)}$$

$$I = \int_{r=r_1}^{r=r_2} \int_{Z=0}^{Z=L} \int_{\theta=0}^{\theta=2\pi} V \frac{rd\theta dZ dr}{r^2 + (Z_1 - Z)^2} e^{-\mu \rho (r-r_1) \csc \phi} \quad \text{EQ. (7)}$$

if a three-term approximation to the exponential is employed:

$$\begin{aligned} I = & 2\pi V \left[ r_2 \left( \tan^{-1} \frac{Z_1}{r_2} - \tan^{-1} \frac{Z_1 - L}{r_2} \right) - r_1 \left( \tan^{-1} \frac{Z_1}{r_1} - \tan^{-1} \frac{Z_1 - L}{r_1} \right) \right. \\ & \left. + \frac{Z_1 - L}{2} \ln \frac{1 + \left(\frac{r_1}{Z_1 - L}\right)^2}{1 + \left(\frac{r_2}{Z_1 - L}\right)^2} + \frac{Z_1}{2} \ln \frac{1 + \left(\frac{r_2}{Z_1}\right)^2}{1 + \left(\frac{r_1}{Z_1}\right)^2} \right] \\ & + 2\pi V \mu \rho \left[ \left( \frac{r_2^2}{2} - r_2 r_1 \right) \left( \sinh^{-1} \frac{Z_1 - L}{r_2} - \sinh^{-1} \frac{Z_1}{r_2} \right) \right. \\ & \left. + \frac{r_1^2}{2} \left( \sinh^{-1} \frac{Z_1 - L}{r_1} - \sinh^{-1} \frac{Z_1}{r_1} \right) \right. \\ & \left. + \left( \frac{Z_1 - L}{2} \right) \left( r_2 \sqrt{\left(\frac{Z_1 - L}{r_2}\right)^2 + 1} - r_1 \sqrt{\left(\frac{Z_1 - L}{r_1}\right)^2 + 1} \right) \right. \\ & \left. - \frac{Z_1}{2} \left( r_2 \sqrt{\left(\frac{Z_1}{r_2}\right)^2 + 1} - r_1 \sqrt{\left(\frac{Z_1}{r_1}\right)^2 + 1} \right) \right. \\ & \left. + (Z_1 - L) r_1 \ln \frac{r_1}{r_2} \left( \frac{\sqrt{\left(\frac{Z_1 - L}{r_1}\right)^2 + 1} + 1}{\sqrt{\left(\frac{Z_1 - L}{r_2}\right)^2 + 1} + 1} \right) \right. \\ & \left. - Z_1 r_1 \ln \frac{r_1}{r_2} \left( \frac{\sqrt{\left(\frac{Z_1}{r_1}\right)^2 + 1} + 1}{\sqrt{\left(\frac{Z_1}{r_2}\right)^2 + 1} + 1} \right) \right] \\ & + \pi V \mu^2 \rho^2 L \left[ \frac{r_2^2 - r_1^2}{2} - 2 r_1 (r_2 - r_1) + r_1^2 \ln \frac{r_2}{r_1} \right] \dots \quad \text{EQ. (8)} \end{aligned}$$

$$\text{for } Z_1 \geq 0, \quad -\frac{\pi}{2} < \tan^{-1} \frac{Z_1 - L}{r_1}, \quad \tan^{-1} \frac{Z_1 - L}{r_2} < \frac{\pi}{2};$$

$$0 \leq \tan^{-1} \frac{Z_1}{r_1}, \quad \tan^{-1} \frac{Z_1}{r_2} < \frac{\pi}{2}; \quad r_1 > 0, \quad r_2 > 0, \quad r_1 \neq r_2.$$

Fig. 33. Dose Rate Equations for Source with Finite Wall Thickness.

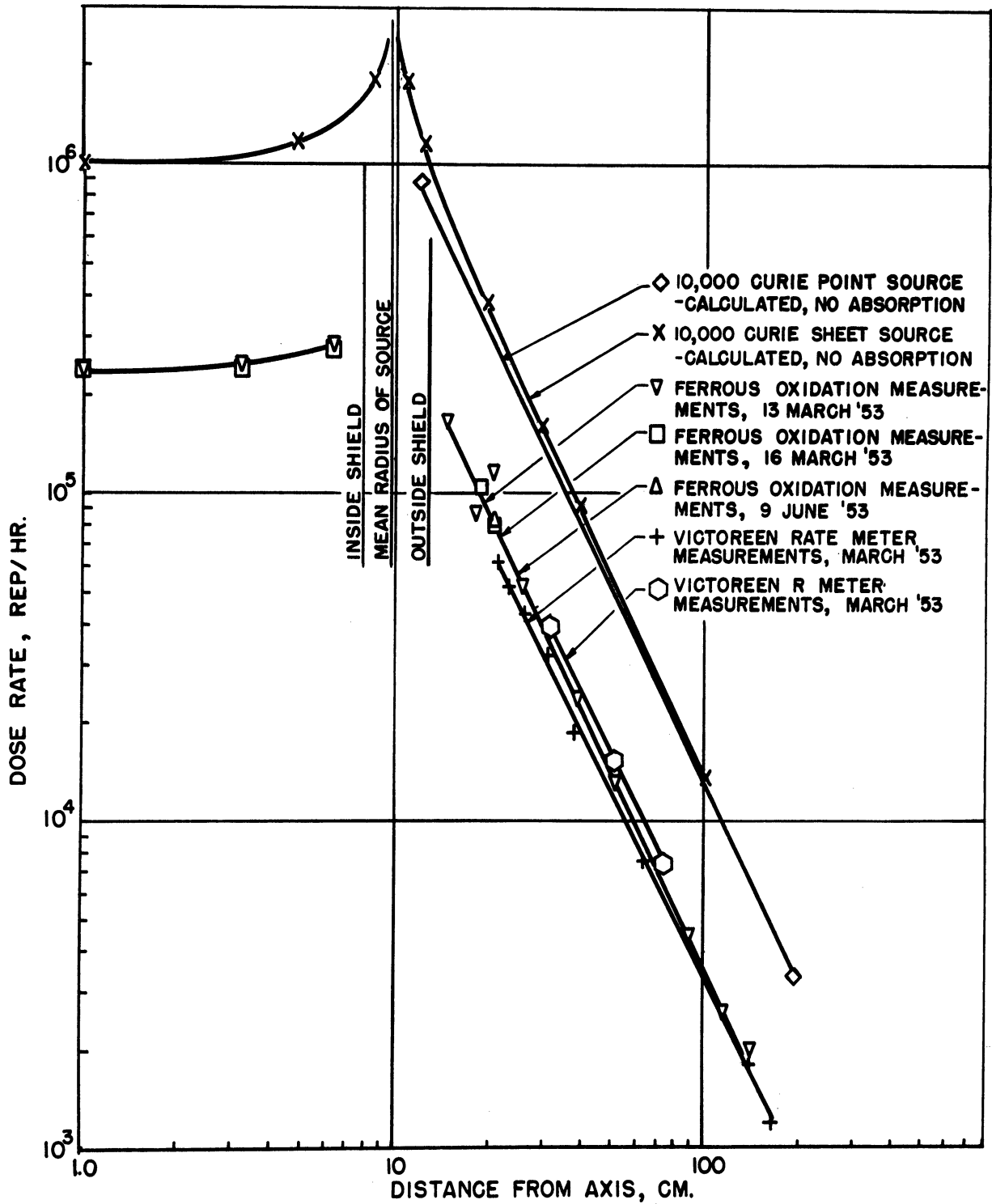


Fig. 34. Dose Rate on Mid-Plane of 10-Kilocurie Source.

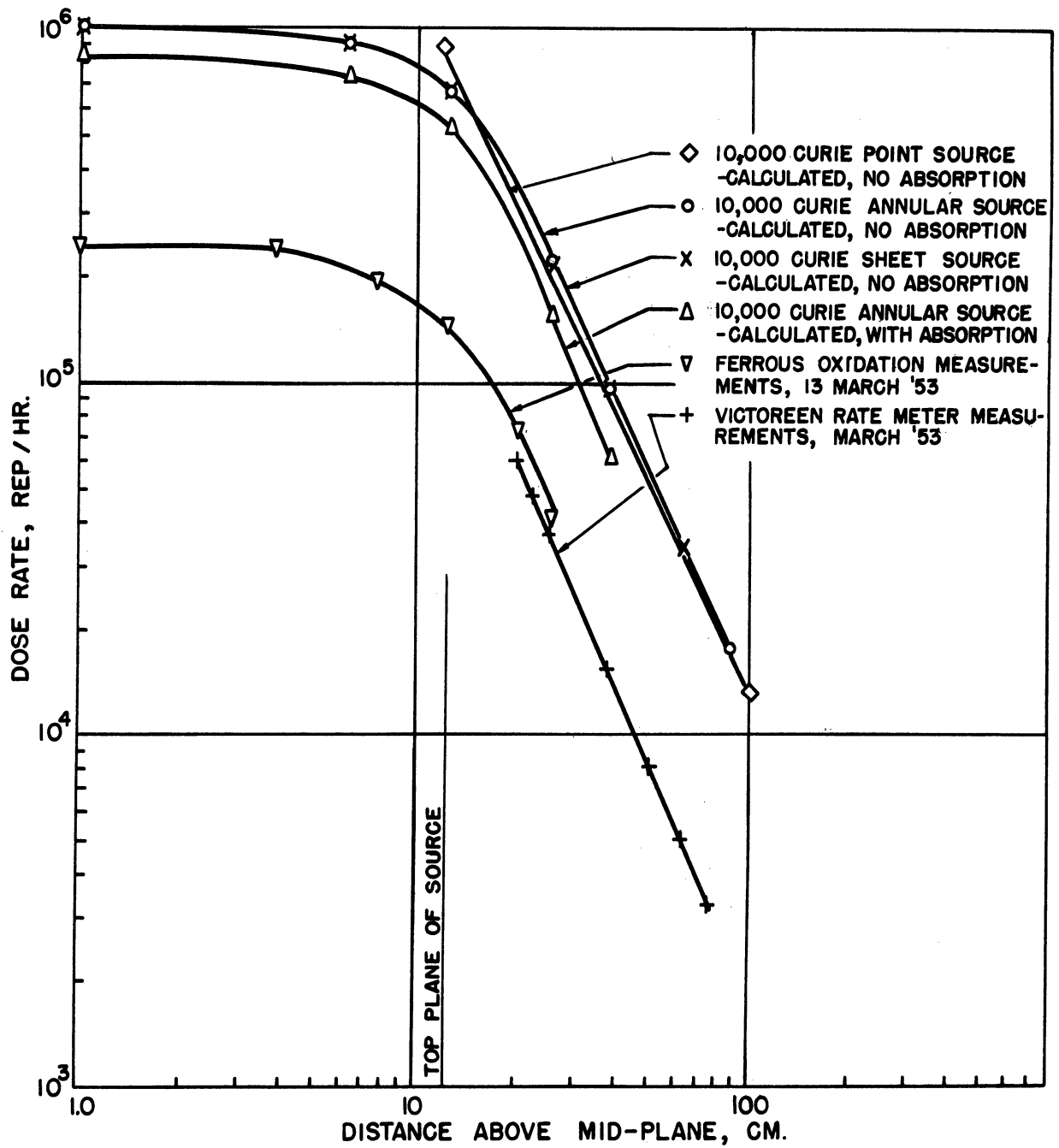


Fig. 35. Dose Rate on Axis of 10-Kilocurie Source.

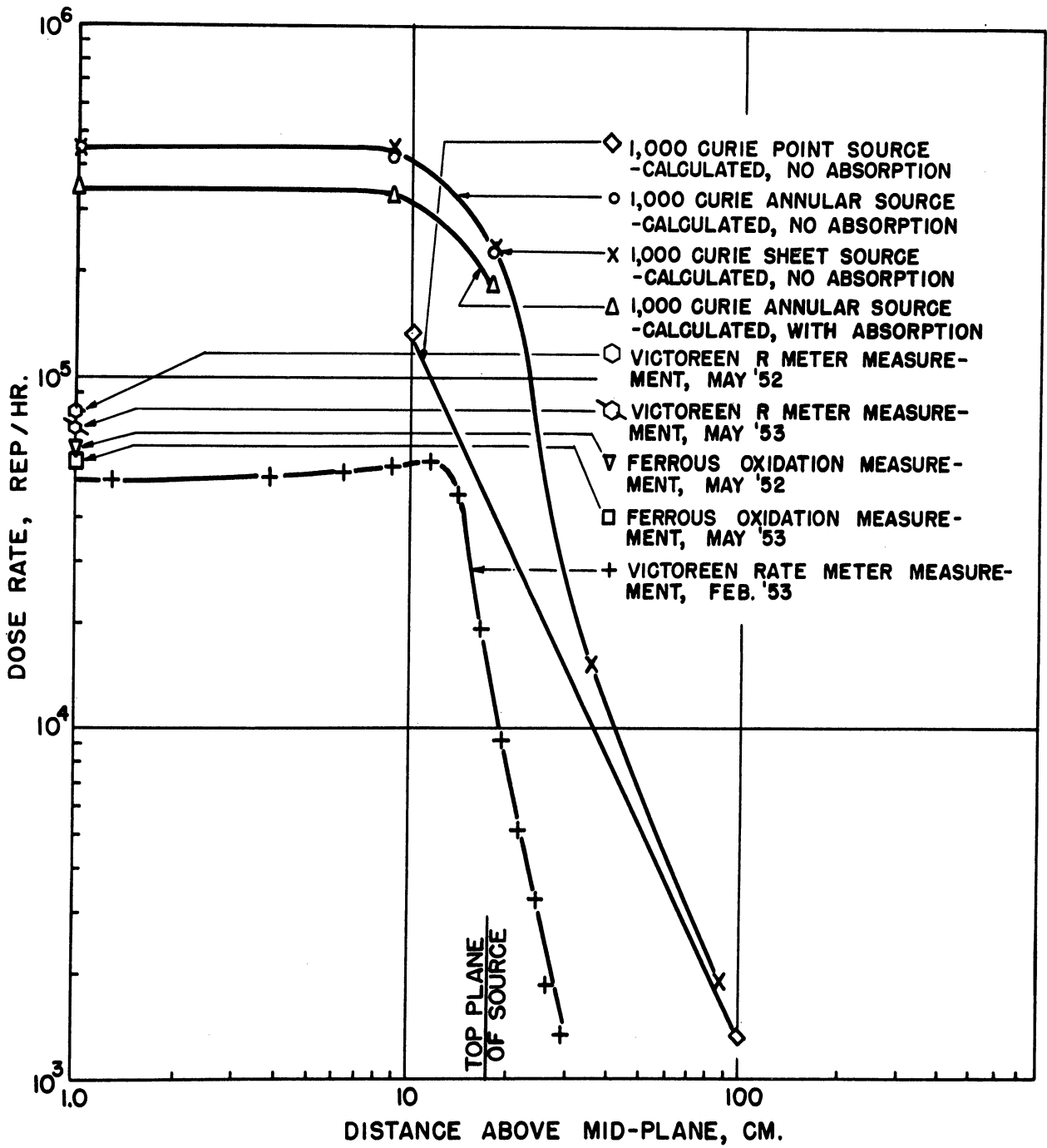


Fig. 36. Dose Rate on Axis of 1-Kilocurie Source.

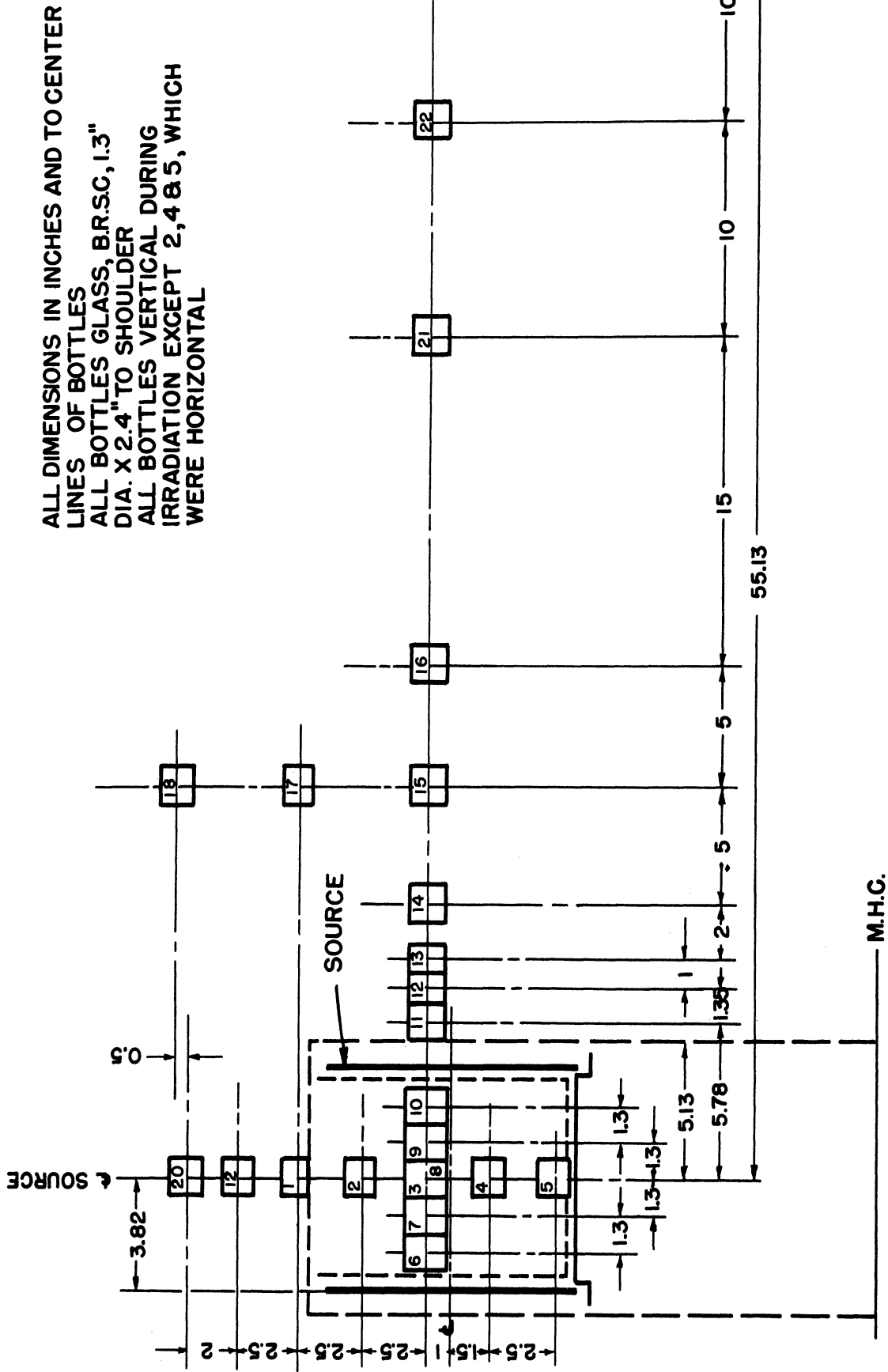


Fig. 37. Location of Dosimetry Samples for Run 132307 with 10-Kilocurie Source.

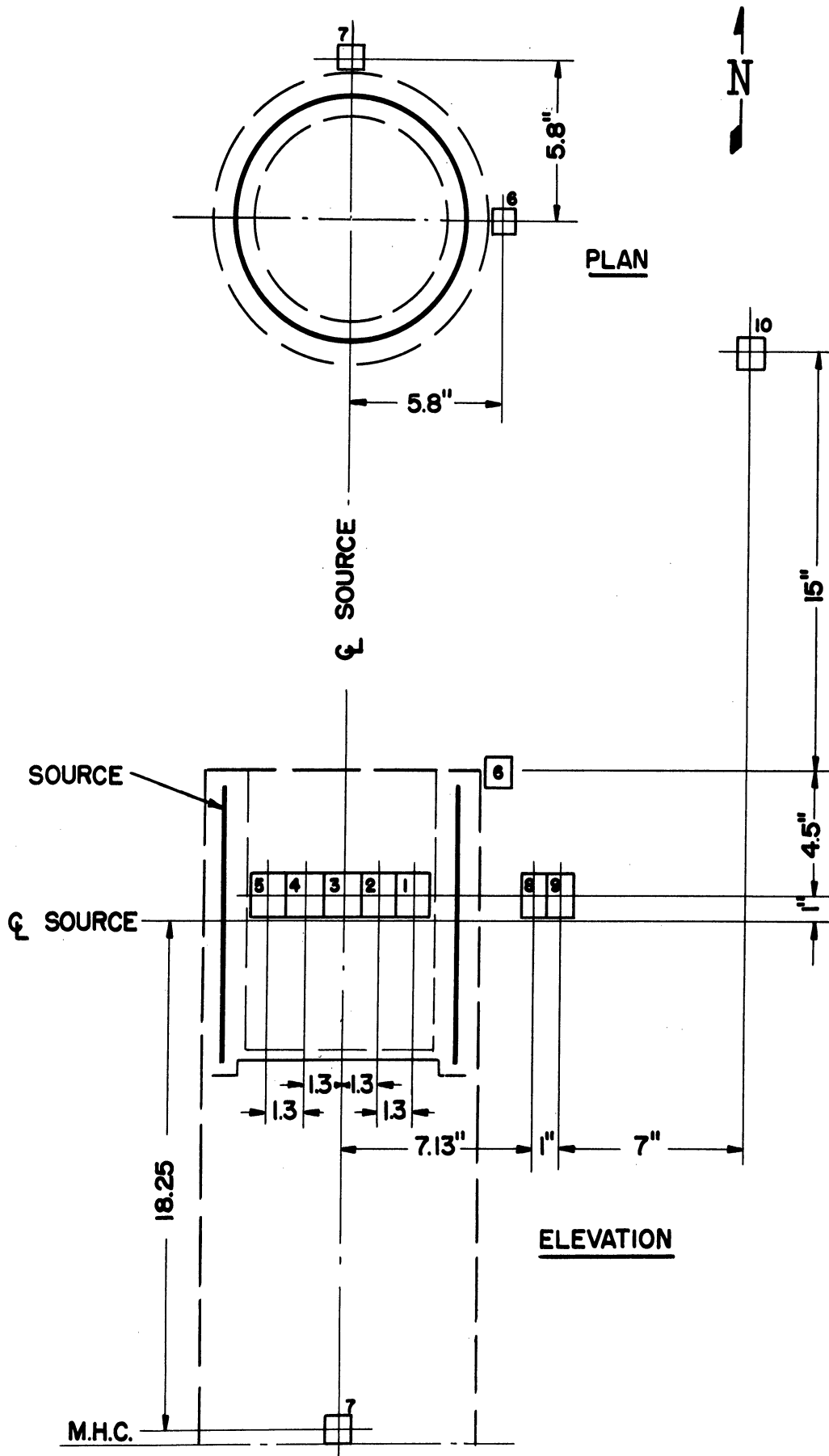


Fig. 38. Location of Dosimetry Samples for Run 132308 with 10-Kilocurie Source.

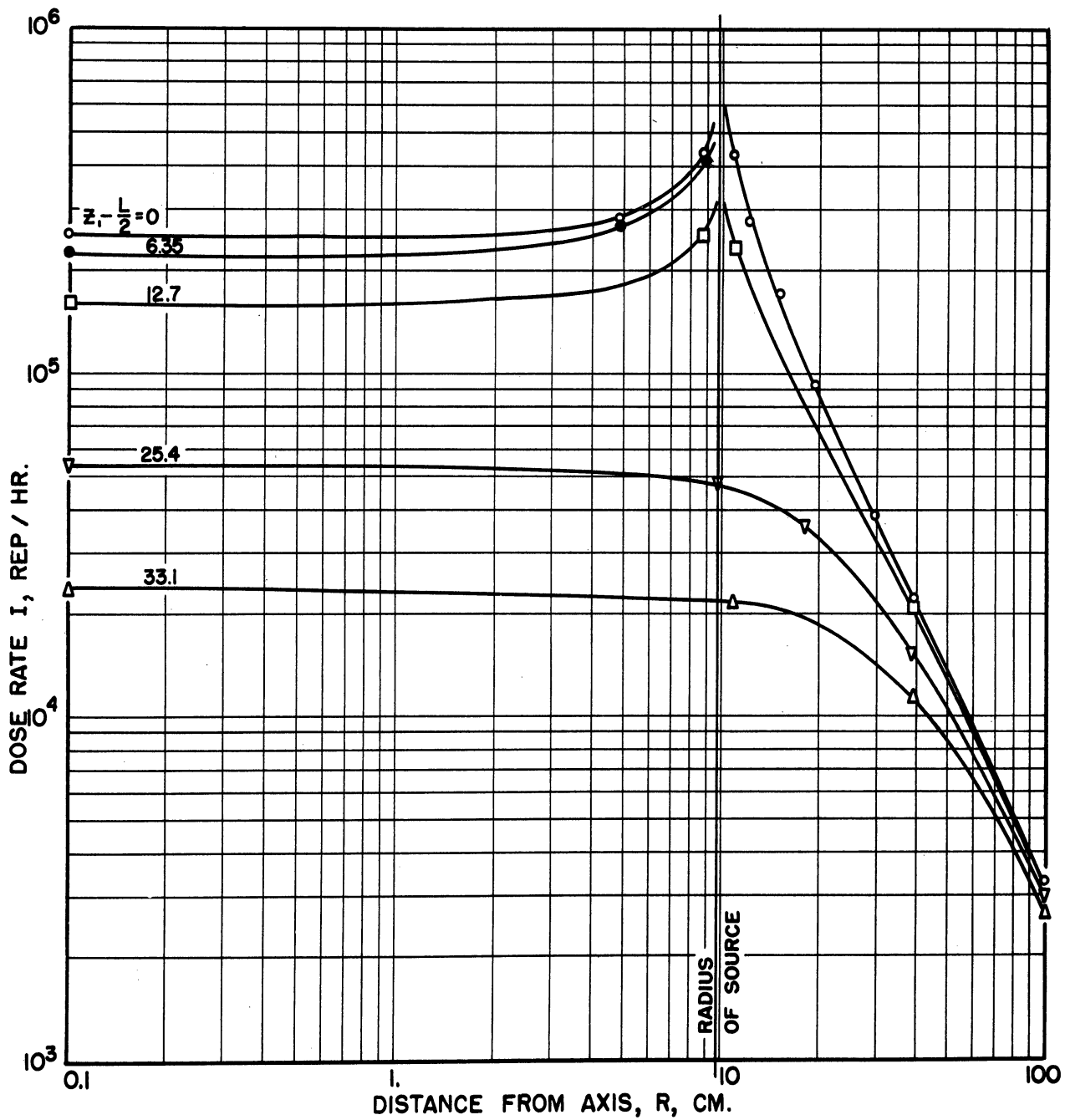


Fig. 39. Dose Rates Parallel to Mid-Plane, Interpolated from Measurements with 10-Kilocurie Source.



## DOSE RATE WITHIN A CYLINDRICAL PRESSURE REACTOR

All the foregoing calculations and dose measurements are for points in air lying at different distances from the sources. In the experiments reported on the polymerization of ethylene, the reaction took place inside a stainless-steel pressure vessel. The dose rate inside this vessel is certainly not the same as that on the outside. Consequently, a series of calculations were made on the intensity of radiation inside the pressure vessel, taking into account the absorption of gamma radiation by the walls of the vessel (see Fig. 46). It is assumed (1) that the source of gamma radiation is a cylindrical sheet of no thickness and of uniform activity per unit area, (2) that the source is transparent to its own radiation, (3) that the dose rate varies inversely with the square of the distance and inversely with an exponential function of absorber thickness, (4) that no absorption occurs inside the reactor, and (5) that secondary radiation from the bomb wall does not affect the dose rate. ~~Non-equilibrium~~ secondary radiation probably does affect the dose rate in the ethylene but this consideration was neglected in computing the dose rates used to calculate G values for the polymerization of ethylene.

Let the terminology be defined as in Fig. 46 and as follows:

$$I = \text{dose rate at } P(R,Z), \text{ rep/hr ;}$$
$$\alpha = \left( \frac{\text{activity of source, curies}}{\text{area of source, cm}^2} \right) \left( \frac{1000 \text{ millicuries}}{\text{curie}} \right) \left( \frac{\text{equiv. roentgen at 1 cm}}{(\text{hr}) (\text{millicurie point source})} \right) ;$$

$\mu$  = absorption coefficient, cm<sup>2</sup>/gram, taken from Snyder and Powell<sup>53</sup>;

A = area of source, cm<sup>2</sup>

$P$  = distance from  $dA$  at  $P(r,Z,\theta)$  to  $P(R,Z)$  ;

$P'$  = distance through bomb wall, cm ;

$K(k)$  = complete elliptic integral of first kind of modulus  $k$ ;

$$k_1 = 2 \frac{\sqrt{Rr}}{R+r} ;$$

$\rho$  = density of bomb wall, grams/cm<sup>3</sup> ; and

$x$  = distance in Fig. 45 from source to point at which  $I$  is measured.

From assumption (3) the following equation may be written:

$$dI = -\mu I dx - \frac{2}{x} I dx . \quad (9)$$

Integration and substitution of limits yields the expressions:

$$I_2 = \left( \frac{x_1}{x_2} \right)^2 I_1 \quad (10)$$

$$I_4 = \left( \frac{x_3}{x_4} \right)^2 I_3 \quad (11)$$

$$\frac{I_3}{I_2} = \left( \frac{x_2}{x_3} \right)^2 e^{-\mu(x_3-x_2)} . \quad (12)$$

Combining Equations (10), (11), and (12) results in the expression:

$$I_4 = \left( \frac{x_1}{x_4} \right)^2 I_1 e^{-\mu(x_3-x_2)} . \quad (13)$$

From Equation (13) we may deduce that the location of an absorber is immaterial as long as it is between the source and point  $P$ . Thus only the thickness of the absorber need be considered.

Now Equation (16) may be written for dose rate on the axis of the bomb (see Fig. 46).

$$P' = b \csc \phi , \quad (14)$$

$$\csc \phi = \sqrt{\frac{R^2 + r^2 - 2Rr \cos \theta + (Z_1 - Z)^2}{R^2 + r^2 - 2Rr \cos \theta}} \quad (15)$$

and

$$dI = \alpha \frac{dA}{p^2} e^{-\mu \rho P'} \quad (16)$$

Equation (16) must be integrated over the entire source, as shown by Equation (17). A three-term approximation to the exponential is employed.

$$I = \int_{Z=0}^{Z=L} 2 \int_{\theta=0}^{\theta=\pi} \alpha r d\theta dZ \left\{ \frac{1}{R^2 + r^2 - 2Rr \cos \theta + (Z_1 - Z)^2} - \frac{\mu b \rho}{\sqrt{R^2 + r^2 - 2Rr \cos \theta + (Z_1 - Z)^2} \sqrt{R^2 + r^2 - 2Rr \cos \theta}} + \frac{\mu^2 b^2 \rho^2}{2!} \frac{1}{(R^2 + r^2 - 2Rr \cos \theta)} - \dots \right\} \quad (17)$$

The first term within braces has been integrated above, in Equations (3) and (5). Integration of Equation (17) yields Equation (18):

$$I = \frac{2\alpha \pi r}{R+r} \left[ F\left(\tan^{-1} \frac{Z_1}{|r-R|}, k_1\right) - F\left(\tan^{-1} \frac{Z_1-L}{|r-R|}, k_1\right) \right] - 2\alpha \mu b \rho \sqrt{\frac{R}{R^2 - r^2}} \int_{Z_1-Z=Z_1-L}^{Z_1-Z=L} \frac{K(k) dk}{1 - (k/k_1)^2} + \frac{\alpha \pi r L \mu^2 b^2 \rho^2}{R^2 - r^2} - \dots, \quad (18)$$

where

$$k = k_1 \frac{(Z_1 - Z)}{\sqrt{(R-r)^2 + (Z_1 - Z)^2}}.$$

Equation (18) holds for

$$Z_1 \geq L > 0, \quad 0 \leq \tan^{-1} \frac{Z_1-L}{|r-R|}, \quad \tan^{-1} \frac{Z_1}{|r-R|} < \frac{\pi}{2}, \quad R \neq r \neq 0.$$

If, however,

$$L \geq Z_1 > 0, \quad R \neq r \neq 0,$$

then

$$\begin{aligned} I &= \frac{2 \alpha \pi r}{R+r} \left[ F\left(\tan^{-1} \frac{Z_1}{\sqrt{\frac{|r-R|}{|r-R|}}}, k_1\right) - F\left(\tan^{-1} \frac{Z_1-L}{\sqrt{\frac{|r-R|}{|r-R|}}}, k_1\right) \right] \\ &- 2 \alpha \mu b \rho \sqrt{\frac{r}{R}} \left[ \int_{\substack{Z_1-Z=0 \\ Z_1-Z=Z_1-L}}^{\substack{Z_1-Z=0 \\ Z_1-Z=Z_1-L}} \frac{K(k) dk}{1 - (k/k_1)^2} + \int_{\substack{Z_1-Z=Z_1 \\ Z_1-Z=0}}^{\substack{Z_1-Z=Z_1 \\ Z_1-Z=0}} \frac{K(k) dk}{1 - (k/k_1)^2} \right] \\ &+ \frac{\alpha \pi r L \mu^2 b^2 \rho^2}{R^2 - r^2} - \dots \end{aligned} \quad (19)$$

Since  $k$ , defined above, is the modulus of an elliptic integral of the first kind,

$$1 \geq k \geq 0.$$

Consequently, for Equation (19) the following definitions are employed.

$$\begin{aligned} k &= k_1 \frac{(Z_1 - Z)}{\sqrt{(R-r)^2 + (Z_1 - Z)^2}} \quad \text{for } Z_1 \geq Z. \\ k &= k_1 \frac{(Z - Z_1)}{\sqrt{(R-r)^2 + (Z_1 - Z)^2}} \quad \text{for } Z > Z_1. \end{aligned}$$

If  $Z_1 \geq L > 0, R = 0, r > 0$  then

$$\begin{aligned} I &= 2 \alpha \pi \left( \tan^{-1} \frac{Z_1}{r} - \tan^{-1} \frac{(Z_1-L)}{r} \right) \\ &- 2 \alpha \mu b \rho \pi \ln \left( \frac{Z_1 + \sqrt{r^2 + Z_1^2}}{(Z_1-L) + \sqrt{r^2 + (Z_1-L)^2}} \right) + \frac{\alpha \pi L \mu^2 b^2 \rho^2}{r} - \dots \end{aligned} \quad (20)$$

where  $0 \leq \tan^{-1} \frac{Z_1}{r}, \tan^{-1} \frac{(Z_1-L)}{r} < \pi/2$ .

If, however,  $L \geq Z_1 \geq 0$ ,  $R = 0$ ,  $r > 0$ , then

$$\begin{aligned}
 I &= 2 \alpha \pi \left[ \tan^{-1} \left( \frac{Z_1}{r} \right) + \tan^{-1} \left( \frac{L-Z_1}{r} \right) \right] \\
 &- 2 \alpha \mu b \rho \pi \ln \left\{ \frac{[(L-Z_1) + \sqrt{r^2 + (L-Z_1)^2}] [Z_1 + \sqrt{r^2 + Z_1^2}]}{r^2} \right\} \quad (21) \\
 &+ \frac{\alpha \pi L \mu^2 b^2 \rho^2}{r} - \dots
 \end{aligned}$$

where  $0 \leq \tan^{-1} \left( \frac{Z_1}{r} \right)$ ,  $\tan^{-1} \left( \frac{L-Z_1}{r} \right) < \pi/2$ . In Equations (18) and (19) terms of the form:

$$\int \frac{K(k) dk}{1 - (k/k_1)^2}$$

may be integrated graphically.

The above expressions have been evaluated for both the 1-kilocurie source and the 10-kilocurie source with reference to the stainless-steel pressure vessel, Fig. 1. The locations studied are indicated in Fig. 47. In Fig. 48 dose rate is plotted against vertical position inside the reactor for the 1-kilocurie source, while Fig. 49 is a similar plot for the 10-kilocurie source. The dose rates for the location of the bomb in the center of the source were calculated separately, and are not shown in Fig. 49. In Fig. 50, the data of Fig. 48 are averaged and plotted against time, assuming that cobalt-60 has a half-life of 5.3 years. In Fig. 51 the data for the 10-kilocurie source (from Fig. 49) are plotted similarly against time.

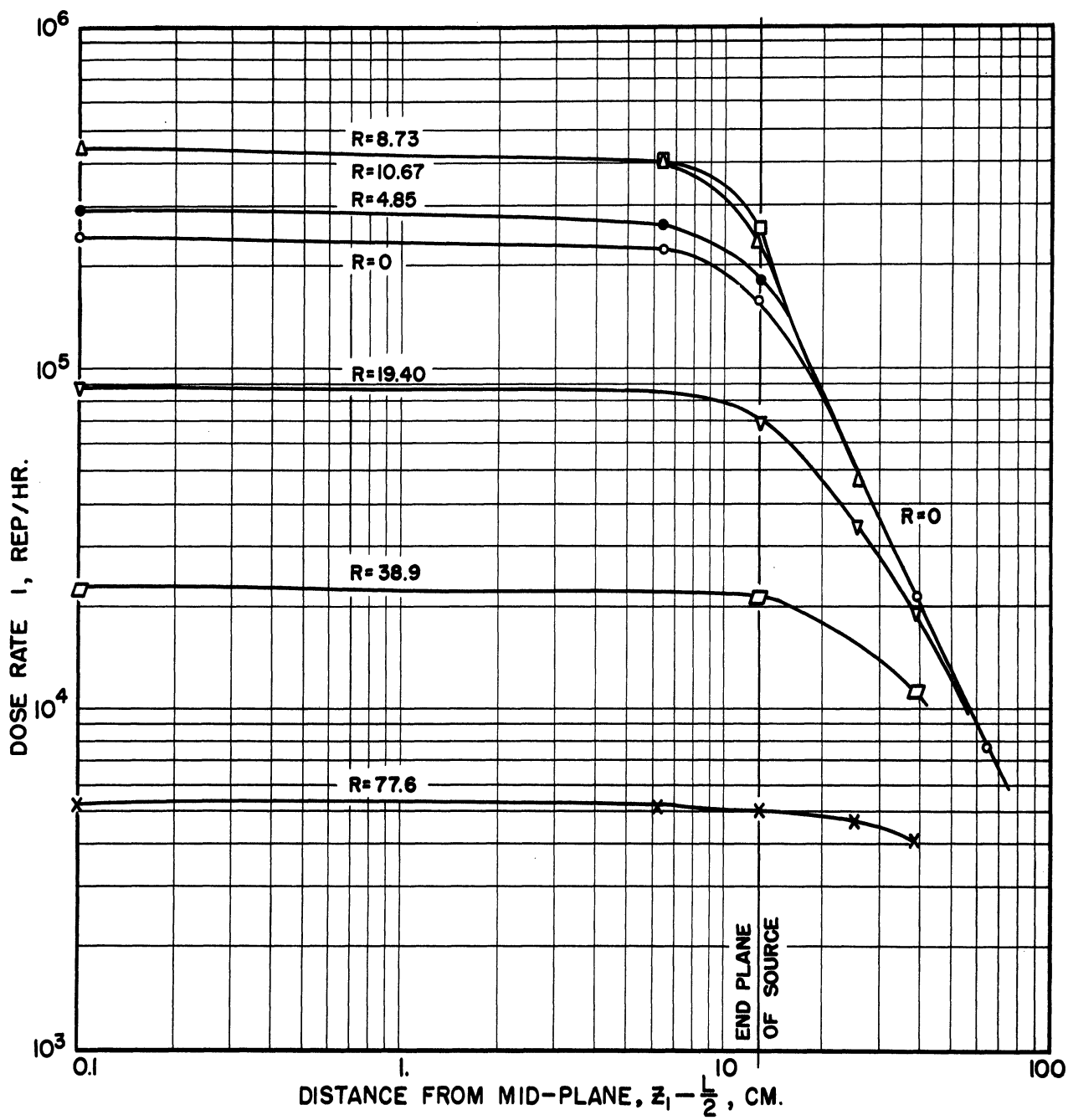


Fig. 40. Dose Rates Parallel to Axis, Interpolated from Measurements with 10-Kilocurie Source.

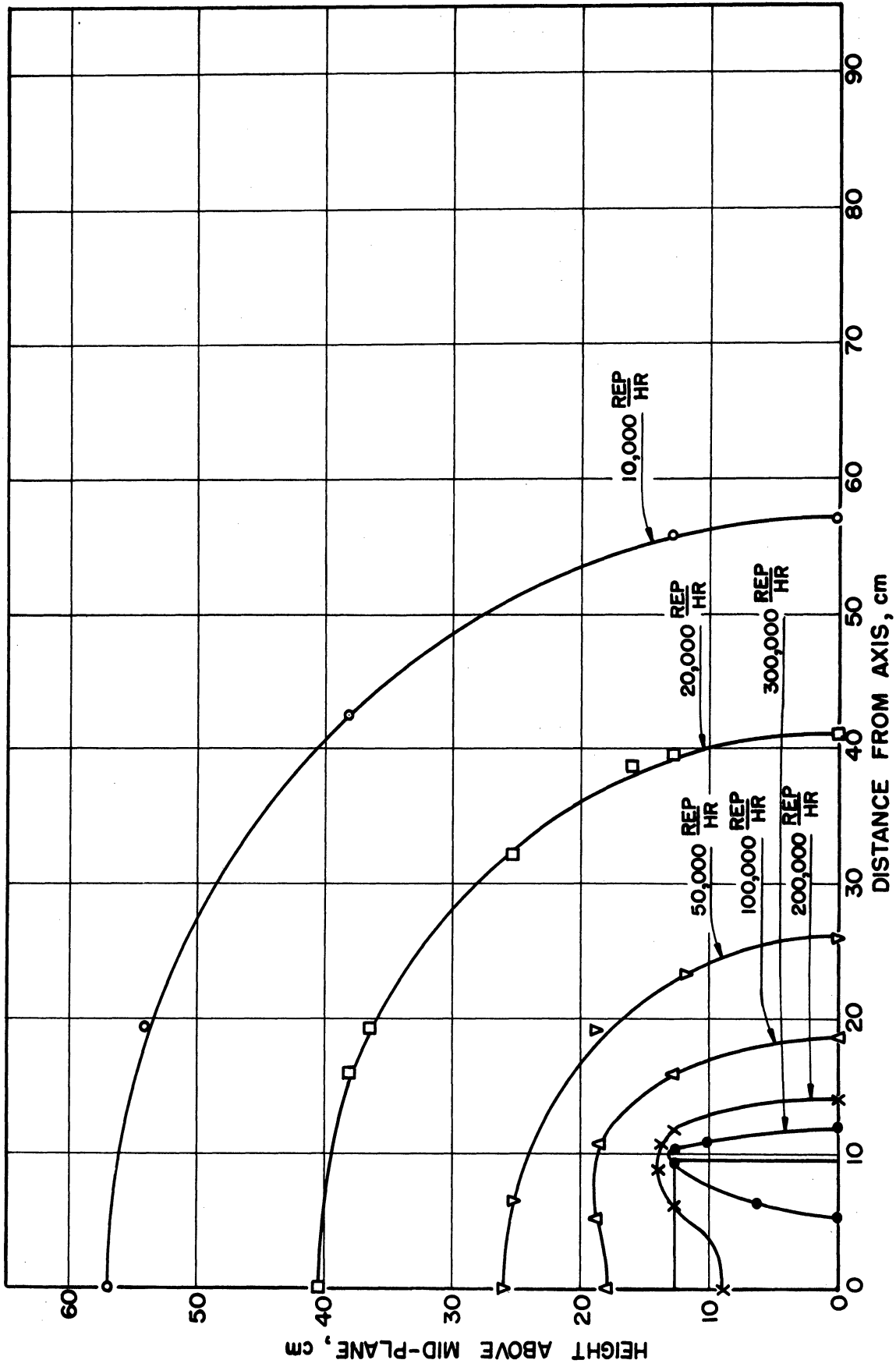


Fig. 41. Isodose Surfaces Interpolated from Measurement with 10-Kilocurie Source.

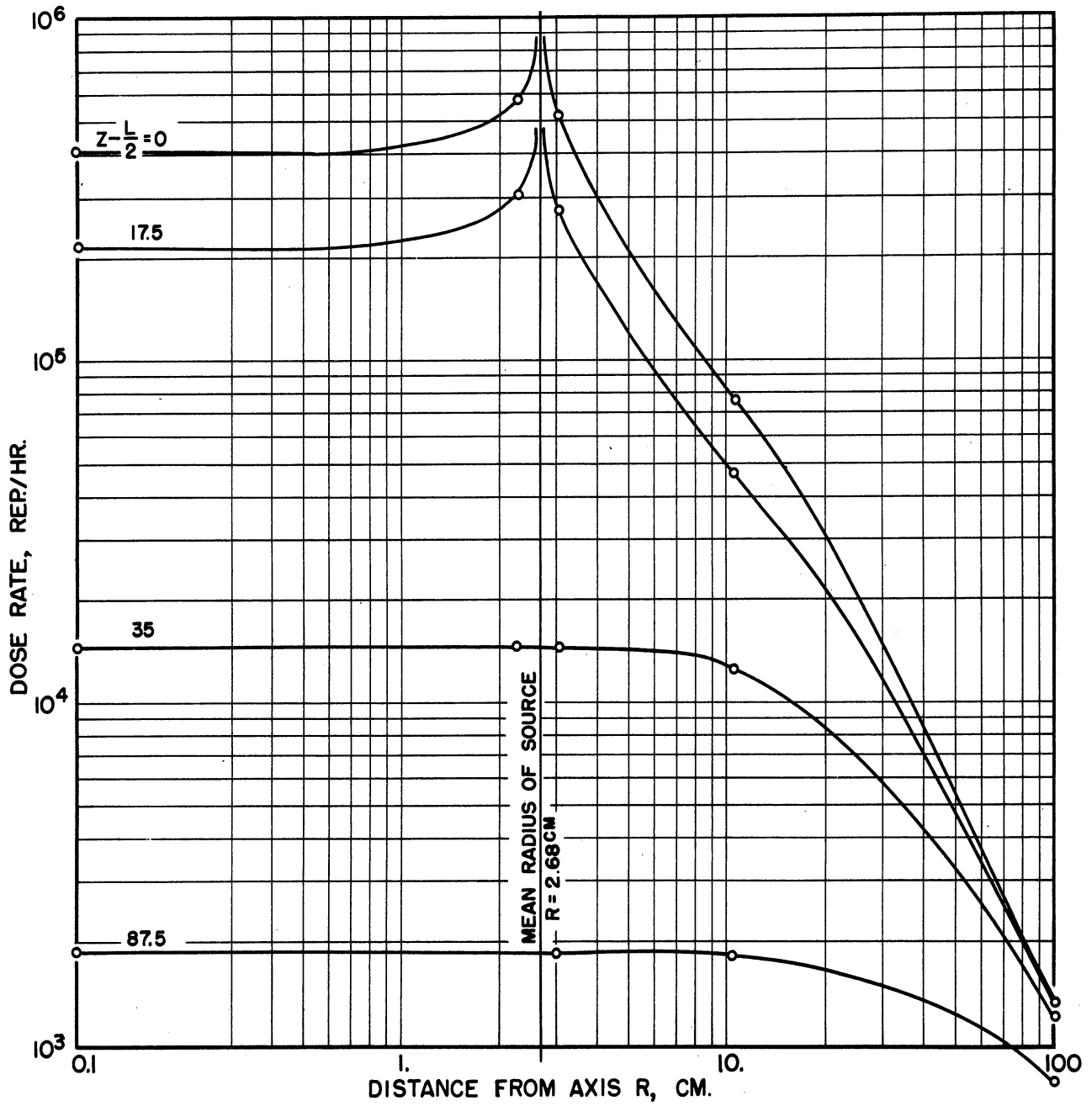


Fig. 42. Calculated Dose Rates Parallel to Mid-Plane with 1-Kilocurie Source.



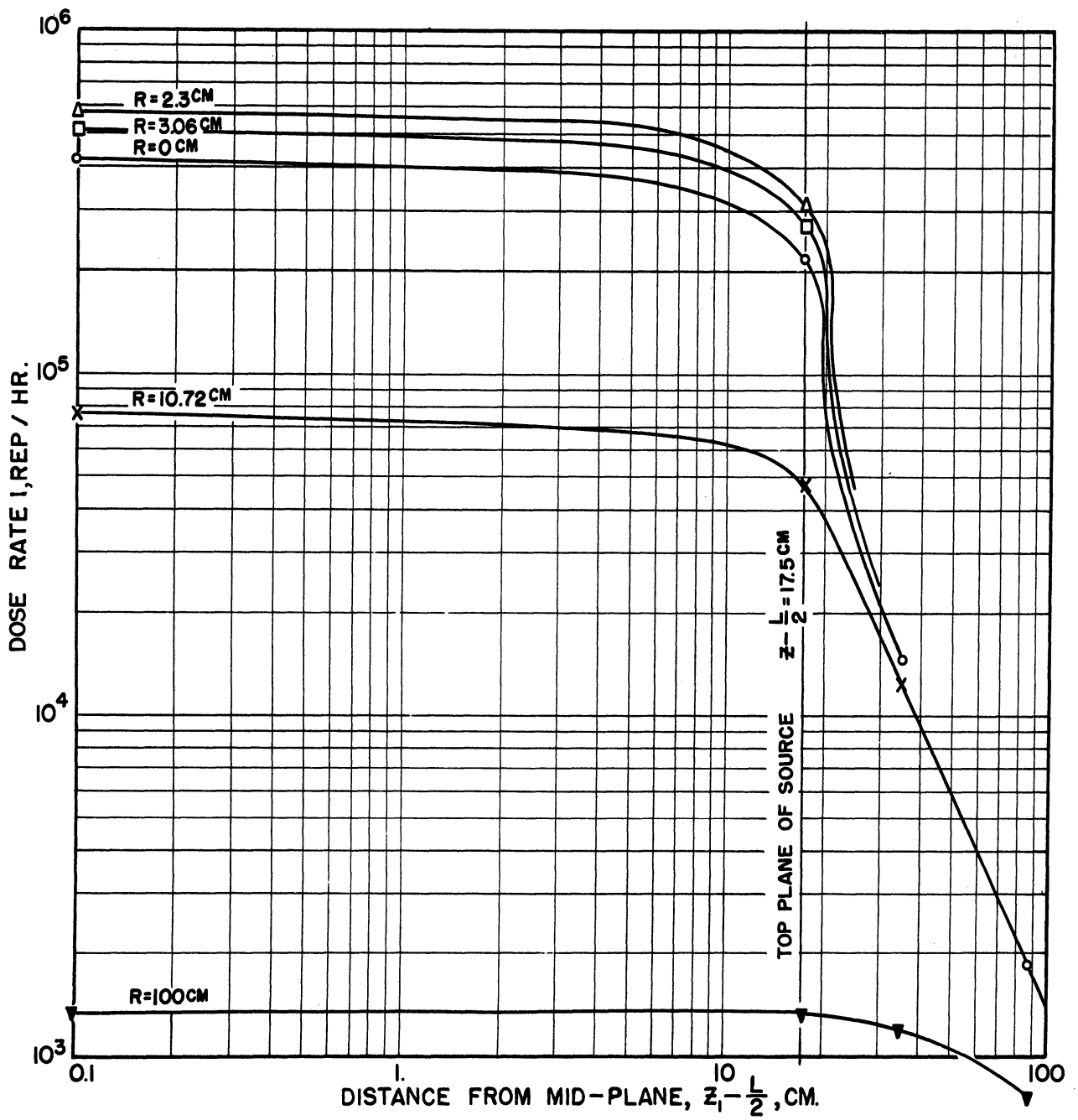


Fig. 43. Calculated Dose Rates Parallel to Axis with 1-Kilocurie Source.

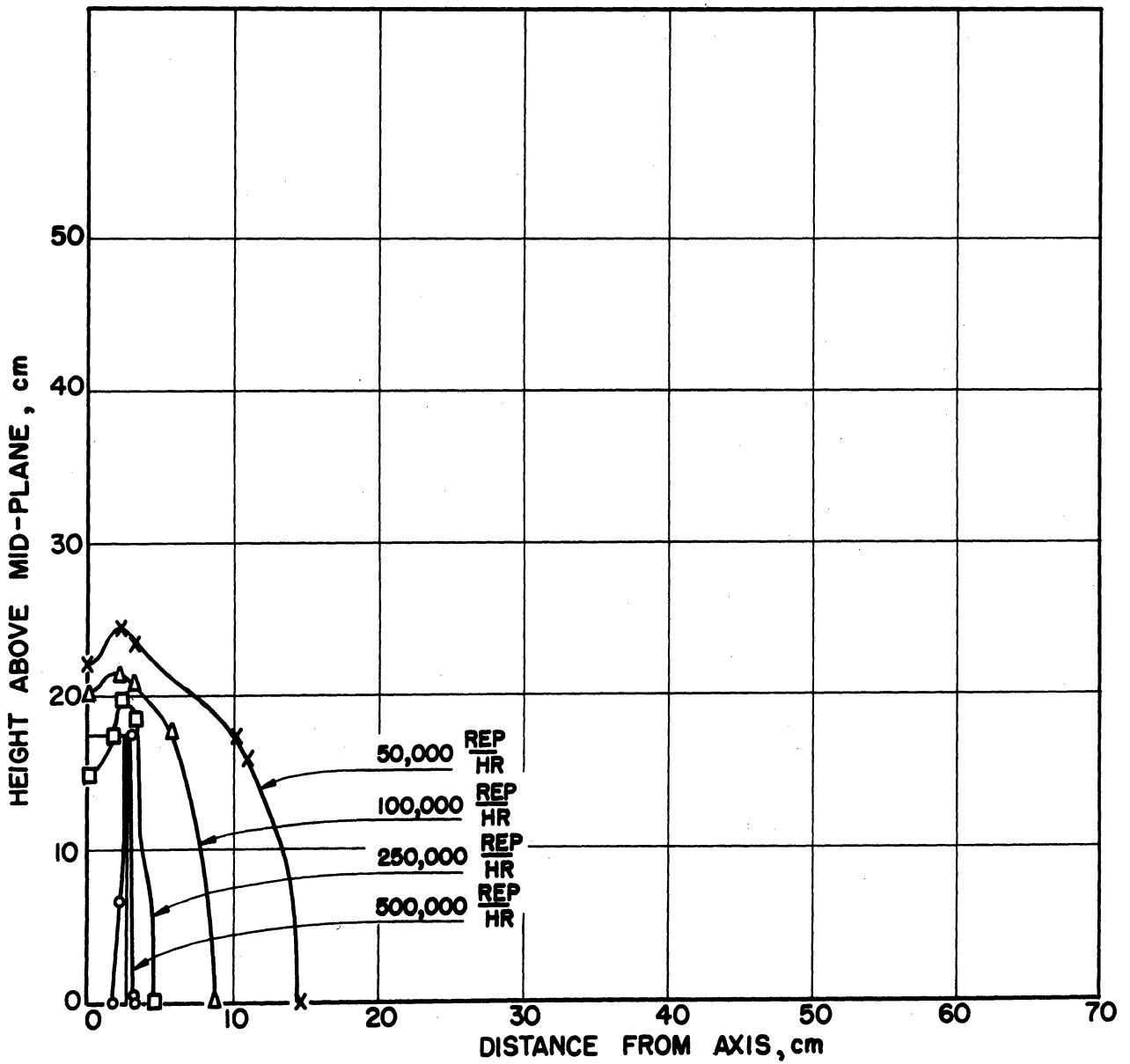


Fig. 44. Calculated Isodose Surfaces with 1-Kilocurie Source.

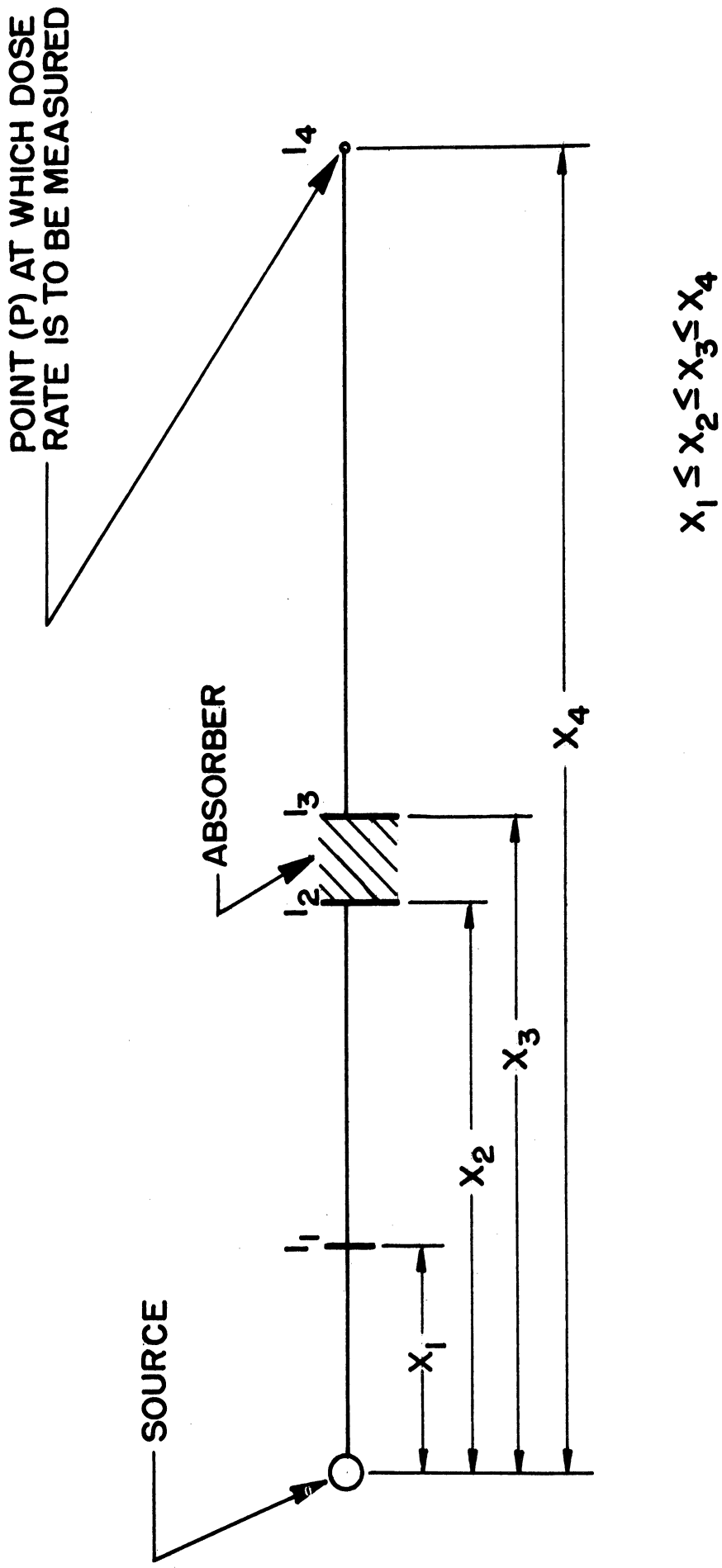


Fig. 45. Diagram for Attenuation by Distance and Absorption.

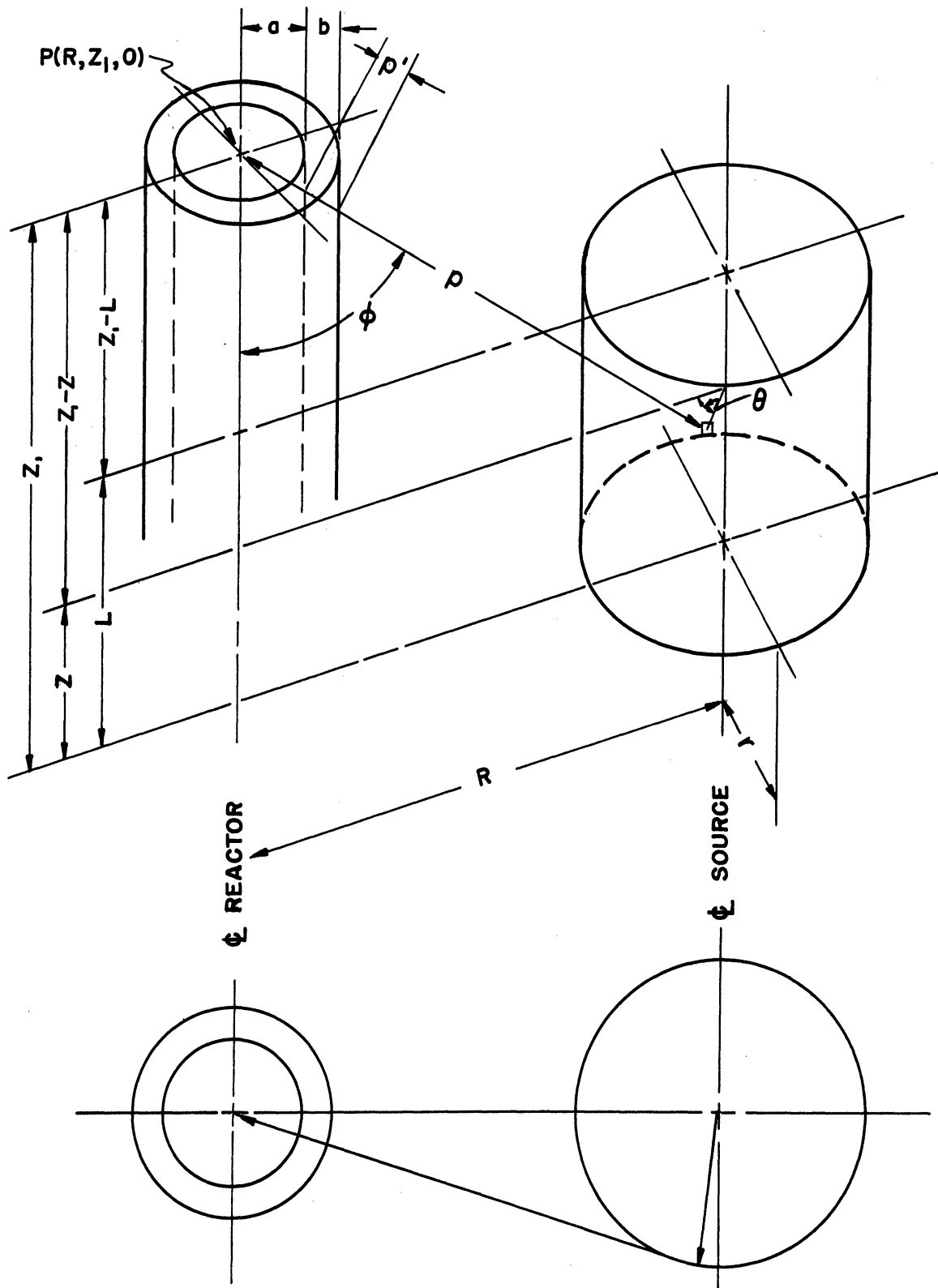


Fig. 46. Diagram for Dose Rate Inside Pressure Vessel.

## PRELIMINARY INVESTIGATIONS

A survey of the literature relating to radiation chemistry indicated that few reactions appeared to be accelerated sufficiently by gamma radiation alone to warrant serious thought of commercial exploitation. However, much of the data reported was secured with the aid of relatively small sources of radiation. It was desired to check some of these results, employing the 1-kilocurie and the 10-kilocurie gamma sources of cobalt-60 at the University of Michigan as described by Anderson, Martin, et al.<sup>5,8</sup>.

### Synthesis of Ammonia

Of the various reactions reported in the literature to be accelerated by radiation, the synthesis of ammonia appeared promising. Boullé<sup>12</sup> investigated the influence of cathode rays and of various metallic catalysts on the kinetics of the ammonia synthesis. D'Olieslager and Jungers<sup>21</sup> investigated some effects of alpha radiation, as did Lind<sup>40</sup>, using alpha rays from radon. In Gmelins Handbuch<sup>26</sup> are reviews of numerous articles dealing with attempted syntheses of ammonia by the use of radiation and electrical discharges. It was thought that if gamma radiation would accelerate the ammonia reaction at a given temperature, then perhaps prevailing industrial rates of reaction could be secured at lower temperatures than those commonly used. Lower temperatures would result in a more favorable percentage of ammonia at equilibrium. Such a circumstance would have permitted the designer of an ammonia plant additional options in the choice of processes to be employed.

Harmer<sup>6</sup> attempted in this laboratory to synthesize and to decompose ammonia at atmospheric pressure by cobalt-60 gamma radiation. The results

failed to indicate the formation or decomposition of ammonia in any experiment. Nessler's reagent, alkalimetry, and combustion tests were used to analyze for ammonia and for hydrogen. It was suspected that the low density of the synthesis mixture and the attendant low absorption of gamma rays were responsible to some extent for the failure to obtain measurable yields of ammonia. However, increasing the pressures to about 100 atm also failed to produce measurable yields, as shown by some tests made at 1200 psig and room temperature. Palladium-109 beta radiation and the pressure vessel illustrated in Fig. 1 were used in these tests. The use of the analytical methods mentioned above for the atmospheric tests indicated no measurable formation of ammonia. The data appear in Table VI.

TABLE VI

## IRRADIATION OF MIXTURE OF NITROGEN AND HYDROGEN WITH PALLADIUM-109 BETA RAYS

Page No.	Time Elapsed, hrs	Time	Date	Curies Pd-109 1st Foil	Pressure, psig 3000 lb/gm, not Calibrated			Temperature, °F
					N <sub>2</sub>	H <sub>2</sub> (by diff.)	Total	
124214	0	2100	17 Jan 52	1.2	300	800	1100	70 <sub>+5</sub>
	0.75	2145					750	70 <sub>+5</sub>
	11.6	0835	18 Jan 52	0.95		705	70 <sub>+5</sub>	

Reactor vented to 505 psig at 11.6. Effluent gas passed through Nessler's reagent. Negative test for ammonia.

However, Selke et al.<sup>46</sup> have obtained measurements of the yields of ammonia in similar experiments, using more sensitive methods of detection. These workers<sup>47</sup> reported yields up to 0.0046 mole percent of ammonia in a reaction mixture of nitrogen and hydrogen exposed to gamma radiation.

The investigation of the ammonia synthesis was suspended after the above results became known. Fortunately the possibility of wishing to

study different reactions had been foreseen in the design of the equipment for studying the ammonia synthesis. Consequently, it was possible to adapt the equipment to the study of other reactions without difficulty.

#### Beta Radiation from Palladium-109

We were also interested in the use of beta radiation as well as gamma radiation for the purpose of promoting chemical reactions. It had been thought that beta radiation, being more completely absorbed than the gamma radiation, would be correspondingly more effective in promoting chemical reactions. The following experiments were devised in order to test this idea when some sources of beta radiation became available for the use of the author and co-workers. These sources were three pieces of palladium-109 foil varying from about 20 to about 100 curies of initial beta activity and were originally procured in connection with some other experiments of the Engineering Research Institute of the University of Michigan.

Beta radiation from palladium-109 was used in an attempt to synthesize ammonia from its elements. See the description of this work under "Synthesis of Ammonia".

Some experiments were conducted as described below in order to test the effect of beta radiation on the rate of drying of some natural oils. A foil of palladium-109 was wrapped in a pliofilm sheath and laid over a 1/4-inch galvanized wire mesh separating it from weighed samples of several different natural oils. Each oil sample was placed on a 2.5-cm-diameter watch glass. A control test, differing only by the absence of radiation, was also set up. Each test was allowed to run for one week. The results are summarized in Table VII. The experimental setup is shown in Fig. 52. From the data in Table VII it was concluded that the irradiation of drying oils with Pd-109 beta radiation did accelerate the drying of some of the samples tested. The effect was of relatively small magnitude, however, and

TABLE VII

## RESULTS OF IRRADIATION OF NATURAL OILS WITH PALLADIUM-109 BETA RAYS

Foil received 1 March 1952.

Material	Percentage Gain in Weight		Remarks	
	<u>Test</u>	<u>Control</u>	<u>Test</u>	<u>Control</u>
Raw Linseed	+7.8	+0.53	tough, rough film	no change
Boiled Linseed	+5.7	+7.0	tough, rough film	tough, rough film
Degummed Soya	+5.8	+0.39	tough, smooth film	no change
Castor	+1.3	-0.58	no change	no change
Refined Menhaden	+9.3	+4.5	tough, smooth film	no change
Cottonseed Pitch	-0.36	-0.19	no change	no change

Schedule of above irradiation

Time	Date	Curies Pd-109 <u>3rd Foil</u>	Remarks Temperature, 70-80°F
0300	2 Mar 52	120	Start irradiation of oils
0800	2 Mar 52	100	
0800	3 Mar 52	33	
0800	4 Mar 52	14	
0800	5 Mar 52	7	
0800	6 Mar 52	4.5	
0800	7 Mar 52	3.4	
0800	11 Mar 52	2.1	
1400	11 Mar 52	2.0	End of irradiation of oils



it was not considered worthwhile to secure more beta sources to continue the investigation.

#### Partial Polymerization of Natural Oils

It was desired to investigate the effects of gamma radiation on some natural fats and oils. Data reported by Sheppard and Burton<sup>48</sup> indicate extensive decomposition of several fatty acids irradiated with alpha particles from radon. Burton<sup>15</sup> reported decarboxylation, polymerization, and hydrogenation of oleic acid irradiated with deuterons. Coolidge<sup>16</sup> reported on the solidification of castor oil by cathode rays outside the generating tube.

Partial polymerization or "bodying" is a necessary step in the processing of some natural oils, and is accomplished by means of prolonged heating under vacuum. A long induction period at high temperature, followed by a rapid reaction, indicated that the reaction proceeds by a free-radical mechanism. The prolonged heating may be needed to form free radicals in sufficient concentrations to initiate the desired reaction successfully. There is evidence that free radicals are formed in some materials by gamma irradiation (see the work of Allen<sup>1</sup>). If free radicals could be formed at the outset instead of by the slow process of thermal formation, then the desired polymerization might follow almost immediately.

The experimental procedure used in testing the effect of gamma radiation from Co<sup>60</sup> on refined soya oil was as follows. Samples of oil in glass containers were irradiated in the 1-kilocurie vault for about 24 hours and then were heated in a glass flask by an automatically regulated gas flame. The flask was evacuated to an absolute pressure of about 1 millimeter of mercury. An air-cooled condenser was connected in series with a water-cooled condenser and the two were placed between the vacuum pump and the flask. Nordco No. 460 grease was used on all standard taper joints.

Data for these tests are given in Table VIII. Samples irradiated and then heated for 6 hours were more viscous than samples not irradiated but heated for 6 hours. The effect appeared to be small, however. The complexity of the reactions in bodying of natural oils is so great that it would be difficult to assess the effects of radiation alone. A study of the bodying of

TABLE VIII

## CHANGES IN VISCOSITY OF SOYA OIL AFTER IRRADIATION AND SUBSEQUENT HEATING

The starting material used in each run was dry, refined, degummed soya oil.\*

Run No.	Irradiation	Temperature, °F	Time of Heating, hr.	Viscosity		Pressure, mm Mercury, Absolute
				G-H	Poises	
11	24 hr, Co <sup>60</sup>	572	6	N+1/3	3.5	1
12	--	572	6	J	2.5	1
13	24 hr, Co <sup>60</sup>	572	6	L	3.0	1
14	24 hr, Co <sup>60</sup>	572	6	L	3.0	1
15	--	572	NG-air leak	--	--	>12
16	24 hr, Co <sup>60</sup>	572	6	L	3.0	1
17	--	572	6.3	L	3.0	1
18	--	572	6.2	J	2.5	1
19	--	572	6	J	2.5	1
26	24 hr, Co <sup>60</sup>	600	6	Z4	63.4	1
27	--	600	NG-air leak	--	--	>10
28	24 hr, Co <sup>60</sup>	600	6	Z4+1/4Z5	69.4	1
29	--	600	NG-boiled over	--	--	1
30	--	600	6	Z1+2/3Z2	33.0	3
31	--	600	6	Z3+1/2Z4	54.8	3-4

\*Donated by Wyandotte, Michigan, plant of Archer-Daniels-Midland Company.

oil by irradiation would not be worth while from an industrial point of view unless a large increase in the rate of reaction could be achieved. Since the effect studied was found to be small, it seemed desirable to drop the work on natural oils and to work instead with some relatively simple, pure materials in order to be able to isolate the effects of radiation. Further work might be done by studying the chemical changes in pure components of the oils when subjected to irradiation as described above.

### Polymerization of Acetylene

A preliminary test was made of the polymerizing effect of gamma radiation on acetylene. Mund and Koch<sup>43</sup> and Lind and Bardwell<sup>37</sup> had reported the polymerization of acetylene by alpha rays from radon. Rosenblum<sup>45</sup> reported the formation of benzene by the irradiation of acetylene with alpha rays from radon. In the following work acetylene was irradiated under pressure in order to find possible evidence of the polymerization of acetylene to benzene under gamma radiation.

Acetylene was irradiated with  $1.9 \times 10^6$  rep in air of cobalt-60 gamma radiation. The acetylene was dissolved in acetone which had first been absorbed in a dried mixture of Portland cement and asbestos. The cakes of cement were placed in the pressure reactor (Fig. 6), which was fitted with an aluminum rupture disc designed to burst at 150 psig. The reactor was evacuated with the cement in place, flushed with nitrogen, and evacuated again. Then 105 grams of acetone was added and acetylene introduced until an equilibrium pressure of 5 psig was reached. The reactor thus charged was irradiated for 24 hours, after which the volatile contents were recovered by immersing the reactor in hot water and heating the discharge pipes with infrared lamps. Subsequently, the reactor was evacuated while being heated in the manner just described. During the heating and evacuation all effluent material was passed through dry-ice traps. The

condensed liquid was distilled in a Podbielniak column, where it was observed that the overhead temperature during the distillation was not significantly different from that of acetone. About 0.2 gram of a brownish, waxy solid was recovered from the pot of the column. This material was insoluble in acetone. No further work was done along this line because of the small yield and indefinite nature of the product.

#### Chlorination of Kerosene and of Benzene

Attention was then turned to investigating the influence of gamma radiation on chlorinations. Alyea<sup>3</sup> reported the addition of chlorine to benzene under alpha radiation from radon. The chlorination of hydrogen under ultraviolet light was studied by Lind and Livingston<sup>39</sup>. The first chlorination studied in this laboratory was that of kerosene. Gaseous chlorine was dissolved in a sample of kerosene. The sample was divided, one half placed in the 1-kilocurie vault and the other half retained in the dark. After irradiation of the test sample both samples were shaken with sodium hydroxide pellets and analyzed for total organic chlorides by the method of Liggett<sup>55</sup>. The data of Table IX indicate no difference between the irradiated and unirradiated samples. The reason for this behavior is probably to be found in the fact that all samples were allowed to stand one week before being analyzed, during which period chlorination probably proceeded to the exhaustion of chlorine both with and without radiation.

Consequently it seemed wise to compare the kinetics of the irradiated and the unirradiated reactions. However, it was thought that such a program of study should be carried out on a pure compound instead of kerosene, which is of uncertain and variable composition. It was tentatively planned to use benzene for these studies. A test by Harmer indicated a rapid, nearly complete reaction of benzene and chlorine to hexachlorocyclohexane under gamma radiation. Slator<sup>50</sup> and Luther and Goldberg<sup>41</sup> have noted

TABLE IX

## IRRADIATION OF MIXTURES OF KEROSENE AND CHLORINE IN 1-KC COBALT-60 GAMMA SOURCE

Page No.	Start Date	Pressure, ATM, ABS	Avg. Temp. °F	Hours Irrad.	Dose Rate Kilorep per hr.	Total Dose Kilo-rep	Sample No.	Percentage, Chlorine	Date of Analysis	Remarks
124216	1 Feb 52	1	70	--	zero	--	1	1.68 1.66	10 Mar 52	Duplicate detns., unirradiated
		1	70	24	63	1500	1	1.42 1.42	14 Mar 52	Duplicate detns., irradiated
124245	1 Mar 52	1	70	--	zero	--	2	1.36 1.37	14 Mar 52	Duplicate detns., unirradiated
		1	70	24	63	1500	2	1.38 1.36	14 Mar 52	Duplicate detns., irradiated

For sample No. 1, Chlorine was dissolved in two separate portions of kerosene and one was irradiated.

For sample No. 2, Chlorine was dissolved in a single portion of kerosene. This was divided in two, and one half was irradiated.

a similar catalytic effect of ultraviolet light on this reaction.

Subsequent investigations conducted in the apparatus portrayed in Fig. 53 indicated that the yield of gamma isomer, valuable as an insecticide, was nearly the same as that ordinarily achieved industrially with the aid of ultraviolet light, i.e., about 12.5 percent by weight of the products of chlorination. This yield was also nearly independent of temperature in the region investigated, i.e., 14°F to 68°F. Recrystallization and extraction procedures were used on some samples to achieve some separation of isomers. A melting-point bar of the design of Dennis<sup>18</sup>, Fig. 54, was constructed to assist in this work. Table X summarizes the data obtained from this series of runs.

#### Oxidation of Sulfur Dioxide

Backstrom<sup>10</sup> and Alyea and Backstrom<sup>2</sup> reported the investigation of the oxidation of sulfur dioxide, both in ultraviolet light and in the dark.

Oxidations of sulfur dioxide were attempted by three procedures. In the first method sulfur dioxide and oxygen were simultaneously bubbled through water in a vessel in the 1-kilocurie vault. The apparatus used was nearly the same as that of Fig. 53, used for the benzene hexachloride experiments. Iodometric-acidimetric titrations as described by Bodenstein and Pohl<sup>11</sup> were used to determine sulfurous and sulfuric acids in the tail-gas scrubbers and in the reactor. Sulfate was determined gravimetrically (Willard and Furman<sup>59</sup>) in both the reactor and tail-gas scrubbers. The results appear in Table XI.

In the second procedure sulfur dioxide and oxygen were admitted to the reactor of Fig. 1, which had previously been evacuated. A heater was silver-soldered to the copper leads inside the reactor. The heater consisted of 18 gauge chromel-A wire coiled on a 1/8-inch arbor, stretched

TABLE X  
IRRADIATION OF MIXTURES OF BENZENE AND CHLORINE IN 1-KC COBALT-60 GAMMA SOURCE

Page No.	Start Date	Pressure, ATM ABS	Avg. Temp. of reaction, °F	Hours Irrad.	Dose Rate Kilo-rep/hr	Total Dose Rep	Percent Benzene (by vol)	Percent Carbon tetrachloride (by vol)	Percent* Gamma Isomer in Benzenehexachloride
129771	11 Aug 52	1	68	0.42	64	27	10	90	11.3 (over chlorinated)
129770	11 Aug 52	1	68	0.33	64	21	20	80	12.5
129773	12 Aug 52	1	14	0.73	64	47	10	90	12.3
129774	12 Aug 52	1	14	0.55	64	35	30	70	12.8

\*Analyses through courtesy of E. I. du Pont de Nemours and Company, Engineering Service Division.

TABLE XI

## IRRADIATION OF MIXTURES OF SULFUR DIOXIDE AND OXYGEN IN 1-KC COBALT-60 GAMMA SOURCE

Page No.	Start Date	Temp. °F	Hours Irrad.	Average Dose Rate Kilorep/hr	Dose, Kilorep	Percentage $\text{SO}_2$ Converted to $\text{SO}_3$ , Based on $\text{SO}_2$ Recovered in Reactor		Procedure
						by iodine method	by gravimetric method	
132184	9 Jan 53	70	1.5	62	93	4.4	---	aqueous $\text{SO}_2+\text{O}_2$
132189	13 Jan 53	70	1.1	62	68	6.1	6.7	aqueous $\text{SO}_2+\text{O}_2$
132192	16 Jan 53	70	0.6	62	37	10.6	6.4	aqueous $\text{SO}_2+\text{O}_2$
132179	16 Dec 52	65-240	2.8	29	81	---	1.3	gaseous $\text{SO}_2+\text{O}_2$
132194	19 Jan 53	56-510	none	--	--	4.4	3.2	liquid $\text{SO}_2+\text{O}_2$
132198	4 Feb 53	296-400	4.3	28.5	120	3.7	1.8	liquid $\text{SO}_2+\text{O}_2$

TABLE XII

## IRRADIATION OF PROPYLENE

Page No.	Start Date	Time	Hours Irrad.	Dose Rate, Rep/hr	Dose, Rep	Temp., °F	Pres., psia	Remarks
132140	9 Feb 53	1313	67.6	29,000	2,000,000	66	145	Out of vault.
132140	18 Feb 53	1000	---	---	---	Room	25-30	0.2--0.3-in.-depth liquid in bottom, quickly evaporated.



to double the close-wound length, and inserted into a 10-mm-O.D. pyrex tube. The tube was then bent into a "U" shape to fit inside the bomb. The reactants were heated by this hot-wire heater while being irradiated in the 1-kilocurie vault. Samples of gas were absorbed in standard iodine contained in an Orsat pipette, using mercury for the levelling fluid. Shrinkage of volume was measured. Then the contents of the pipette were back-titrated with thiosulfate and then with alkali. In addition some of the gas was absorbed in water and sulfate was determined gravimetrically, as for the aqueous solutions described above. The results appear in Table XI.

A third procedure used to study the oxidation of sulfur dioxide was to liquefy sulfur dioxide in the open body of the reactor, Fig. 1, seal the reactor, warm to room temperature, and place the reactor in the 1-kilocurie vault. The assembled reactor, or bomb, was then heated to a temperature of about 500°F, and oxygen was slowly bubbled into the liquid sulfur dioxide. The bomb was cooled, the gas vented and absorbed in water, and the sulfurous and sulfuric acids determined by iodometric-acidimetric and by gravimetric methods, as before. Results of these tests also appear in Table XI. Under the conditions used, irradiation evidently did not accelerate significantly the oxidation of sulfur dioxide.

#### Reaction of Carbon Dioxide with Hydrogen

A test was made to determine whether carbon dioxide and hydrogen would react in the presence of gamma radiation. The purpose of this work was to test the possibility of formation of formaldehyde and similar oxygenated hydrocarbons.

Carbon dioxide was therefore introduced into the evacuated bomb to a pressure of 680 psia. Hydrogen was added until the pressure was 1070 psia, and the bomb was then irradiated in the 1-kilocurie source for 16 hours in November, 1952. No reaction was observed.

### Polymerization of Isobutylene

Polyisobutylene is of some importance as a plastic, and an attempt was therefore made to polymerize isobutylene by means of gamma radiation.

Isobutylene was liquefied in the open body of the bomb; the bomb was then sealed, warmed to room temperature, and irradiated for about 100 hours in the 1-kilocurie source. The irradiations took place at intervals over a period extending from July to October, 1952. The contents of the bomb were vented to a dry ice trap. About 103 ml of liquid was obtained. The contents of the trap were then poured into a still flask through a vertical condenser cooled by circulating methanol which had been indirectly cooled by dry ice. The still flask was heated by warm water, a reflux was maintained in the vertical condenser, and the overhead was conducted to a dry-ice trap. The distillate was colorless liquid, presumably isobutylene, and the residue left in the flask was a dark straw color. The residue amounted to about 1 ml and had an odor similar to a terpene.

### Polymerization of Propylene

Liquid propylene was irradiated for 67.6 hours at a dose rate of about 25,000 rep/hour, and the results are reported in Table XII. A small quantity of a volatile liquid was found in the reactor when it was vented and opened. Some polymerization therefore took place, but the yield was not measured.

### Polymerization of Ethylene

Acetone and ethylene were introduced into the pressure reactor and irradiated. Some fluffy white powder was obtained. The acetone was added originally to release free radicals on radiolysis and to initiate the chain polymerization of the ethylene.

### Discussion of Preliminary Investigations

If gaseous systems are subjected to higher pressures, their densities are increased. The resulting increased densities cause increased absorption of gamma radiation. Consequently a reaction promoted by gamma radiation in a gaseous system should be accelerated by increased pressure.

Accordingly, some preliminary work was undertaken as noted in the preceding section, to find reactions occurring under pressure which would be accelerated by gamma radiation. Pressure reactions promoted by gamma radiation would be interesting from an industrial point of view because the radiation can pass through the walls of pressure vessels and promote reactions where other forms of radiation could not be used.

The polymerization of ethylene appeared to be the most promising reaction in this category to study further. The yields of polyethylene obtained were not large, but were somewhat larger than those for any of the other reactions studied, except for the chlorinations. In addition, polyethylene is one of the most important of the industrial plastics, and there is currently great interest in the development of manufacturing facilities for this material. Accordingly, further investigations were confined to the study of the polymerization of ethylene by means of gamma radiation.

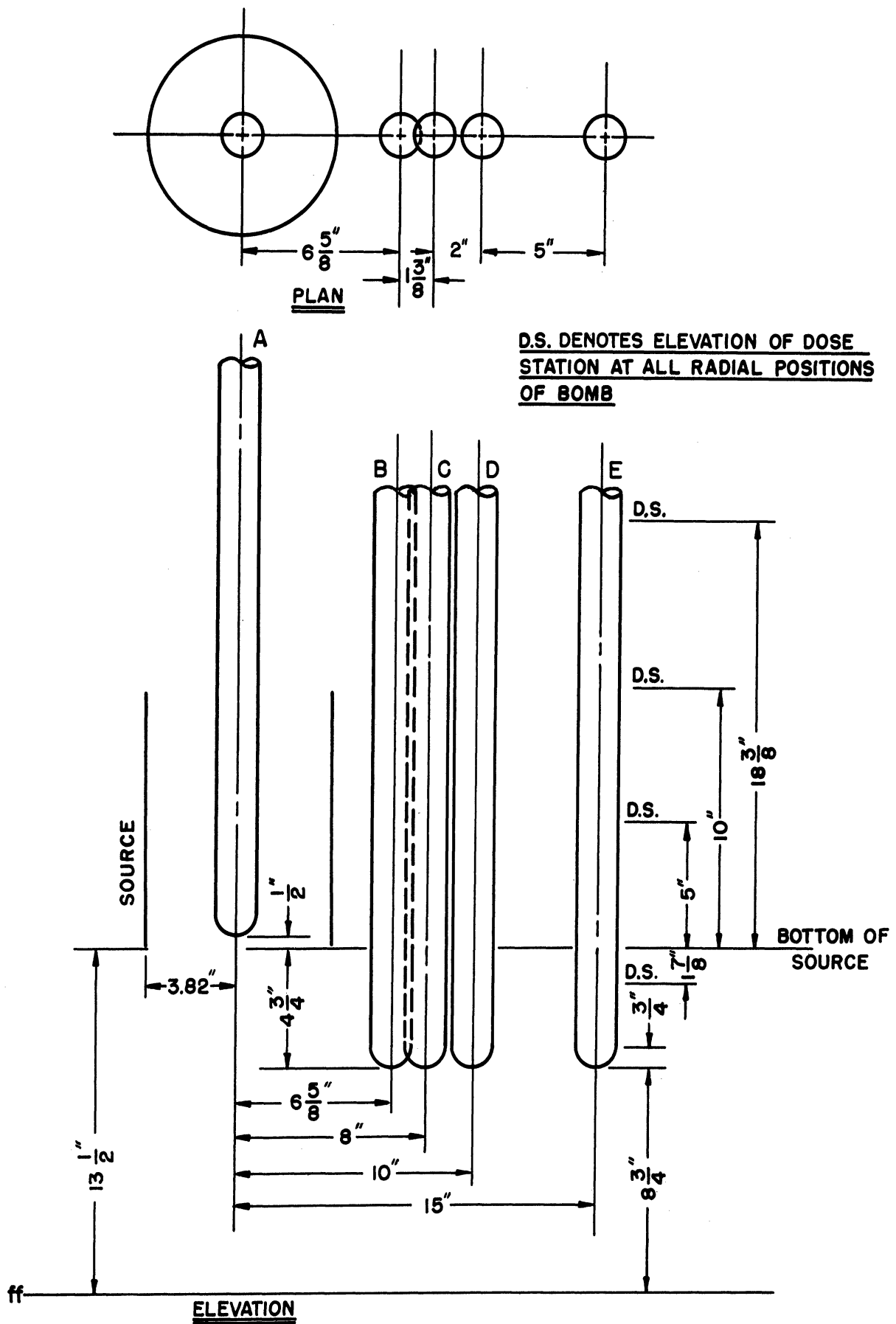


Fig. 47. Location of Pressure Reactor for Dose Rate Studies with 10-Kilocurie Source.

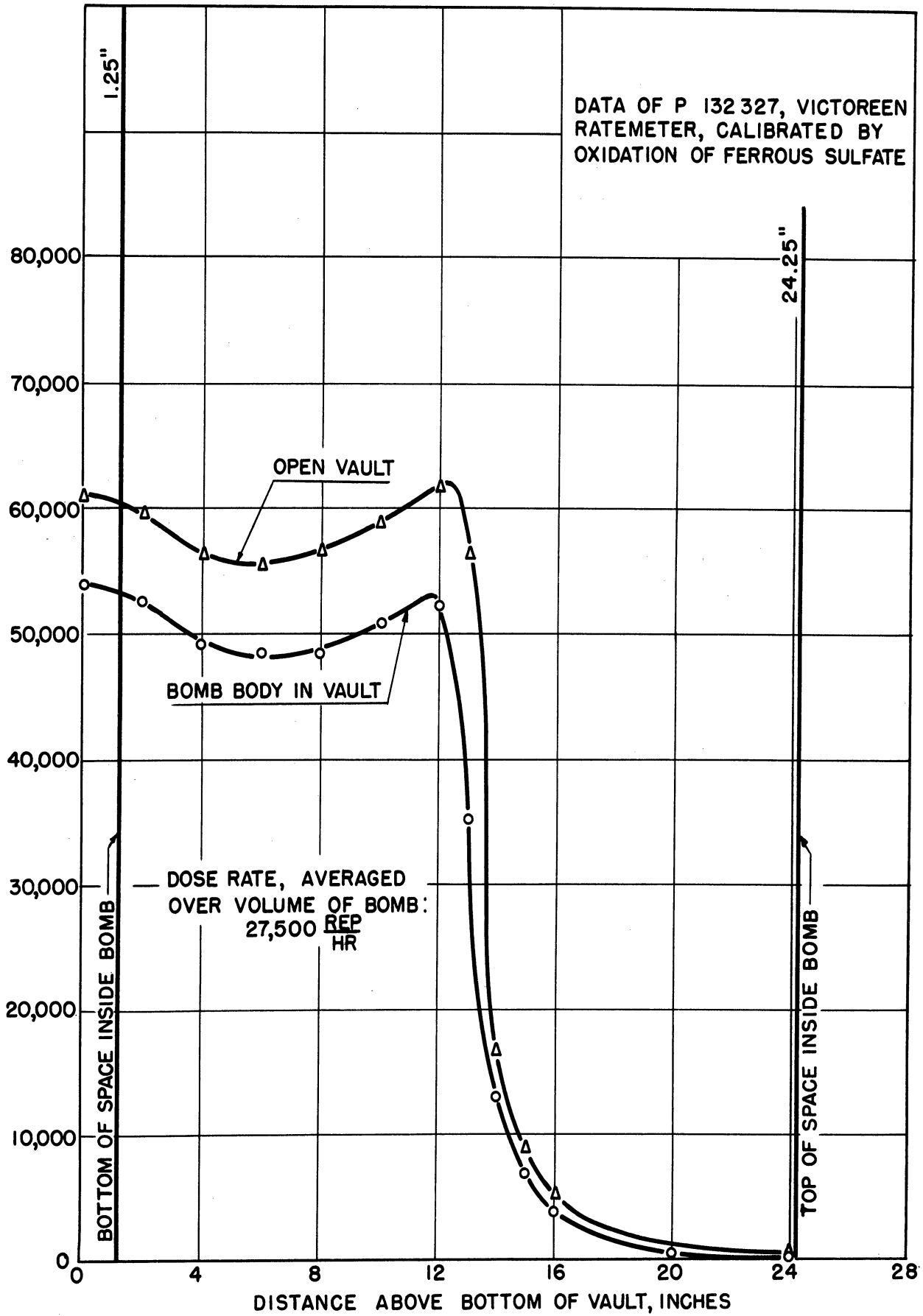


Fig. 48. Dose Rates Inside Pressure Reactor with 1-Kilocurie Source.

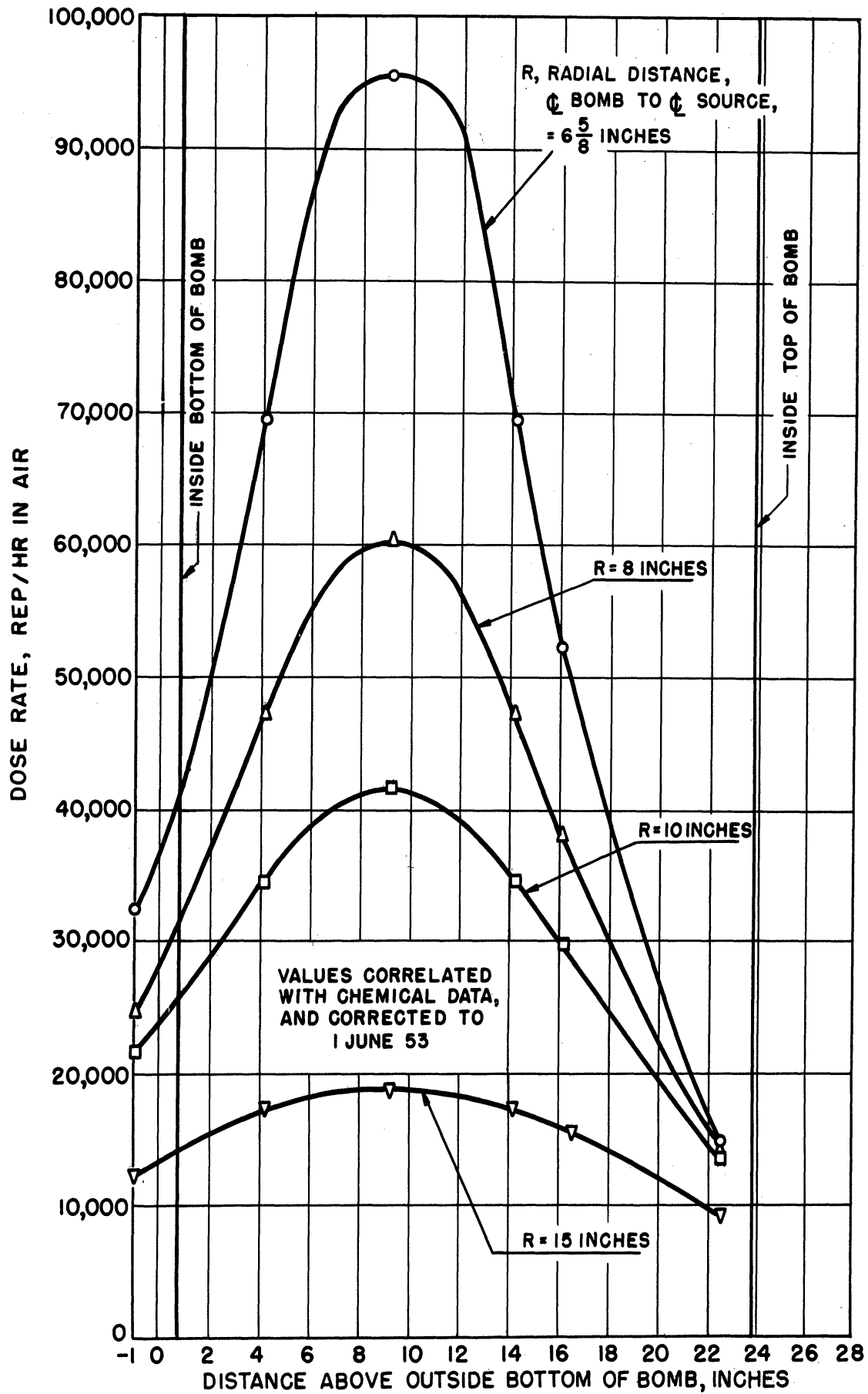


Fig. 49. Dose Rates Inside Pressure Reactor with 10-Kilocurie Source.

## POLYMERIZATION OF ETHYLENE

### Prior Work

Ethylene has been polymerized under various conditions, yielding polymers of widely different properties. At temperatures of 572-1292°F and pressures of 0.2 to 70 atmospheres, ethylene has been polymerized to liquids in the presence of iron, silica, or zinc chloride (Ellis<sup>22</sup>). Such liquids have been of interest principally as fuels for internal-combustion engines and have consisted of mixtures of lower olefins and paraffins. Ethylene has also been polymerized by the use of catalysts consisting of peroxides<sup>62,64,67</sup>, or elementary oxygen<sup>29,63</sup>, as well as by the use of other catalysts<sup>32,65</sup>, to yield products of molecular weights varying from a few hundred to tens of thousands. Such polyethylenes display physical properties ranging from oils when of lower molecular weight to waxlike solids when of intermediate molecular weight and plastic solids when of high molecular weight. These materials are used for a variety of purposes. Planned capacity for the production of polyethylene was reported by Stenerson<sup>54</sup> to be about 200,000 tons per year by 1955. Peroxide- or oxygen-catalyzed reactions were conducted at temperatures of 32 to 752°F by Robertson<sup>68</sup> and by Roedel<sup>69</sup>, although the lower or middle range of temperatures is often preferred in order to produce materials of higher molecular weight. Pressures of 1000 to 2000 atmospheres are often used in order to obtain materials of higher molecular weights.

Ethylene has been polymerized at 77°F and about 1 atmosphere by Lind, Bardwell, and Perry<sup>38</sup> using alpha radiation from radon to initiate the reaction. The products were liquids reported to be olefins of higher molecular weight, and also gases, reported to be hydrogen and methane.

Ethylene has also been observed to polymerize when irradiated with ultraviolet light. LeRoy and Steacie<sup>33</sup> noted that the metal sensitizers cadmium, zinc, and mercury accelerated the polymerization of ethylene irradiated with ultraviolet light and simultaneously caused some dehydrogenation to acetylene. In this work temperatures ranged from 77 to 572°F and pressures from 15 mm to 400 mm of mercury absolute. Danby and Hinshelwood<sup>17</sup> investigated the polymerization of ethylene by ultraviolet light at 572°F and pressures to 400 mm of mercury absolute, as sensitized by acetone, by diethyl ketone, and by acetaldehyde. Taylor and Emeleus<sup>56</sup> found that the polymerization of ethylene was photosensitized by ammonia at 68 to 212°F and 5 to 15 cm of mercury, and the same authors found<sup>57</sup> that methyl and ethyl amines at 2 to 25 cm of mercury and temperatures to 392°F showed similar behavior. These reactions were studied in the gas phase; solid polyethylene was not isolated or studied.

Ethylene has been polymerized by gamma radiation. This reaction has been studied by Bretton et al.<sup>13</sup> at 1 atmosphere and at temperatures ranging from room temperature to 372°F. The products were solids, usually yellowish or brown in color. Other properties of the solids were not reported.

#### Polymerization of Ethylene by Means of Gamma Radiation

Investigative Procedure. As was noted in the section on Preliminary Investigations, one or two initial tests indicated that ethylene could be polymerized by gamma radiation at moderately high rates. As explained above, these observations formed the basis for the decision to study this reaction in greater detail.

The results obtained on resumption of this work were disappointing, however, since the later runs produced very erratic results. Moreover, as noted in Table XIII, the yields decreased considerably.



TABLE XIII

IRRADIATION OF ETHYLENE

Order No.	Page No.	Starting Date	Psig Initial	Psig Final	Avg. P, psi	Avg. Temp., °F	Grams Polymer	Hours Irrad.	Grams Polymer per Hour	A = G-Moles Reacted (Metric Ton)(Megavey)	Averaged over Reactor Dose Rate (Gillorep/Hr)	Total Dose (Megavey)	Other Reactants	Source	Position of Reactor	Mfr.	Cylinder No.	Remarks
2	132113	19 Dec 52	830	785	822	69	1.64	69.7	0.024	608.	2.02	1. MI acetone	1 kc			Matheson	FF 737	
3	132118	12 Jan 53	820	795	822	70	0.666	61.	0.011	485.	28.9		1 kc			"	"	
4	132147	5 Mar 53	1330	1350	1325	250	0.292	17.2	0.017		29.5		10 kc	8" NE 9" up		"	"	
5	132149-II	7 Mar 53	820	775	797	50	0.004	0.9	0.0003	12.7	42.		10 kc	8" NE 9" up		"	"	
1	132159	26 Nov 52	790	780	800	68	0.394	42.	0.009	298	29.5	1. MI acetone	1 kc			"	"	
6	132250	10 Mar 53	810	715	777	50	0.167	16.2	0.010	94.5	96.		10 kc	g on g		"	"	
7	132252	11 Mar 53	1430	1330	1395	200	1.04	16.1	0.06	51.3	82.5		10 kc	Base at Base		"	"	
8	132253	12 Mar 53	698	692	710	45	1.48	87.7	0.017	423.	42.0		10 kc	8" NE 9" up		"	"	
9	132254	17 Mar 53	635	655	660	45	--	23.3	--		42.0	650 psi N <sub>2</sub> and vent, chg. C <sub>2</sub> H <sub>4</sub>	10 kc	8" NE 9" up		"	"	
10	132255	18 Mar 53	800	710	710	45	0.68	21.5	0.004	865.	42.0		10 kc	8" NE 9" up		"	"	
11	132256	19 Mar 53	840	760	815	420	0.301	13.5	0.025	1800.	29.3		10 kc	8" NE 9" up		"	"	
12	132258	23 Mar 53	810	70	455	45	0.010	39.	0.0003	12.5	41.9	10 MI acetone	10 kc			"	"	Leak
13	132259	26 Mar 53	788	185	485	61	--	15.3	--		95.5		10 kc	g on g		"	"	
14	132263-I	4 May 53	1600	1425	1528	72	--	21.9	--		27.7		10 kc	Base at Base		"	"	
15	132263-II	5 May 53	620	595	623	72	0.022	23.	0.001	45.8	27.7		10 kc			"	"	
16	132264	7 May 53	615	600	622	69	<0.0001	20.7	<0.000005	<0.25	27.6		100 MI O <sub>2</sub>			"	"	
17	132265	8 May 53	680	608	631	67	<0.0001	21.4	<0.000005	67.5	27.5		25 MI O <sub>2</sub>			"	"	
18	132266	9 May 53	394	377	601	72	0.094	25.6	0.0013	67.5	27.5		5.0 MI O <sub>2</sub>			"	"	
19	132267	11 May 53	617	575	603	75	~0.001	17.0	~0.00005	3.1	27.5		2.0 MI O <sub>2</sub>			"	"	
20	132268	11 May 53	617	575	603	75	0.037	24.5	0.0006	36.6	27.5		10.0 MI O <sub>2</sub>			"	"	
21	132269	12 May 53	605	590	612	71	0.057	21.8	0.0014	71.	27.5		10.0 MI O <sub>2</sub>			"	"	
22	132270	13 May 53	637	629	638	66	0.016	14.8	0.0011	54.	27.5		10.0 MI O <sub>2</sub>			"	"	
23	132271	4 Jun 53	550	525	553	70	0.031	16.8	0.002	94.	27.5		10 kc	8" SW 13"-1/8" up		"	"	
24	132276	7 Jul 53	490	490	505	76	0.021	22.1	0.001	65.	27.0		10 kc			"	"	
25	132277	8 Jul 53	460	460	475	78	--	20.1	--	0.0	27.0		10 kc			"	"	
26	132278	9 Jul 53	460	455	473	73	0.011	18.3	0.0006	43.1	27.0		95 MI air			"	"	
27	132279	10 Jul 53	445	440	458	~75	0.136	69.8	0.002	147.	27.0		215 mm CO <sub>2</sub>			"	"	
28	132280	13 Jul 53	426	395	425	87	Least, save al grams	16.5	--		27.0		33 mm SO <sub>2</sub>			"	"	
29	132281	14 Jul 53	430	420	440	81	0.015	20.0	0.001	52.2	27.0		AlO <sub>3</sub>			"	"	
30	132282	15 Jul 53	420	410	430	79	0.057	23.2	0.028	184.	27.0		1 atm SO <sub>2</sub>			"	"	
31	132284	16 Jul 53	420	385	417	83	2.692	64.9	0.167	241.	27.0		55 parts SO <sub>2</sub>			"	"	
32	132285	17 Jul 53	395	70	246	83	30.9	64.9	0.485	2450.	27.0		23-98 gm SO <sub>2</sub>			"	"	
33	132287	20 Jul 53	400	390	410	85	--	64.9	--		0		27.9 gm SO <sub>2</sub>			"	"	
34	132293	3 Aug 53	810	790	815	80	0.028	17.0	0.012	357.	26.8		1 kc			Ohio Chem.	028087	
35	132294	4 Aug 53	930	910	925	76	0.472	16.8	0.024	445.	26.8		1 kc			"	"	
36	132295	5 Aug 53	615	610	628	76	0.010	16.0	0.0026	70.	26.8		1 kc			Matheson	FF 737	
37	132297	6 Aug 53	955	950	968	75	4.45	15.7	0.0625	30.	26.8		Alk. pyrogallol			"	"	
38	132350	10 Aug 53	320	320	335	75	0.005	15.7	0.0003	35.6	26.8		1 kc			"	"	
39	132351	11 Aug 53	985	965	990	80	0.084	16.3	0.005	67.	26.8		1 kc			"	"	
40	132353	12 Aug 53	945	930	950	75	0.085	14.6	0.006	112.	26.8		1 kc			"	"	
41	132354	13 Aug 53	860	840	865	80	0.150	16.3	0.009	112.	26.8		1 kc			"	"	
42	132355	14 Aug 53	870	855	877	74	1.70	65.6	0.0668	698.	26.8		1 kc			"	"	
43	132356	14 Aug 53	925	900	922	70	0.309	11.8	0.0231	509.	26.7		1 kc			Ohio Chem.	028087	
44	132359	17 Aug 53	1015	970	1000	72	0.428	18.5	0.0231	551.	26.7		1 kc			"	"	
45	132359	18 Aug 53	1015	970	1000	72	0.428	18.5	0.0231	551.	26.7		1 kc			Matheson	5772	
46	132360	21 Aug 53	920	865	902	71	~0.005	17.8	~0.0002	7.3	26.7		1 kc			"	"	
47	132361	24 Aug 53	825	785	820	79	2.6	15.7	0.040	82.	26.7		1 kc			"	"	
48	132362	25 Aug 53	975	946	975	79	0.029	14.0	0.0021	28.0	26.5		1 kc			"	"	
49	132363	26 Aug 53	1200	1000	1115	90	21.5	116.5	0.185	2380.	26.5		1 kc			Carbide and		In small to medium lumps, slightly off white, moderately coherent
50	132366	5 Sept 53	1010	924	980	77	4.9	90.5	0.0941	730.	26.5		1 kc			Matheson	5772	Powdery, in small, soft lumps, white
51	132369	9 Sept 53	1005	925	980	73	--	17.0	--	0.0	26.5		1 kc			"	"	
52	132370	10 Sept 53	1000	970	1000	70	1.5	21.3	0.0705	790.	26.5		1 kc			Carbide and		
53	132372	11 Sept 53	513	475	510	60	0.16	34.5	0.0064	298.	26.5		1 kc			Carbide and		
54	132373	14 Sept 53	1500	960	1245	~70	51.3	262.7	0.195	2200.	26.5		Acetaldehyde			Matheson	5772	Had to be cut out of bomb. Some fines, all coherent, white
55	132375	25 Sept 53	1570	1080	1315	~65	43.6	71.8	0.607	1915. avg	89.6		10 kc	On g		"	"	
56	132376	30 Sept 53	1780	1110	1450	79	12.5	17.0	0.18 avg	745. avg	29.5		10 kc	On g		U.S. Ind. Chem.	I 1065	White, soft powder, very small lumps
								28.8		58.0	1.67		10 kc	On g				Had to be cut out of bomb. Some fines, all coherent, white

At first it was thought that the decrease in rate of reaction was caused by the presence of oxygen in the system, and therefore a number of runs were made in which a known amount of oxygen was introduced. Although the results of these runs showed a dependence of the extent of reaction on the amount of oxygen, as shown in Fig. 55, the effect was far smaller than the decrease in reactivity from the early runs to the later runs. (see Figs. 56 and 57). Therefore, it seemed unlikely that oxygen alone could be responsible for inhibiting the reaction.

Other ideas were therefore advanced in order to account for the erratic polymerization rates observed. It was suggested that some polyethylene might be present in the storage cylinders and introduced during charging of the reactant to the pressure reactor; however, the conditions usually required for the polymerization of ethylene were unlikely to have prevailed in the storage cylinder.

Another possibility was that some unknown inhibitor was present erratically, or that some unknown promoter was absent erratically. The substances most likely to fall into these categories were impurities in the ethylene, gases from the air, materials used in cleaning the reaction equipment, and the reaction equipment itself. The latter possibility was tested tentatively by allowing polymer to accumulate on the walls of the reactor and then checking the rate of reaction in a subsequent run; no influence on the rate of reaction was noted. The influence of various solvents and other materials thought possibly to have been present accidentally in the successful runs was checked by adding the following materials successively to separate batches of the reactant ethylene: acetone, acetaldehyde, air and acetone, air and water, carbon dioxide, sulfur dioxide, and aluminum chloride. Sulfur dioxide and aluminum chloride were the only additives producing detectable effects, and the latter material produced a typical tar instead of the white

powder sought. The addition of sulfur dioxide resulted in the production of a white powder at relatively high rates of reaction. However, this powder proved to have a sulfur content rather close to that of the equimolar addition product of sulfur dioxide and ethylene. See Fig. 58. Matthews and Elder<sup>61</sup> and Snow and Frey<sup>52</sup> have reported similar reactions between sulfur dioxide and olefins under ultraviolet light.

Next the composition of the reactant gases was examined in some detail. The ethylene was analyzed (see Table XIV) immediately on removal from the storage cylinders, after charging to the reactor but before irradiation, and on removing from the reactor after irradiation. Components determined were "soluble in bromine", carbon dioxide, oxygen, carbon monoxide, paraffin hydrocarbons, and nitrogen. Higher olefins and acetylenic compounds were not detected separately by the methods used.

A series of tests was made in order to remove possible oxygen or other volatile gases from the ethylene. The bomb was evacuated, ethylene was charged under cylinder pressure, and then the ethylene was condensed by immersing the bomb in a flask containing dry ice. The bomb was then vented until the pressure had dropped to a predetermined value or until a given volume of gas had been released. The ethylene was then vaporized and the bomb and contents irradiated as before.

Experimental Procedure. In this work ethylene was irradiated with cobalt-60 gamma radiation while at room temperature and at pressures of 250 to 1600 pounds per square inch pressure. Some tests were made in which ethylene was reacted alone and some in which the ethylene was mixed with other reactants. A stainless-steel bomb (Figs. 1 and 2) was used as the reaction vessel. The bomb was evacuated to a pressure of less than 1 mm of mercury absolute. Ethylene was added to the bomb from a cylinder. Pressures up to about 75 atmospheres and room temperature were the usual physical conditions employed. The bomb was then placed in either the 1-kilocurie source or the

TABLE XIV

## ANALYSES OF ETHYLENE FROM STORAGE CYLINDERS AND FROM REACTOR

<u>Material No.</u>	<u>Mfg. No.</u>	<u>%CO<sub>2</sub></u>	<u>%O<sub>2</sub></u>	<u>%CO</u>	<u>%N<sub>2</sub></u>	<u>% Combustible as marked</u>	<u>Number of Determinations</u>
1	Math FF737	0.06	0.02	0.02	0.15	0.1 propane?	duplicate
2	Math 5772	0.06	0.02+	0.00	0.07	0.29 propane	duplicate
3	OC G28087	0.10+	0.02+	0.00+	0.47 total	ethane?	single sample
4	C and C JK370331	0.37	0.02	0.05	1.7	0.8 pentane	triplicate
5	USI IC-1065	0.08	0.05	0.005(?)	0.21	0.45 methane	duplicate

TABLE XIV (cont)

## ANALYSES OF ETHYLENE FROM STORAGE CYLINDERS AND FROM REACTOR

Material No.	Dose	G	Page No.	%CO <sub>2</sub> *	%O <sub>2</sub> *	%CO*	%N <sub>2</sub>	%Combustible as marked	Number of Determinations
4	3.09	2380	132363	0.37 0.62	0.02 0.07+	0.05 0.07	0.00	3.8 ethane	duplicate; first sample of 1 l. or more
2	2.40	730	132366	0.06 0.05	0.02 0.008	0.00 0.002	0.12	0.14 ethane(?)	duplicate
2	0.45	0	132369	0.06 0.02	0.02 0.05	0.00 0.01	0.22 total	-?-	duplicate
4	0.57	790	132370	0.37 0.34	0.02 0.01	0.05 0.01+	2.49 total	-?-	duplicate
2	0.91	298	132372	0.06 0.05+	0.02 0.005	0.00 0.00	0.23 total	-?-	duplicate; acetaldehyde added
2	6.97	2200	132373	0.06 0.05	0.02 ≤0.01	0.00 0.00	0.09	0.18 methane	single
3	6.43	1915	132375	0.10 0.11	0.02 0.02	0.00 0.009	0.16	0.32 ethane (?)	single
5	4.29	745	132376	0.08 0.07	0.05 0.009	0.005(?) 0.00	0.10	0.63 methane	single

\*Top, before irradiation  
Bottom, after irradiation  
(no removal by distillation and no addition to ethylene unless noted)

10-kilocurie source until the proper dose had been accumulated. After irradiation, the bomb was removed from the source, the unreacted ethylene was vented and analyzed by an Orsat analyzer and the accumulated polymer was removed mechanically.

Results of Polymerization of Ethylene. A white, solid polyethylene resulted from the irradiation of ethylene with cobalt-60 gamma rays. The yield of polymer was found to be quite small until the system had received a dose of about 1/2 megarep. The yield increased rapidly to a value of about 2500 gram-moles reacted/(metric ton)(megarep) at about 3 megarep, and remained nearly constant up to doses of 7 megarep, the highest dose studied (see Fig. 58). (It should be noted that 1 gram-mole reacted/(metric ton)(megarep) is equivalent to 0.97 molecule reacted per 100 electron-volts.) About one-third of the monomer was polymerized in three days in the center of the 10-kilocurie source. The thermodynamic properties of ethylene were taken from the work of York and White<sup>60</sup>.

#### Discussion of Polymerization of Ethylene

From Fig. 58 it can be seen that the yield of polymer per unit of energy absorbed from the radiation, the G value for the reaction, is a function of the total dose of radiation. This relation is evidently due to the presence of an induction period for the reaction. No correlation could be observed between contents of the following gases in the monomer and the yield as a function of dose: carbon dioxide, oxygen, carbon monoxide, hydrogen, paraffin hydrocarbons, nitrogen, and sulfur dioxide. It appeared, however, that the venting of noncondensable gases from the liquid ethylene did increase the initial rate of reaction to some extent. The data for the analyses of gases before and after irradiation are given in Table XIV.

Average values of dose rates used in these studies varied from about 30 kilorep/hour to about 90 kilorep/hour. It should be noted, however,

that errors exist in the method of calculating the dose rates used in estimating the G values. A Victoreen ratemeter was used to measure the dose rates on the axis of the bomb. This instrument would detect the secondary photons produced by scatter from the wall of the bomb, but probably would not detect the scattered electrons. These scattered electrons would be quite effective in producing chemical reaction because nearly all their energy would be imparted to the chemical system. Consequently it can be seen that more ionization probably occurred than was taken into account by the calculations, in which the effect of the bomb wall was neglected. The effect of this error is that the G values given are too high.

On the other hand, as a calculation device, the primary beam was assumed to undergo no appreciable absorption within the ethylene in the bomb. Rather, the beam was assumed to maintain within the bomb a value which would be attained in the axis if the bomb were full of air. It was recognized, of course, that absorption within the ethylene was assumed to be causing the reaction. If account were taken of absorption of primaries within the ethylene, then somewhat greater credit for initiating reaction would have to be given to each primary photon, and this would increase the G values given.

Thus, neglect of nonequilibrium secondaries and neglect of the absorption gradient of primary gamma intensity within the ethylene compensate each other to some extent. The importance of accounting for the above errors in dosimetry is recognized. However, the complexity of the problems of measurement would seem to indicate the desirability of pursuing this work further in future studies. Therefore, the values given for G in Fig. 58 should be regarded as relative rather than absolute, since all determinations were made in the same equipment and using similar procedures.

No consistent effect of pressure on the G value could be noted.

Elevated temperatures were investigated only briefly, but preliminary results indicated that considerably increased rates of polymerization would result in irradiated systems at temperatures of 200-400°F as compared with those obtained at room temperature.

### Evaluation of the Polyethylene Product

General. The polyethylene obtained as a result of gamma irradiation of ethylene was subjected to a brief program of evaluation. The properties considered most basic to an understanding of the material were investigated. Most experimental work was concerned with determinations of solution viscosity, melt viscosity, density, and tensile strength. Melting points of some samples were also determined. Molecular weights were estimated from the determinations of viscosities of solutions and of melts. Crystallinity was estimated from determinations of density. The other measurements were made by conventional means.

These measurements and derived quantities probably need no further explanation, with the exception of the concept of crystallinity of a polymer. The degree of crystallinity of a polymer is measured by the degree to which the molecules of polymer are arranged parallel to each other. An arrangement of parallel molecules results in a repetitive structural pattern such as that found among the molecules of a crystal. A random orientation of molecules similar to a pile of jackstraws might be expected to be less dense than a parallel arrangement such as that just described, and it has been found that percentage crystallinity may be correlated with the density of polyethylene (see Kirk-Othmer<sup>31</sup>). Some explanation is given in the following paragraph of the manner of presenting the data obtained from experiments on the polymer.



The properties of the polyethylene are presented as functions of the radiation yield of the polymerization reaction because of the reasons given below. In addition molecular weight and crystallinity are presented as functions of dose. The radiation yield of the polymerization of ethylene may be expressed as the G value, the number of molecules of ethylene which undergo polymerization for every 100 electron-volts of energy absorbed from radiation. Lind<sup>36</sup> has shown that in many gaseous systems, approximately one molecule reacts per ion pair formed in the system. In the irradiation of ethylene a variable number of molecules, usually much greater than one, react for each ion pair formed. The polymerization of ethylene is therefore evidently a chain reaction. For this calculation it is assumed that one chain is initiated for every ion pair formed, that all chains are of equal length, and further that the formation of each ion pair requires 32.5 electron-volts of energy, a value approximately correct for gases at one atmosphere. The densities of ethylene under the conditions of reaction were greater than at one atmosphere and therefore the energy required per ion pair may be quite different from the value given. The G value may therefore be divided by three to give the approximate number of molecules reacted for each ion pair formed, and this result may then be multiplied by the molecular weight of the monomer in order to arrive at the molecular weight of the polymer.

Consequently, the G value is directly proportional to the molecular weight which would be expected of the polymer if the above assumptions held. Furthermore, the properties of a polymer are frequently found to be functions of its molecular weight. It therefore seems advantageous to consider the properties of the polyethylene as functions of the G value.

The results of most determinations could be correlated against the G value, or radiation yield, somewhat better than they could against dose, although the G value has been shown to be a function of dose. See Fig. 58,

where it is indicated that the G value was about 0.1 to 1.0 until about 0.5 megarep had been received. The G value then increased rapidly with increasing dose until it reached a nearly constant value of about 2000 molecules per 100 electron-volts for doses of about 3 to 7 megarep.

Experimental. All the samples of polyethylene were white. Some were fluffy powders and others were tough, coherent masses.

Portions of each of the samples of polyethylene which occurred in yields of 4 grams or more were molded into sheets as an operation preliminary to further examinations. A two-compartment mold was used, one compartment at a time. Samples were placed between aluminum foil in the mold, preheated to 300°F, pressed to 1000 psi, and cooled to about 125°F under pressure. The resulting sheets were 2.5 by 4 by 0.025 inch. All such sheets proved to have the characteristic milky, translucent appearance of polyethylene. The sheets molded from the powders were brittle, while those from the tough reaction products were also tough.

Molecular weights were estimated from viscosities of solutions, measured as follows: Solutions of some samples were prepared in concentrations of 0.01 percent and of 0.125 percent by weight in tetralin. Viscosities of these solutions and of the tetralin were measured in modified Ostwald pipettes at 212°F. Specific viscosities were calculated and divided by the respective concentrations. The resulting ratios were plotted as a function of the concentration of polymer, and the plots were extrapolated to zero concentration to give intrinsic viscosity. Intrinsic viscosity was assumed to be directly proportional to molecular weight. The concentration was computed in units of gram moles of monomeric ethylene per liter of solution. The constant of proportionality was computed by the author to cause the observed value for the molecular weight of Bakelite DYNH to agree with the value of 20,000 for the weight average molecular weight given by Dienes and Klemm<sup>20</sup>. The

value of the constant was computed in this way to be  $0.42 \times 10^{-4}$  liter per gram. See also the work of Tani<sup>55</sup> on intrinsic viscosities of polyethylene in tetralin.

The method of Dienes and Klemm<sup>20</sup> was used to estimate molecular weights from melt viscosities. Viscosities were measured in a parallel-plate plastometer with an attached dial gauge reading to 0.01 millimeter. The entire assembly was placed in an oven. Temperatures of 248°F and of 266°F were used. The samples were placed between sheets of aluminum foil about 1-1/2 mils thick. The thickness of the sheets of foil was measured in the plastometer before each determination.

Crystallinity was estimated by correlation with density (see Kirk-Othmer<sup>31</sup>). Densities were determined by the use of Archimedes' principle. Weighings were made directly in water, after the sample had first been degassed by use of reduced pressure while it was immersed in water.

Tensile properties of the polyethylenes were examined by the following procedure. Specimens for testing were cut from the molded sheets by means of a die. The resulting specimens were 0.079 by 0.025 inch in the smallest cross section. The narrowest section was 1-1/2 inches long. Tension was applied in Gardner-Parks testing machine shown in Fig. 266 of Gardner<sup>24</sup>. This machine had a capacity of 2.5 kilograms.

Melting points were determined on a melting-point bar of the design of Dennis<sup>18</sup> (see Fig. 54).

Discussion. The results of evaluation of the properties of the radiation-polymerized polyethylene are summarized in Table XV. The molecular weight is plotted as a function of radiation yield in Fig. 60. The molecular weights and crystallinities are plotted as functions of dose in Fig. 61.

The significance of the determination of molecular weights by means of solution viscosity is not clear. The values obtained were assumed to be

TABLE XV

## PROPERTIES OF POLYETHYLENE PRODUCED

Page Number	Dose, Megarep	Radiation Yield, A	Melting Point, °F Lower/Upper	Density g/cm. <sup>3</sup>	Ultimate Tensile, psi	Elongation, Percent at rupture	Crystallinity Percent	Molecular Weight by Melt Viscosity	Molecular Weight by Solution Viscosity
132250	1.55	95	219/226						
132268	0.61	37	216/225						
132269	0.58	71	205/217						
132276	0.60	63	207/214						
132281	0.54	52	196/205						
132297	1.91	750	241/244	0.951	450	4	77	26,300	insol.
132362	0.37	28	234/235						
132363	3.09	2400	248/689	0.941	2200	42	71	34,400	insol.
132366	2.40	730	210/248	0.951	770	2	77	28,100	4200
132369	0.45	0.1							
132370	0.57	790	203/252						8800
132372	0.91	298	199/207						insol.
132373	6.97	2200	234/720	0.943	2100	29	72	40,500	insol.
132375	6.43	1900	241/610	0.941	2300	79	71	37,300	insol.
132376	4.29	745	241/244	0.951	630	3	77	11,900	3700
Bakelite DYNH				0.921	1500	550	61	21,800	20,000 assumed

weight average molecular weights, based on the weight average molecular weight of Bakelite DYNH of 20,000 (see Table XV). However, differences in crystallinity and cross linking, mentioned above, may invalidate the comparison of the thermally polymerized sample with the radiation-polymerized samples.

Determinations of molecular weight by melt viscosity may be subject to similar criticism. As shown in Figs. 60 and 61, the molecular weights determined by solution viscosity do not agree well with those determined by melt viscosity. Neither do the molecular weights from solution viscosity appear to display any regular variations with dose or with G value, in contrast to the regular behavior of molecular weights from melt viscosities. The reasons for these discrepancies are not clear.

Values of crystallinity are plotted as a function of radiation yield in Fig. 63. The crystallinities varied from about 77 percent for samples of low radiation yield to about 71 percent for samples of high radiation yield. All these samples were of considerably higher crystallinity than was the Bakelite DYNH, which had a crystallinity of about 61 percent. It is possible that the radiation-polymerized samples were of higher crystallinity than the thermally polymerized sample of DYNH because the temperature of polymerization was lower for the radiation-polymerized samples. The samples of low radiation yield would be expected to be more highly crystalline than those of high radiation yield, since radiation yield has been shown to increase with dose (Fig. 58), cross-linking and branching would probably also increase with dose, and increases in either cross-linking or branching would cause decreased crystallinity.

Tensile properties are reported in terms of stress as a function of strain in Fig. 62. The irradiated samples all have properties similar to those of a brittle material. The samples subjected to higher doses

have higher tensile strengths and are more ductile than those subjected to lower doses of radiation. Such behavior would be likely if the irradiation increased cross-linking and branching. The Bakelite DYNH shows the characteristic elongation of several hundred percent before rupture. See Kirk-Othmer<sup>31</sup>, p. 942. Ultimate tensile stress as a function of radiation yield is plotted in Fig. 63. The ultimate tensile stress increased markedly with radiation yield and consequently with dose. A set of structural properties such as those just described for the radiation-polymerized polyethylene might be desirable for certain applications, but the properties differ from those of most polyethylene currently marketed.

Melting points are plotted as a function of radiation yield in Fig. 64. Curves are given for both the upper and the lower ends of the melting-point range. The results show that there is a small increase in the temperature of initial softening with increase in radiation yield, and that there is a large increase in the temperature of complete melting. The higher melting points indicate higher degrees of cross-linking as a result of the higher doses of radiation, and are thus in conformity with the results of the other determinations mentioned above.

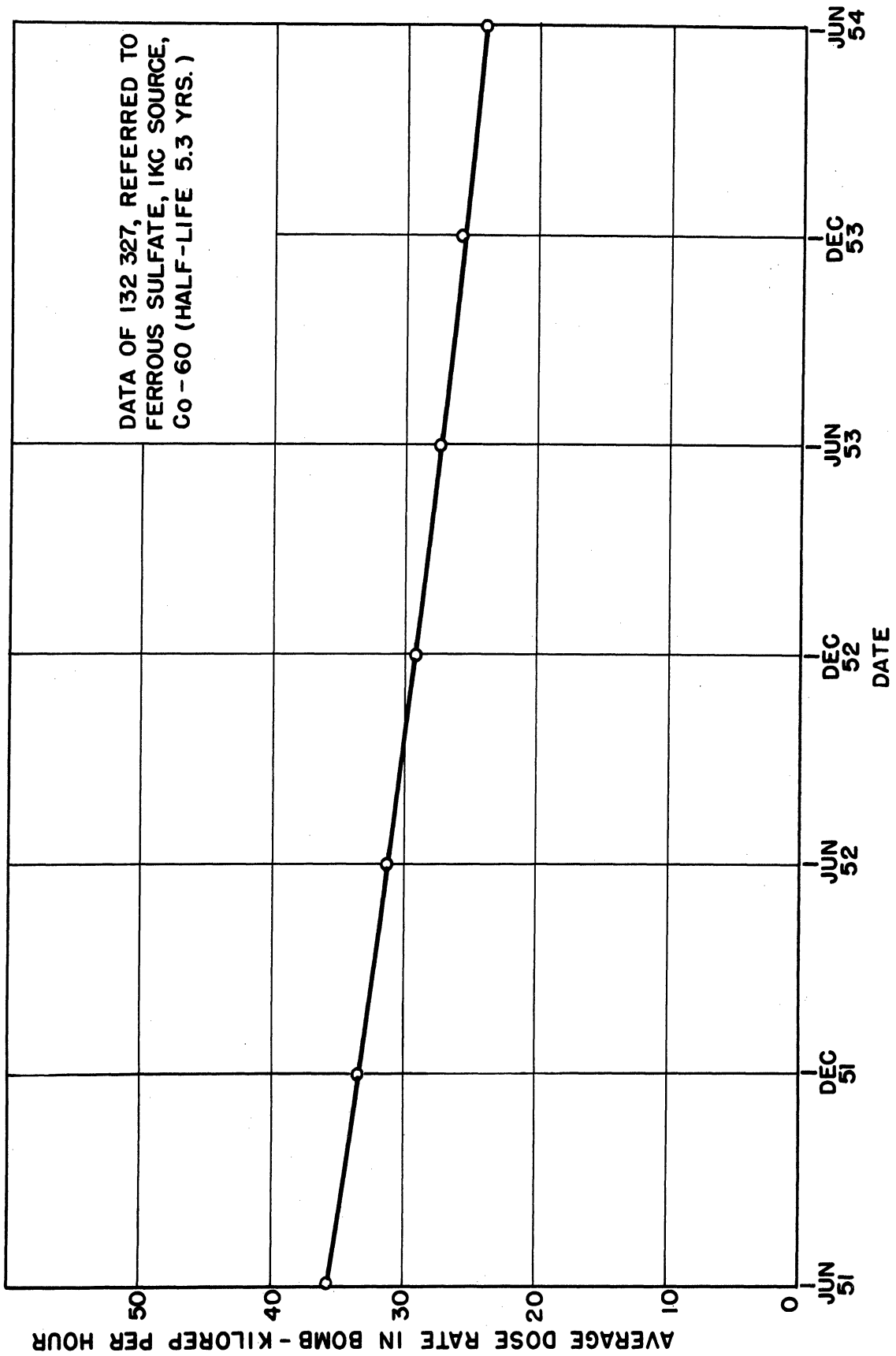


Fig. 50. Average Dose Rate Inside Pressure Reactor as Function of Time with 1-Kilocurie Source.

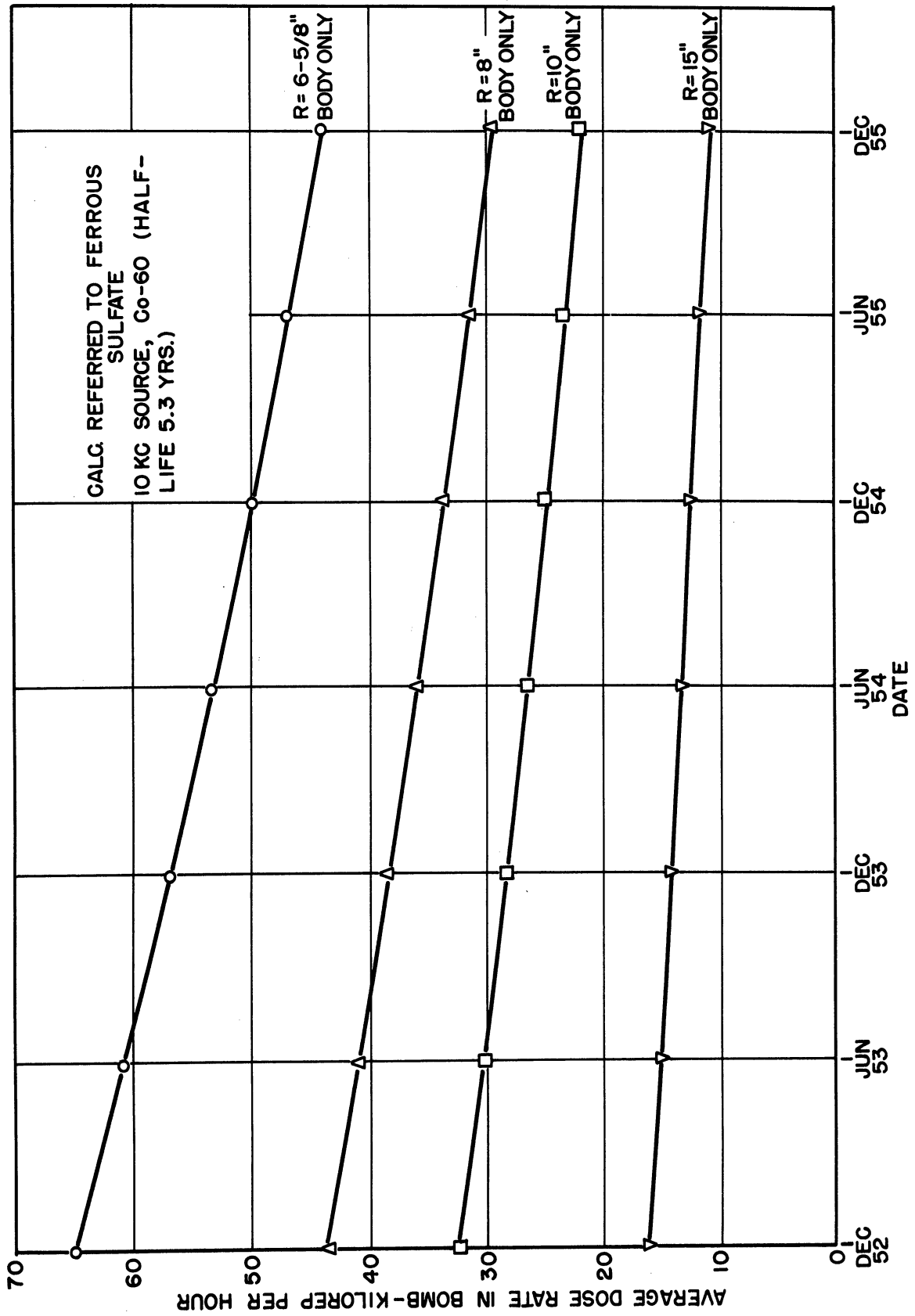


Fig. 51. Average Dose Rates Inside Pressure Reactor as Function of Time with 10-Kilocurie Source.



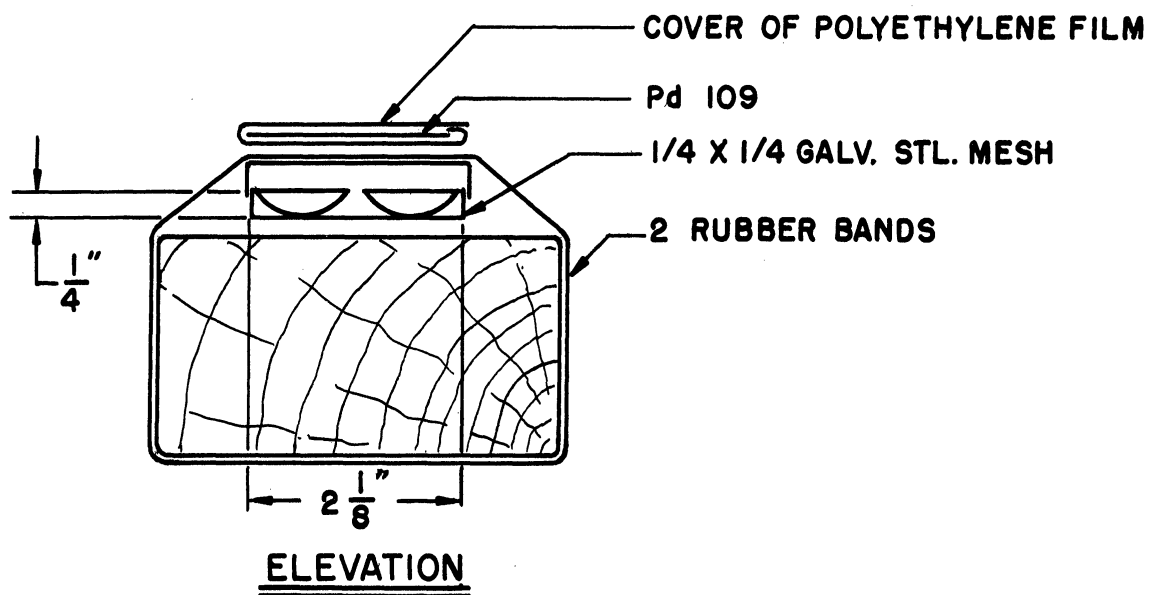
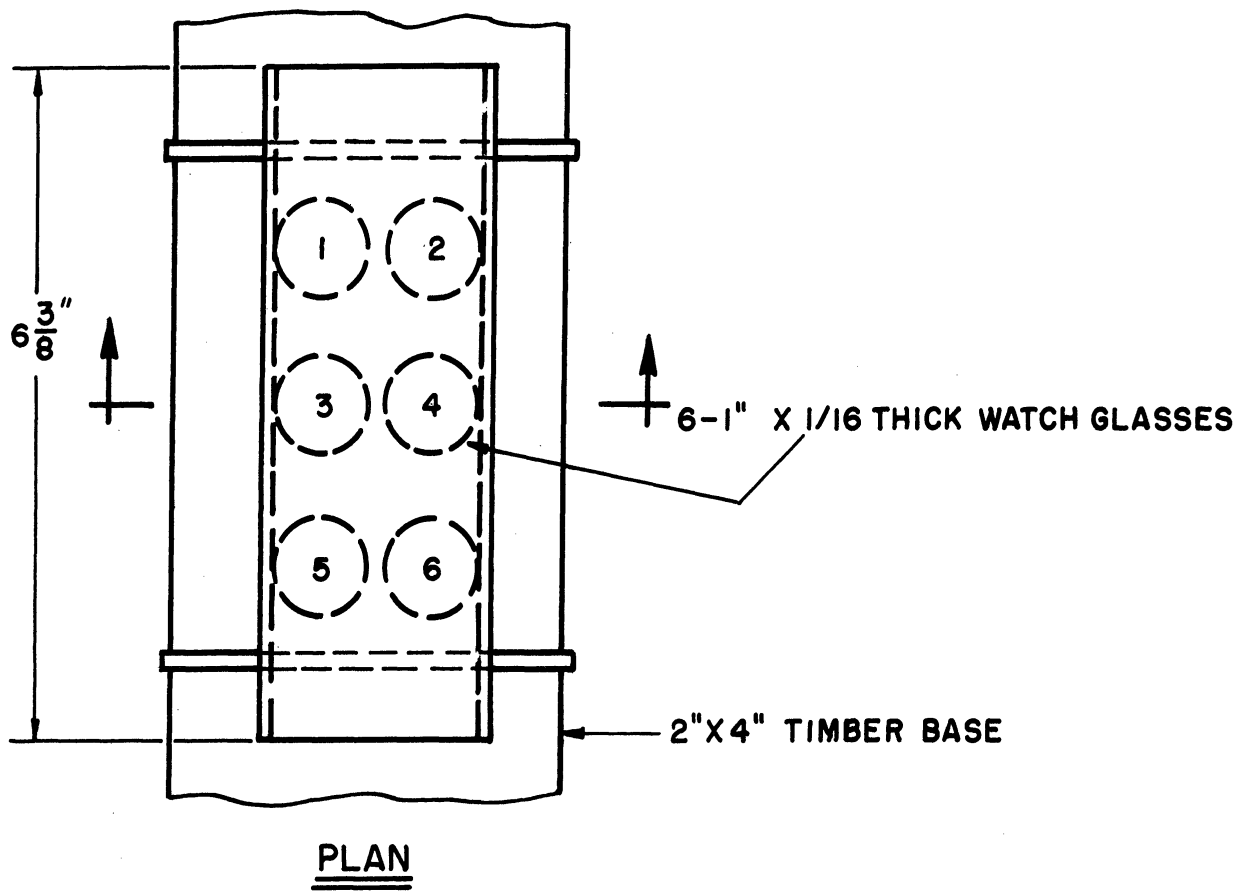


Fig. 52. Apparatus for Drying of Natural Oils by Palladium-109 Beta Rays.

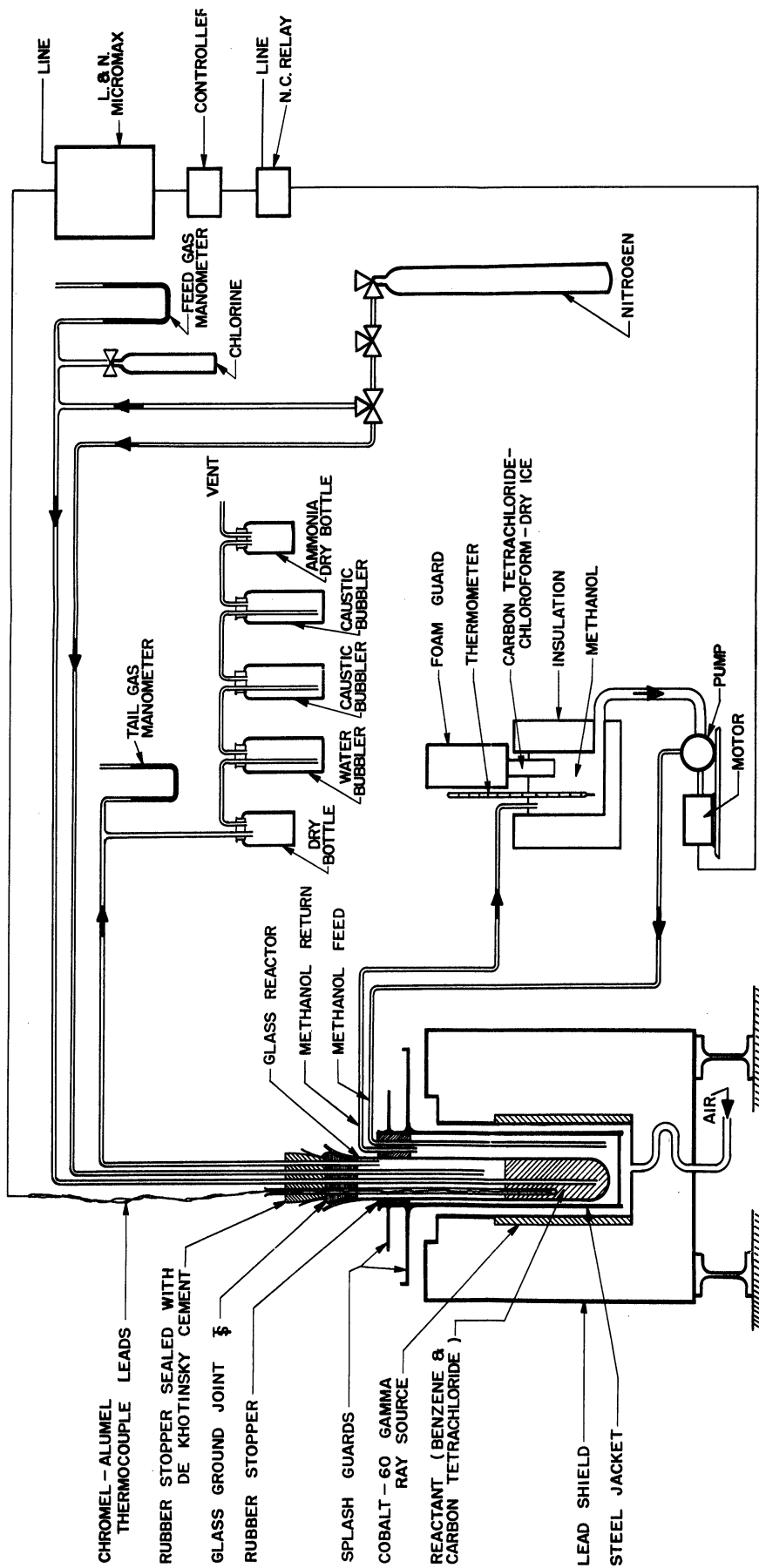


Fig. 53. Flow Sheet for Additive Chlorination of Benzene in Cobalt-60 Gamma Ray Source.

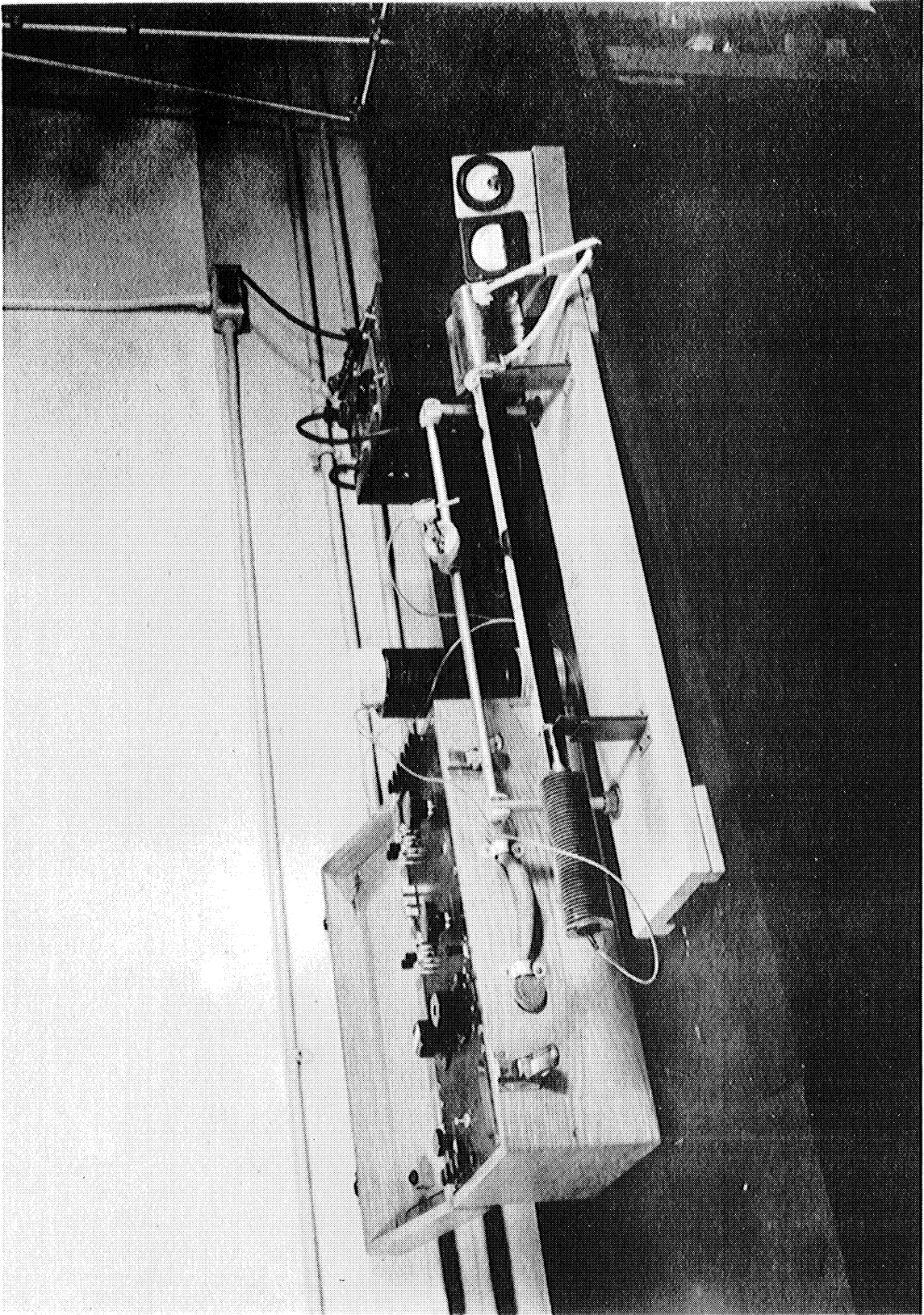


Fig. 54. Melting-Point Bar.

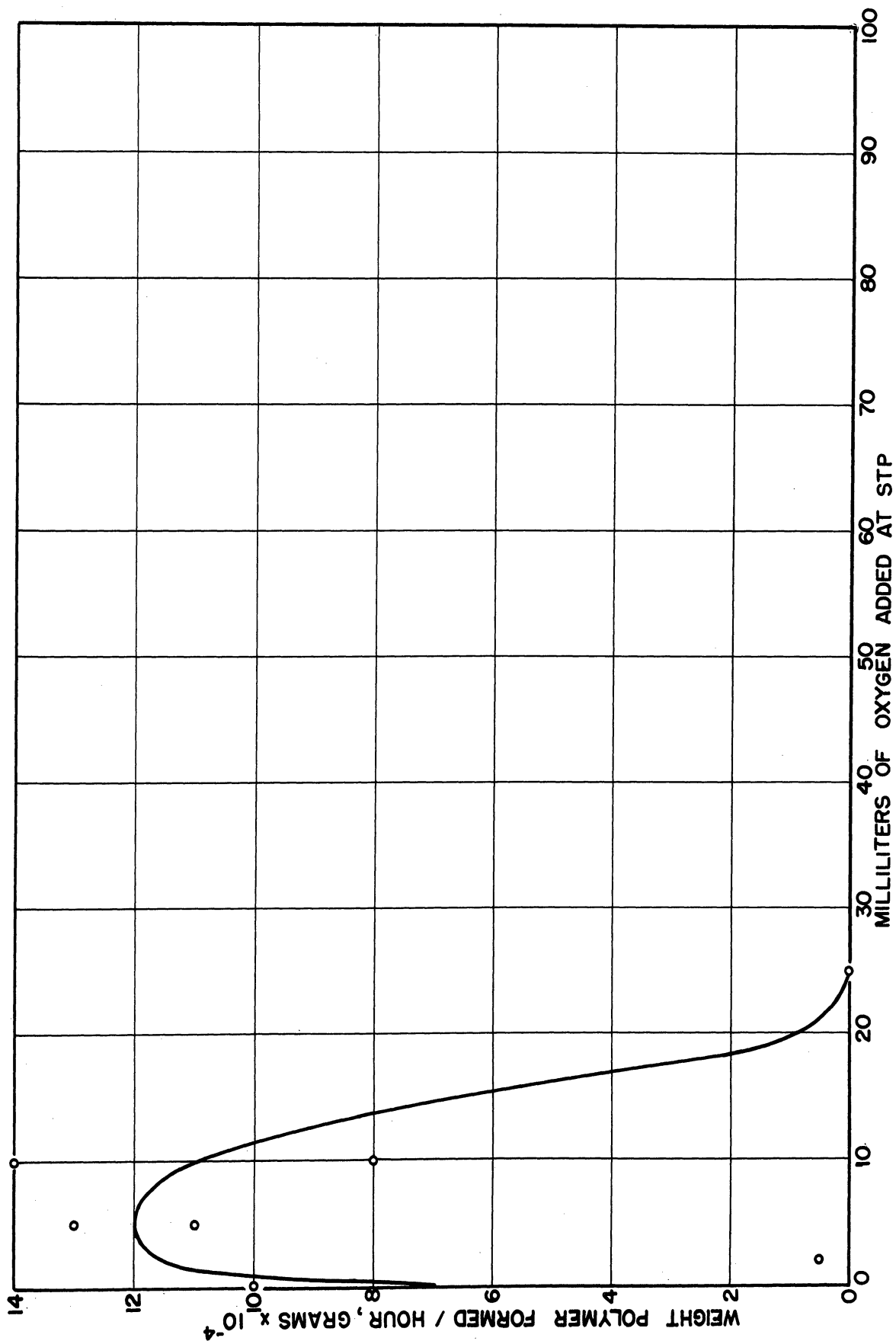


Fig. 55. Influence of Oxygen on Polymerization of Ethylene.

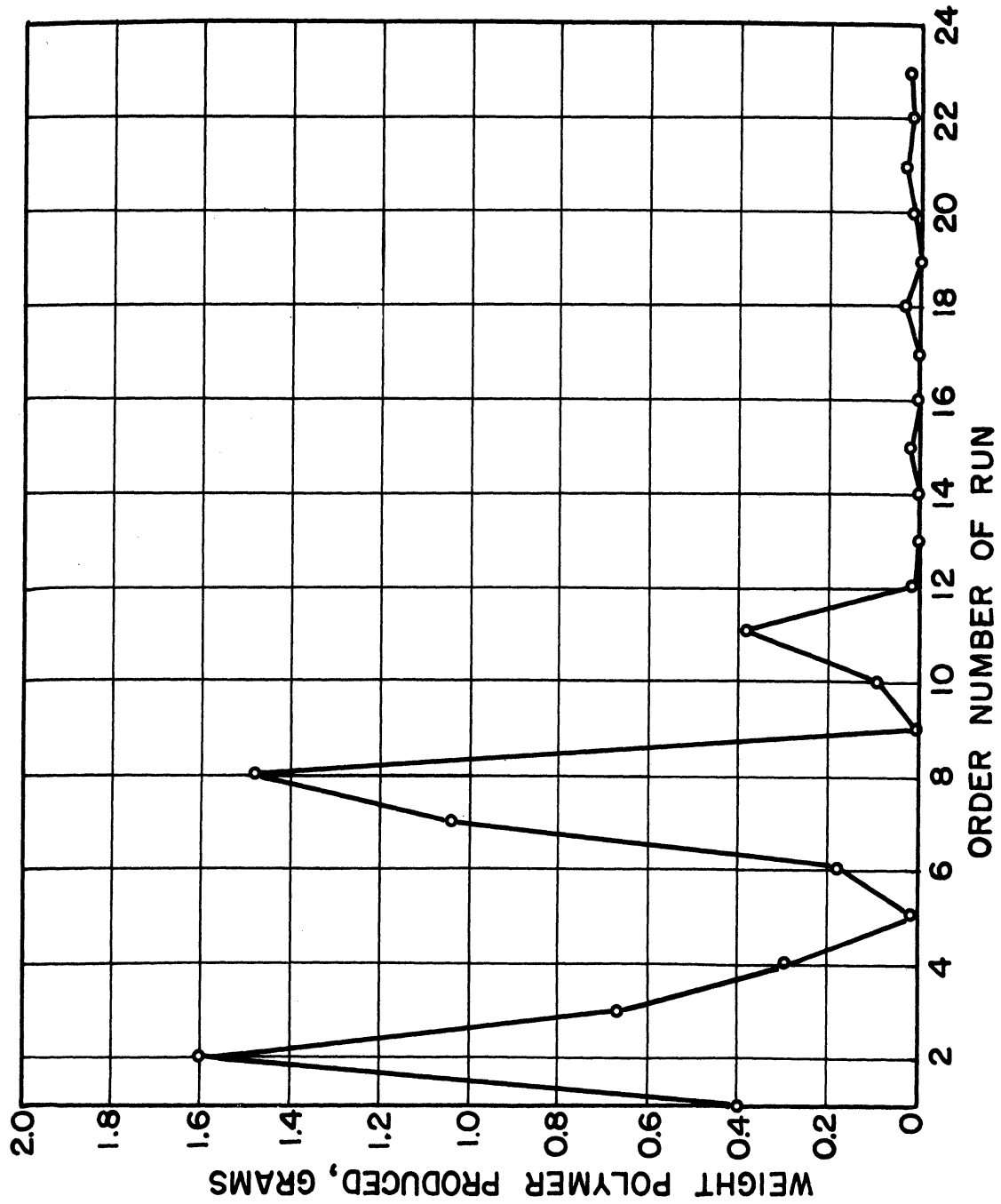


Fig. 56. Yield as Function of Order of Run in Polymerization of Ethylene.

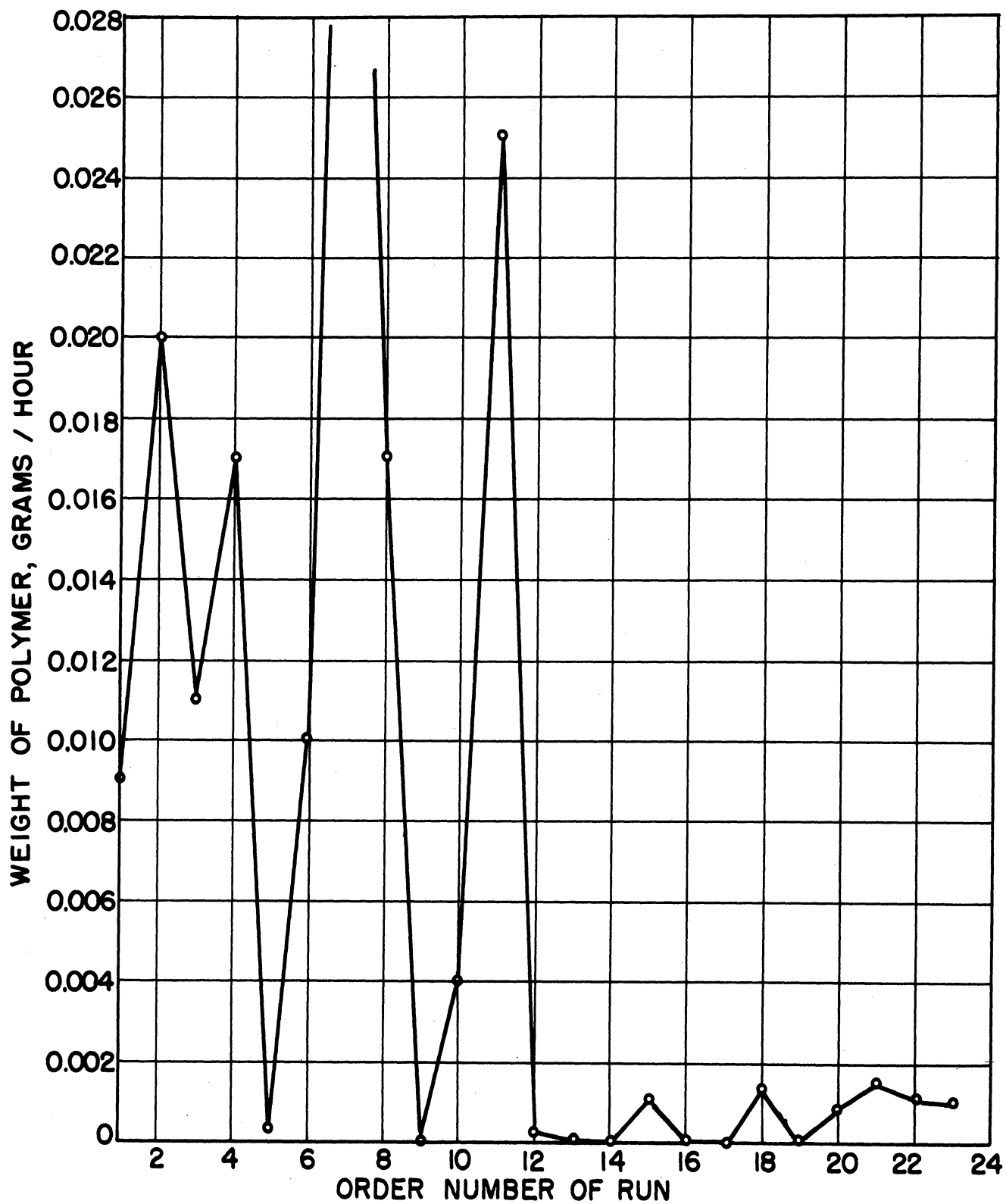


Fig. 57. Rate as Function of Order of Run in Polymerization of Ethylene.

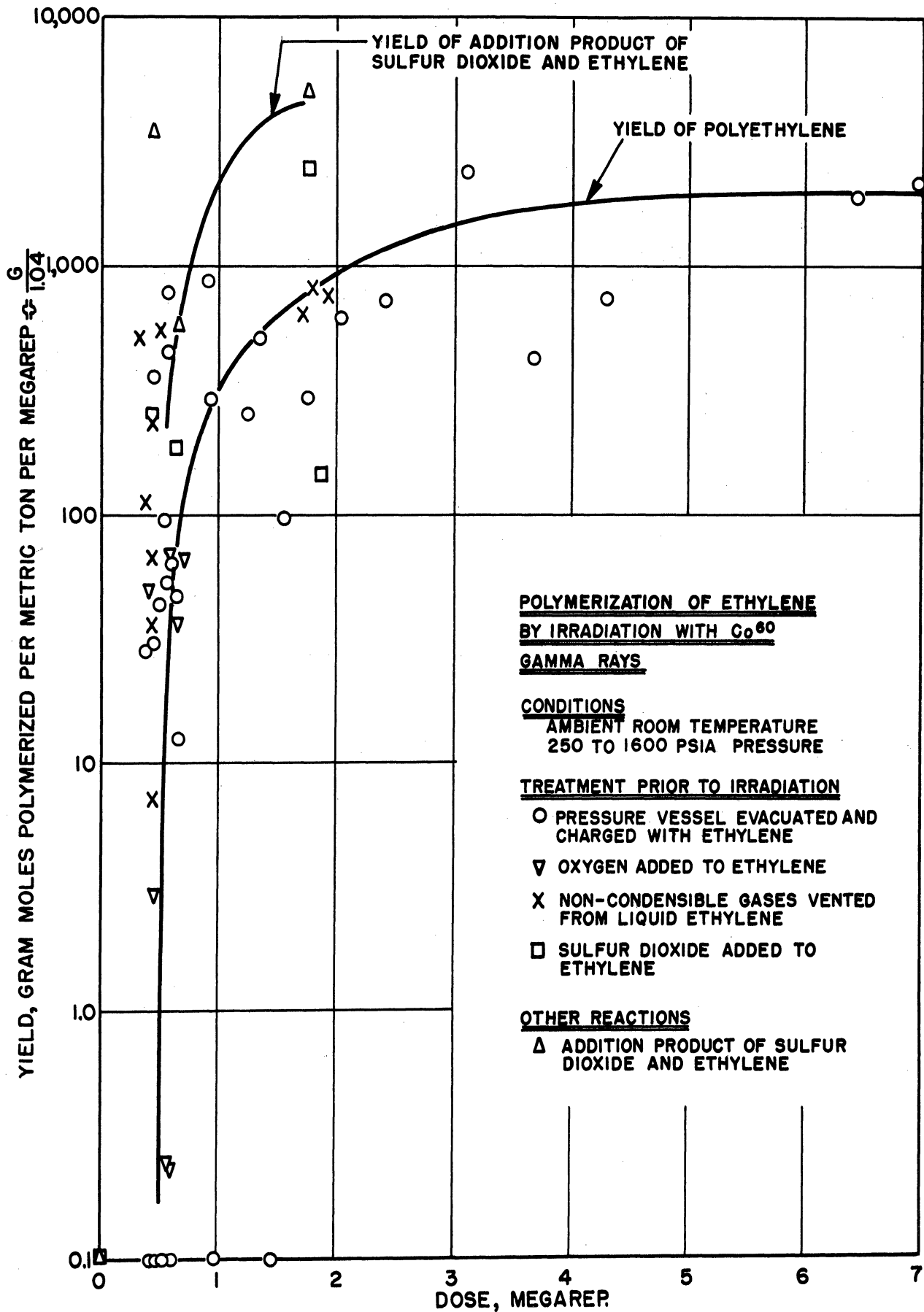


Fig. 58. Radiation Yield as Function of Dose of Radiation in Polymerization of Ethylene.

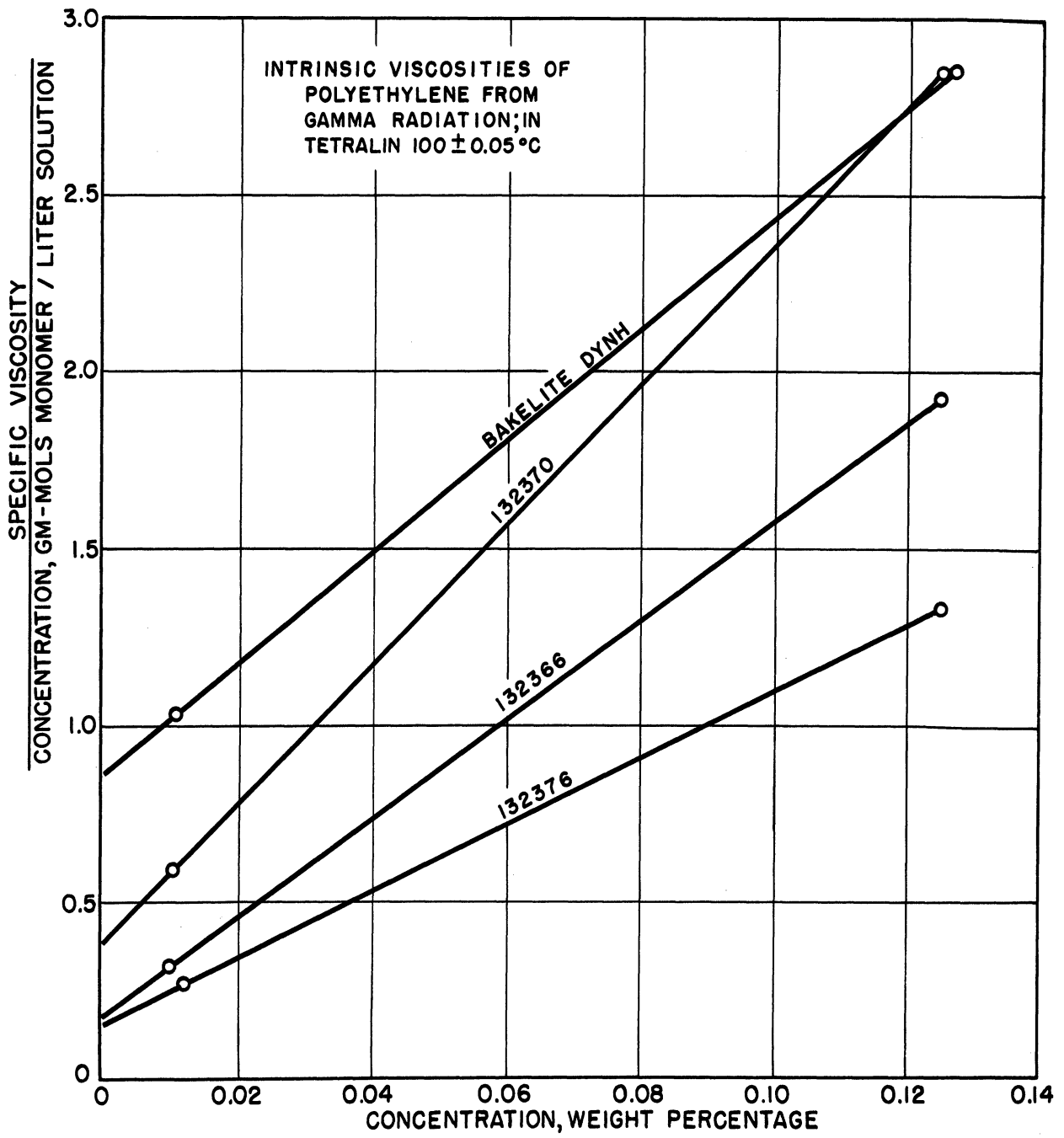


Fig. 59. Solution Viscosity Determinations on Polyethylene.



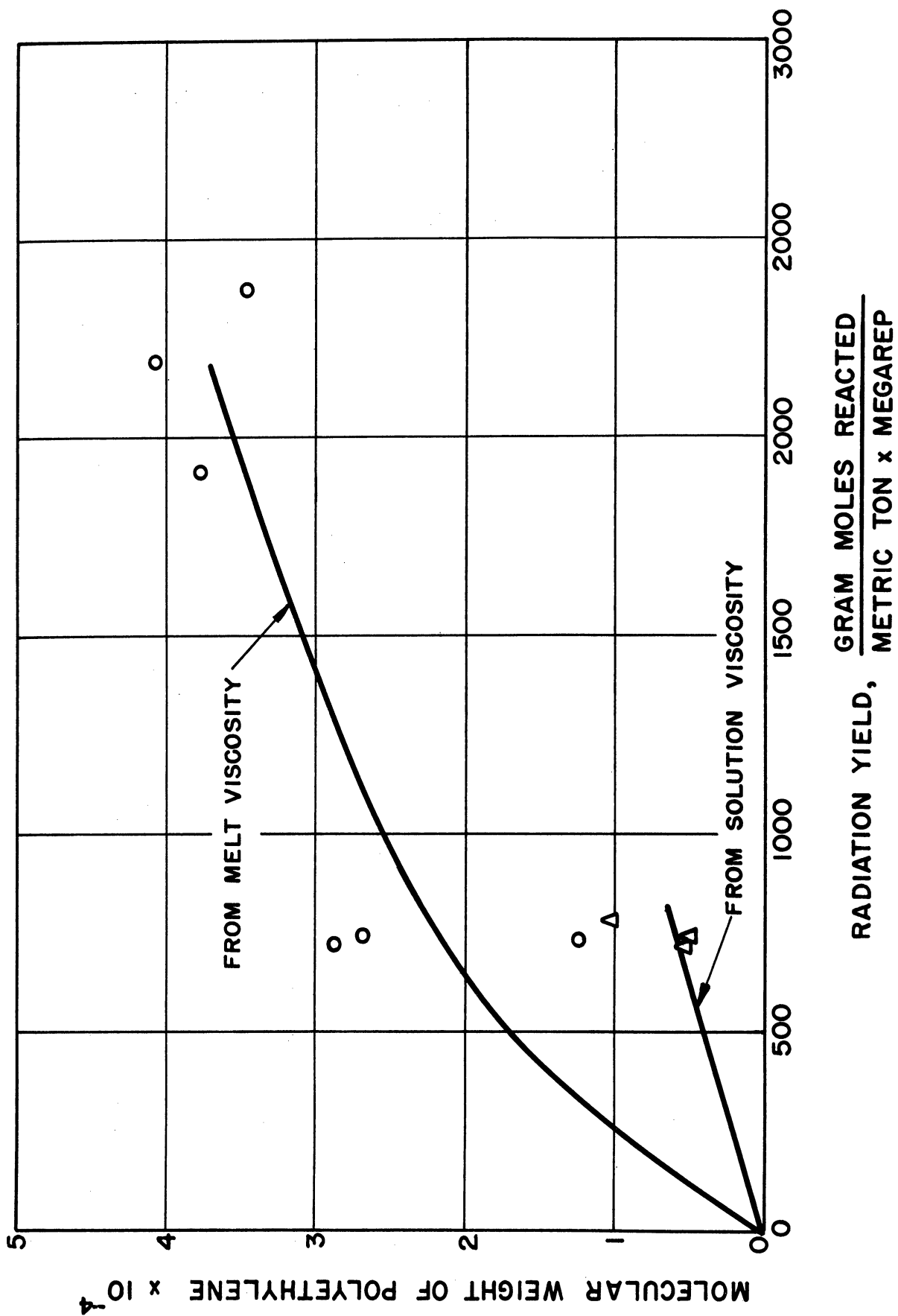


Fig. 60. Molecular Weight as Function of Radiation Yield of Polyethylene.

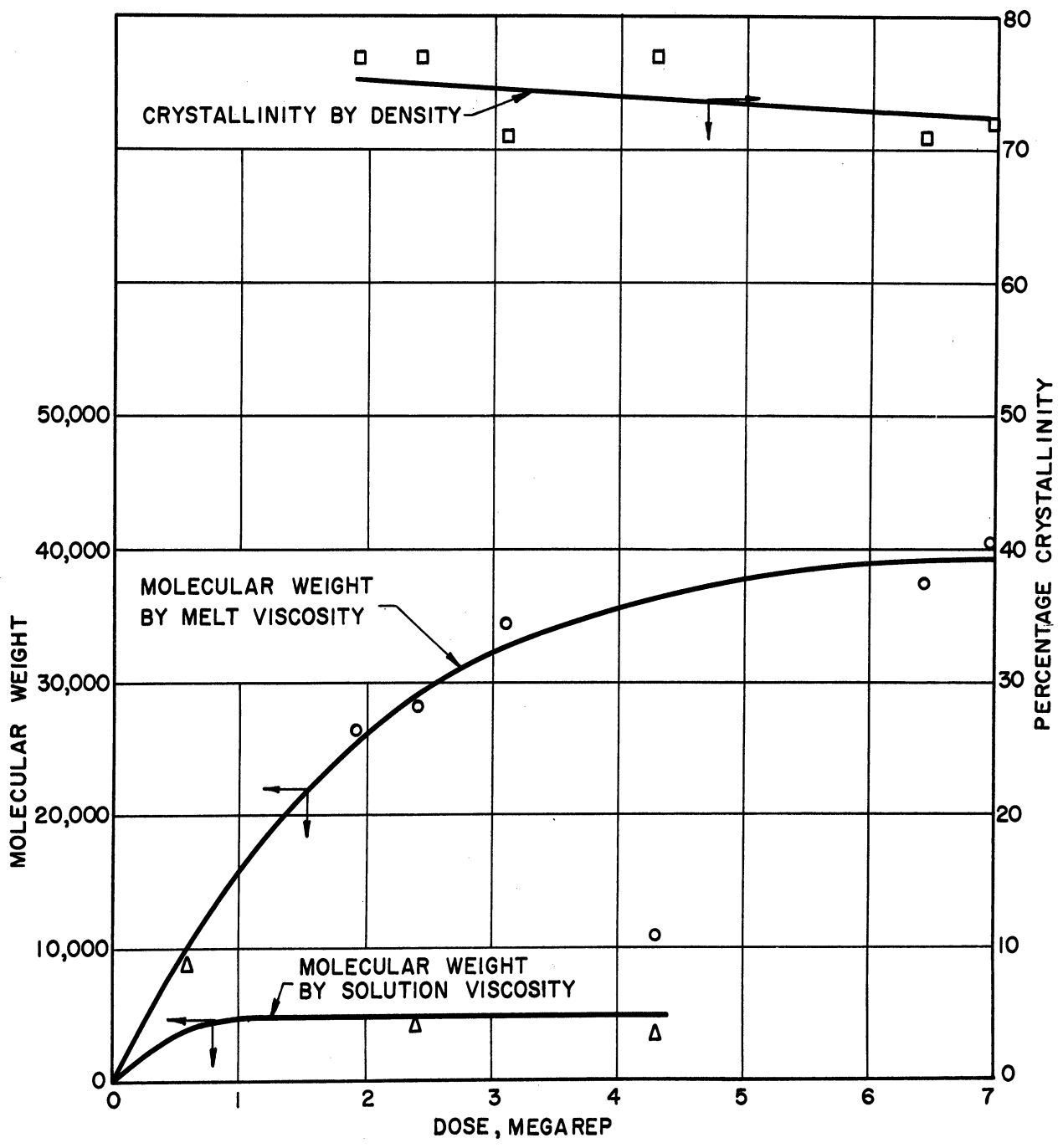


Fig. 61. Molecular Weight and Crystallinity as Functions of Radiation Dose for Polymerization.

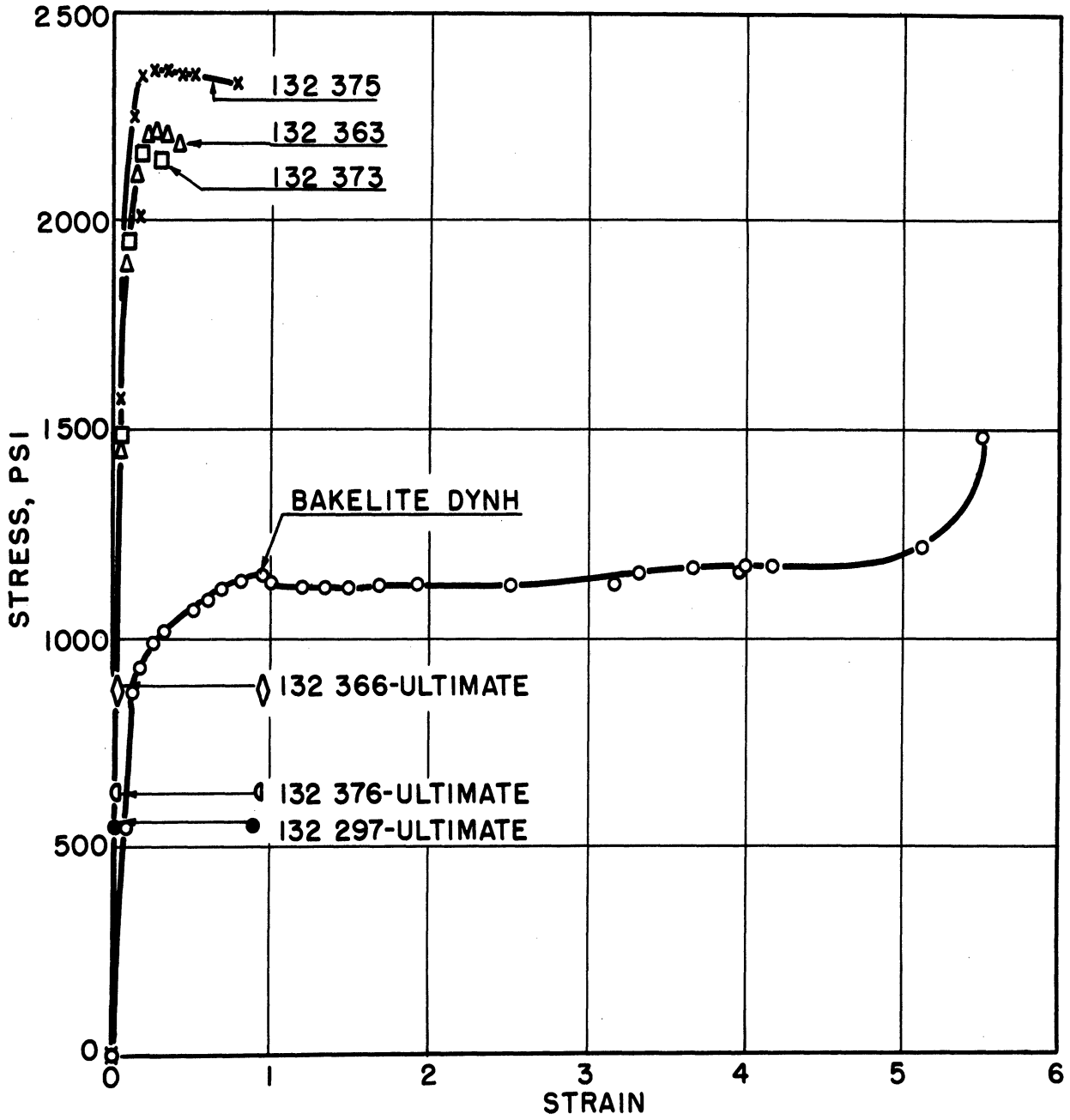


Fig. 62. Stress-Strain Plots for Test Specimens of Polyethylene.

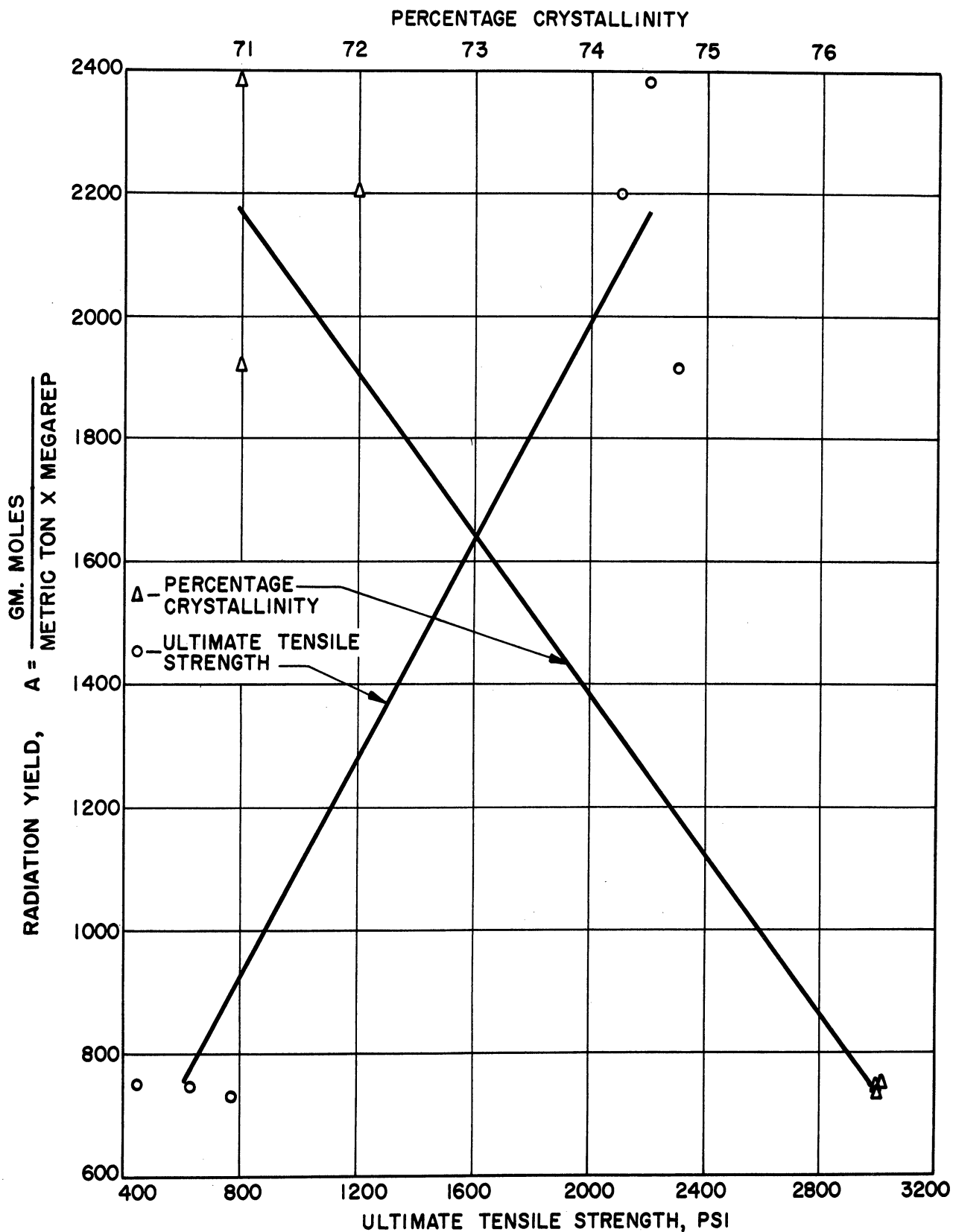


Fig. 63. Crystallinity and Tensile Strength as Functions of Radiation Yield for Polyethylene.

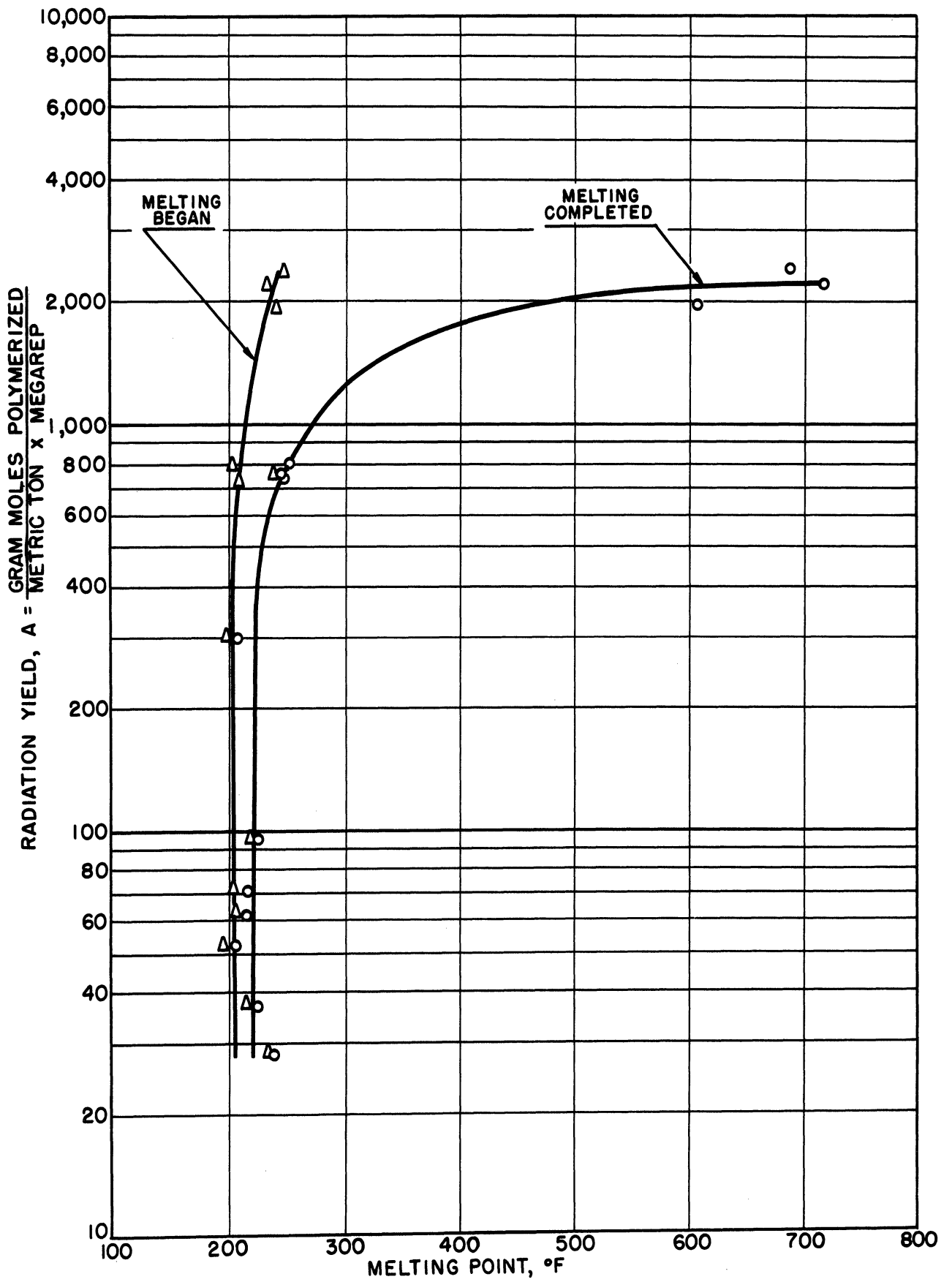


Fig. 64. Melting Points as Functions of Radiation Yield of Polyethylene.

SUGGESTIONS FOR FUTURE WORK IN THE PROMOTION OF  
CHEMICAL REACTIONS BY GAMMA IRRADIATION

Polymerization of Ethylene

It would be of interest to investigate further the polymerization of ethylene under gamma radiation with the objective of determining the cause for the induction period observed for the polymerization. It seems possible that small concentrations of impurities are responsible for the induction period. However, it is also possible that such an induction period might be characteristic of the gamma-induced polymerization and independent of chemical parameters.

If the ethylene could be caused to polymerize immediately on subjection to radiation at the same rate observed after the induction period, then a continuous process for the polymerization might be developed. Such a procedure would permit closer control of those properties of the polymer which are dependent on total dose of radiation.

It would also be interesting to study the electrical properties of the polyethylene made by gamma irradiation.

As mentioned above, under "Discussion of the Polymerization of Ethylene," elevated temperatures in conjunction with irradiation caused greater rates of polymerization of ethylene than did irradiation alone. It would be interesting to investigate further the influence of both elevated temperatures and irradiation on the polymerization of ethylene. Some suggestions for such a program were advanced by Anderson, Martin, et al.<sup>9</sup>, based on some of the foregoing studies of radiation chemistry and on the work of Kennard<sup>30</sup>.

Other Reactions

The reaction between ethylene and sulfur dioxide proceeds rapidly enough under gamma radiation that it should be possible to secure much information concerning the behavior of this reaction. It would be of interest to determine the physical properties of the resulting polymer when molded into massive form.

The acceleration of the drying of natural oils appeared to be interesting in preliminary experiments (Table VII). Additional work on this topic might be of interest.

Since chlorinations appear to be a class of reactions generally promoted by gamma radiation, it would be of interest to procure data on rates and yields of such reactions. Such results could then be compared with other methods commonly used to initiate the chlorination reaction.

## CONCLUSIONS

From the foregoing work the following conclusions were drawn:

- (1) Ethylene was polymerized by exposure to gamma radiation from cobalt-60. The rates of reaction were sufficiently large that further work on this reaction appears to be promising.
- (2) Polyethylene formed by gamma irradiation was subjected to a preliminary evaluation. The polymer was found to be denser, less ductile, and of a higher ultimate strength than Bakelite DYNH polyethylene. Molecular weights of the radiation-polymerized materials increased with dose of radiation to a value of about 40,000 when estimated from melt viscosities. Most samples were insoluble in tetralin and estimates of molecular weights from solution viscosities were not conclusive. Crystallinities estimated from densities varied from 71 to 77 percent.
- (3) Benzene reacted with chlorine in the presence of gamma radiation from cobalt-60 to form benzene hexachloride at large rates of reaction. The benzene hexachloride was found to have a content of the gamma isomer of about 12 percent, or approximately the same as that resulting from the reaction activated by ultraviolet light.
- (4) The polymerizations of soya oil, acetylene, isobutylene, and propylene were accelerated to small extents by gamma irradiation. The oxidation of drying oils was accelerated by palladium-109 beta-irradiation.
- (5) The synthesis of ammonia from nitrogen and hydrogen, the oxidation of sulfur dioxide, and the reaction of carbon dioxide and hydrogen were not measurably affected by cobalt-60 gamma irradiation.



- (6) With the exception of reactions such as the polymerization of ethylene and certain chlorinations, most of the chemical systems examined were remarkable for the small magnitude of any effects caused by gamma radiation originating in 1/4 to 3 kilocuries of cobalt-60. Such information may be regarded as indicative of the relative stability toward gamma radiation of many chemical systems.
- (7) The activities of the cobalt-60 sources were calculated from measurements of dose and were found to be about 30 percent of the values obtained previously from nuclear-reactor calculations.
- (8) It was found that no unusual difficulties resulted from the operation of a pressure vessel at 2000 psi and 50 to 400°F within a hollow cylinder of cobalt-60 encased in aluminum.

## APPENDIX

### Design Data for Bomb

- (1) Design conditions: 2000 psig, 650°F.
- (2) Maximum operating conditions: same as for (1).
- (3) Materials of construction: AISI type 304 stainless steel with AISI type 347 rod in welds.  
Bolts: ASTM A-193.  
Nuts: AISI type 304 plate, bored perpendicular to plane of rolling.  
Gaskets: 1-1/4-inch-I.D. x 1-1/2-inch-O.D. x 3/32-inch thick single-jacketed asbestos gaskets with copper cladding.  
Electrical fittings: Fixed Nitrogen Research (as described by Ernst<sup>23</sup>) with Teflon pressure cones.  
Tubing fittings: Fixed Nitrogen Research and Ermeto fittings.
- (4) Designed according to recommendations of the ASME Boiler Code, Section VIII<sup>4</sup>. Parts of the design were checked by the methods given by Sliepcevich<sup>51</sup>.
- (5) All welding radiographed.
- (6) Bomb and auxiliary tubing subjected to 2800-psi hydrostatic test before use.

### Assembly Instructions for Bomb

- (1) Clean the interior and the gasket seats.
- (2) Check to see that all passages are open.
- (3) Assemble electrical fittings, Teflon cones, and electrical and thermocouple leads in head.

- (4) Check electrical leads for continuity and grounds.
- (5) Attach carefully to the head any internal fittings to be used. Use special rack to hold assembly during this operation.
- (6) Screw body-flange on body.
- (7) Place body in holding rack.
- (8) Place gasket on seat or in retaining groove.
- (9) Place head on body.
- (10) Assemble bolt studs and nuts but do not tighten.
- (11) Tighten the head bolts. Use alternate tightening sequence, checking separation of flanges by means of a feeler gauge.
- (12) Attach tubing and auxiliary fittings to head.

#### Operating Instructions for Bomb

- (1) Attach pressure gauge to external fittings for safety, even if not required for operation.
- (2) Attach rupture disc, suitably anchored, to external fittings.
- (3) After assembly of the bomb, test for leaks with soap solution, and then test with a Freon alcohol-lamp assembly.
- (4) If internal fittings are in used in the bomb, vent the pressure slowly to avoid overstressing the internal fittings.

#### Definition of "Radiation Yield"

Below is described the method used for reporting the yields of polyethylene produced by gamma irradiation. The quantities A, B, and G, mentioned below, are referred to elsewhere as the radiation yield. It was desired to report yields of chemical reactions in the units generally used, such as the quantity G, mentioned by Burton<sup>14</sup>. G is the yield of a reaction in terms of molecules reacted per 100 electron-volts of energy absorbed from radiation. However, it was also desired to report yields in terms more closely related

to engineering usage. It was observed that both requirements could be met by an arrangement which will now be described. The observation was made that the yield in units of G, molecules reacted per 100 electron-volts absorbed, is numerically almost equal to the yield reported in units of what we have called A, gram moles reacted per metric ton subjected to 1 megarep. This relation is demonstrated below:

$$\begin{aligned}
 & \left[ \frac{\text{gram moles reacted}}{\text{metric ton x megarep}} \right] \times \frac{6.02 \times 10^{23} \text{ molecules}}{\text{gram mole}} \times \frac{\text{metric ton}}{10^6 \text{ grams}} \\
 & \times \frac{\text{megarep}}{10^6 \text{ rep}} \times \frac{\text{gram x rep}}{93 \text{ ergs}} \times \frac{1.6 \times 10^{-12} \text{ ergs}}{\text{electron-volt}} \times \frac{100 \text{ (electron-volts)}}{100 \text{ electron-volts}} \\
 & = 1.04 \times \frac{\text{gram moles reacted}}{\text{metric ton x megarep}} \times \frac{\text{molecules x metric ton x megarep}}{\text{gram mole x 100 electron-volts}} \\
 & = G, \frac{\text{molecules reacted}}{100 \text{ electron-volts}}
 \end{aligned}$$

Therefore

$$A, \frac{\text{gram moles reacted}}{\text{metric ton x megarep}} = \frac{G}{1.04}, \frac{\text{molecules reacted}}{100 \text{ electron-volts}}$$

By means of a similar procedure, the following relation can also be established:

$$B, \frac{\text{pound moles reacted}}{\text{metric ton x megarep}} = \frac{G}{518}, \frac{\text{molecules reacted}}{100 \text{ electron-volts}}$$

This method of reporting yields was applied as follows. The yield of polyethylene in grams was divided by the molecular weight of ethylene, 28.04, to give gram moles reacted. The weight of ethylene charged to the bomb was estimated from measurements of pressure and temperature and from the data of York and White<sup>60</sup>. The weight of ethylene charged was computed in units of metric tons, and therefore is the weight of material assumed to absorb radiation. The dose rates used in this work were values averaged

over the length of the axis of the pressure vessel for the positions in which it was placed for these experiments. The average dose rate so found was multiplied by the total time during which exposure to the radiation occurred. With some simplification the following relation was developed:

$$A, \quad \frac{\text{gram moles reacted}}{\text{metric ton} \times \text{megarep}} = \frac{\text{weight fraction ethylene reacted} \times 10^6}{\text{molecular weight of ethylene} \times \text{dose, megarep}} .$$

## BIBLIOGRAPHY

1. Allen, A.O., Chemical Effects of Ionizing Radiation on Simple Inorganic Compounds and Aqueous Solutions, U.S. Atomic Energy Commission, MDDC-363, 1946.
2. Alyea, H.N., and Backstrom, H.J., J. Am. Chem. Soc. 51, 90 (1929).
3. Alyea, H.N., "Chain Reactions Produced by Light and by Alpha Radiation", J. Am. Chem. Soc. 52, 2743 (1930).
4. American Society of Mechanical Engineers, Boiler Construction Code, Section VIII, Unfired Pressure Vessels, 1950.
5. Anderson, L.C., Martin, J.J., et al., Utilization of the Gross Fission Products, Progress Report 1 (C00-86), Eng. Res. Inst., Univ. of Mich., Project M943, August, 1951.
6. Anderson, L.C., Martin, J.J., et al., Utilization of the Gross Fission Products, Progress Report 2 (C00-90), Eng. Res. Inst., Univ. of Mich., Project M943, January, 1952.
7. Anderson, L.C., Martin, J.J., et al., Utilization of the Gross Fission Products, Progress Report 3 (C00-91), Eng. Res. Inst., Univ. of Mich., Project M943, June, 1952.
8. Anderson, L.C., Martin, J.J., et al., Utilization of the Gross Fission Products, Progress Report 4 (C00-124), Eng. Res. Inst., Univ. of Mich., Project M943, March, 1953.
9. Anderson, L.C., Martin, J.J., et al., Utilization of the Gross Fission Products, Progress Report 5 (C00-196), Eng. Res. Inst., Univ. of Mich., Project M943, November, 1953.
10. Backstrom, H.L.J., J. Am. Chem. Soc. 49, 1460 (1927).
11. Bodenstein, M., and Pohl, W., Z. fur Elek. 11, 373 (1905).
12. Boullé, Andre, "Catalysis by Cathodic Projection", Bull. Soc. Chim. 10, 361-71 (1943).
13. Bretton, R.H., et al., Effect of Gamma Radiation on Hydrocarbon Gases, Progress Report IV (NYO-3311), Dept. of Chem. Eng., Yale Univ., October 30, 1952.
14. Burton, M., J. Phy. Coll. Chem. 51, 611 (1947).
15. Burton, V.L., "The Effects of Radioactivity on Oleic Acid", J. Am. Chem. Soc. 71, 4117 (1949).

16. Coolidge, W.O., "High-Voltage Cathode Rays Outside the Generating Tube", Science 62, 441-2 (1925).
17. Danby, C.J., and Hinshelwood, C.N., Proc. Roy. Soc. (London) A179, 169 (1941).
18. Dennis, L.M., and Shelton, R.S., J. Am. Chem. Soc. 52, 3128-32 (1930).
19. Dewes, R.A., and Goodale, E.E., Utilization of the Gross Fission Products, SO-1100, General Electric Laboratory, December, 1951.
20. Dienes, G.J., and Klemm, H.F., "Theory and Application of the Parallel-Plate Plastometer", J. App. Phys. 17, 458 (1946).
21. D'Olieslager, J.F., and Jungers, J.C., Bull. Soc. Chim. Belg. 40, 75 (1931).
22. Ellis, C., The Chemistry of Petroleum Derivatives, The Chemical Catalog Co., Inc., New York, 1934.
23. Ernst, F.A., Ind. Eng. Chem. 18, 664 (1926).
24. Gardner, H.A., and Sward, G.G., Physical and Chemical Examination of Paints, Varnishes, Lacquers, and Colors, 10th ed., Gardner, 1946.
25. Gibson, W.B., et al., Industrial Uses of Radioactive Fission Products, Stanford Res. Inst., Stanford Univ., Project No. 361, 1951.
26. Gmelins Handbuch der anorganischen Chemie, 8 Auf., Nr. 4, Lief. 2, Deut. Chem. Ges., Berlin, 1936.
27. Hancock, Harris, Elliptic Integrals, Wiley, New York, 1917.
28. Hayner, J.H., Ind. Eng. Chem. 44, 472 (1952).
29. Hopff, H., and Goebel, S., Modern Plastics 23, No. 9 (1946).
30. Kennard, Earle H., Kinetic Theory of Gases, 1st ed., McGraw-Hill, New York, 1938.
31. Kirk-Othmer, Encyclopedia of Chemical Technology, Vol. 10, 1953, pp. 938-57.
32. Kooijman, P.L., and Ghijsen, W.L., Rev. Trav. Chim. 66, 673-9 (1947).
33. LeRoy, D.J., and Steacie, E.W.R., J. Chem. Phys. 10, 676 (1942).
34. Levin, J.S., and Hughes, D.J., "Flux Depression and Self Protection in the Production of Radio-cobalt", Nucleonics 11, No. 7, 8 (1953).
35. Liggett, L., Private Communication.
36. Lind, S.C., The Chemical Effects of Alpha Particles and Electrons, 2nd ed., The Chemical Catalog Co., New York, 1928.

37. Lind, S.C., and Bardwell, D.C., "Chemical Effects in Ionized Gases", Science 62, 422-24 (1925).
38. Lind, S.C., Bardwell, D.C., and Perry, J.H., J. Am. Chem. Soc. 48, 1556-75 (1926).
39. Lind, S.C., and Livingston, R., J. Am. Chem. Soc. 52, 593 (1930).
40. Lind, S.C., J. Am. Chem. Soc. 53, 2423-4 (1931).
41. Luther, R., and Goldberg, E., Z. physik. Chem. 56, 43 (1906).
42. Marinelli, L.D., Quimby, E.H., and Hine, G.J., Am. J. Roentg. and Rad. Ther. 59, 260 (1948).
43. Mund, W., and Koch, W., J. Phys. Chem. 30, 289-93 (1926).
44. Mund, W., J. Phys. Chem. 30, 890 (1926).
45. Rosenblum, Charles, "Benzene Formation in the Radiochemical Polymerization of Acetylene", J. Phys. and Coll. Chem. 52, 474-8 (1948).
46. Selke, W.A., et al., Utilization of Waste Fission Products in Chemical Reactions, NYO-3327, AT(30-1)-1187, January 20, 1952.
47. Selke, W.A., et al., Utilization of Waste Fission Products in Chemical Reactions, NYO-3328, AT(30-1)-1187, May 5, 1952.
48. Sheppard, C.W., and Burton, V.L., "The Effects of Radioactivity on Fatty Acids", J. Am. Chem. Soc. 68, 1636-39 (1946).
49. Siri, W.E., Isotopic Tracers and Nuclear Radiations with Applications to Biology and Medicine, McGraw-Hill, New York, 1949.
50. Slator, A., Z. physik. Chem. 45, 540 (1903).
51. Sliepcevich, C.M., Design, Construction and Operation of a High-Pressure, High-Temperature Plant, Ph.D. Thesis, Univ. of Mich., 1947.
52. Snow, R.D., and Frey, F.E., Ind. Eng. Chem. 30, 176 (1938).
53. Snyder, W.S., and Powell, J.L., Absorption of Gamma Rays, AECD-2739, 1949.
54. Stenerson, H., Chem. and Eng. News 30, 4572 (1952).
55. Tani, H., Chem. High Polymers (Japan) 4, 151-7 (1947).
56. Taylor, H.S., and Emeleus, H.J., J. Am. Chem. Soc. 52, 2150 (1930).
57. Taylor, H.S., and Emeleus, H.J., J. Am. Chem. Soc. 53, 3370 (1931).
58. Weiss, Jerome, "Chemical Dosimetry Using Ferrous and Ceric Sulfates", Nucleonics 10, 28-31 (1952).



59. Willard, H.H., and Furman, N.H., Elementary Quantitative Analysis, 3rd ed., Van Nostrand, New York, 1940.
60. York, R., and White, E.F., Trans. Am. Inst. Chem. Engr. 40, 227 (1944).
61. British Patent 11,635, F.E. Matthew and H.M. Elder, 1914.
62. British Patent 584,794, E.I. du Pont de Nemours and Company, 1947.
63. British Patent 588,143, C.O. Strather to Carbide and Carbon Chemicals Corporation, 1947.
64. British Patent 591,335, E.I. du Pont de Nemours and Company, 1947.
65. U.S. Patent 2,436,256, W.E. Hanford and P.L. Salzberg to E.I. du Pont de Nemours and Company, 1948.
66. U.S. Patent 2,439,528, M.J. Roedel to E.I. du Pont de Nemours and Company, 1948.
67. U.S. Patent 2,450,451, L. Schmerling to Universal Oil Products Company, 1948.
68. U.S. Patent 2,468,111, J.A. Robertson to E.I. du Pont de Nemours and Company, 1949.

